Multi-Objective Vertiport Location Optimization for a Middle-Mile Package Delivery Framework: Case Study in the South Holland Region

MSc Thesis Control & Operations

Victor Petit

Technische Universiteit Delft

TU Delft

Multi-Objective Vertiport Location Optimization for a Middle-Mile Package Delivery Framework: Case Study in the South Holland Region

MSc Thesis Control & Operations

by

Victor Petit

to obtain the degree of Master of Science
at the Delft University of Technology,
to be defended publicly on Friday July 12th at 14:00.

Student number:	4858522	
Project duration:	11 September, 2023 – 12 July, 2024	
Thesis committee:	Prof.dr.ir. J.M. Hoekstra	Chair
	Dr. M.J. Ribeiro	Daily Supervisor
	Dr. R. Merino-Martinez	Examiner

An electronic version of this thesis is available at http://repository.tudelft.nl/.

TU Delft

Acknowledgements

The submission of this Master's thesis marks the end of my academic journey at the Faculty of Aerospace Engineering at the TU Delft. As my interests in aviation were sparked from a young age with my father being an airplane spotter hobbyist, the decision to choose Aerospace Engineering as a field of study was a rather logical one. I have very much enjoyed my time in Delft, as I got the opportunity to develop my academic skills, work on interesting projects, perform case-studies, do an internship and finally write this thesis, all whilst expanding my social network. I have met a lot of inspiring people along the way and I have had the privilege to make a lot of new friends.

I would like to express my gratitude to my supervisor Marta Ribeiro for her support during the entirety of this thesis. You were always available for any questions I had and often helped me, whenever I got stuck or was not sure how to approach certain problems. The meetings that we had every two weeks helped me very much in the process as I always got a fresh batch of motivation after the discussions we had. Your ideas and critical insight have been essential for this Master's thesis.

In addition, I would like to express my gratitude towards my family and friends. Your support and distractions from the hard studying have made the past 6 years in Delft very enjoyable and have kept me going throughout my studies. I would especially like to thank Vincent for his help, feedback, sparring sessions and the nice study sessions we had together throughout both of our theses. Thank you to my parents for always supporting me and expressing your pride of my academic achievements. This has driven me to always do my best and consequently has helped me greatly to achieve my academic goals. Another special thanks goes out to Judith for her unconditional support throughout the process and for her help to keep me motivated in good times and in bad times.

I would like express my extreme gratitude to my sister Alexa, who is both my academic and life role model. Your support and the countless amount of talks we had during these past 6 years when I wasn't feeling my best were essential for both my academic achievements and my overall happiness. I will forever be grateful for all your support and our friendship as brother and sister. I could not have done it without you.

To conclude, I feel a bit sad that my student time is over as I look back at it with great joy. Nevertheless, I look forward to the next steps in my career and the opportunities that I might get. Who knows what the future will hold.

Victor Petit
Delft, June 2024

Contents

List of Figures

List of Tables

List of Abbreviations

AHN	Actueel Hoogtebestand Nederland
CAGR	Compound Annual Growth Rate
CBS	Central Bureau of Statistics
CSFL	Continued Safe Flight and Landing
CTR	Control Zone
DBI	Davies-Bouldin Index
DES	Discrete Event Simulation
DOD	Depth of Discharge
EASA	European union Aviation Safety Agency
EMS	Emergency Medical Services
eVTOL	electrical Vertical Take-Off and Landing
FAA	Federal Aviation Administration
FATO	Final Approach and Take-off Area
GA	Genetic Algorithm
GIS	Geographic Information System
HLP	Hub Location Problem
HP	Heliport
ICAO	International Civil Aviation Organization
ILP	Integer Linear Programming
ILT	Inspectorate of Environment and Transport
IM	Intensification Memory
IP	Integer Programming
KPI	Key Performance Indicator
LAP	Location Allocation Problem
LMD	Last-Mile Delivery
LVNL	Luchtverkeersleiding Nederland
Mass-GT	Multi-Agent Simulation System for Goods and Transport
MILP	Mixed Integer Linear Programming
MIP	Mixed Integer Programming
MMD	Middle-Mile Delivery

MP	Master Problem
MTM	Medium Term Memory
O-D	Origin-Destination
RTHA	Rotterdam The Hague Airport
SA	Safety Area
SOC	State Of Charge
SP	Sub Problem
STM	Short Term Memory
sUAS	small Unmanned Aerial Systems
TAT	Turn Around Time
TLOF	Touchdown and Lift-Off Area
TSA	Tabu Search Algorithm
UAM	Urban Air Mobility
UAS	Unmanned Aerial System
UAV	Unmanned Aerial Vehicle
UTM	Unmanned Traffic Management system
VLO	Vertiport Location Optimizatio
VNS	Variable Neighbourhood Search
VP	Vertiport

I

Scientific Paper

Multi-Objective Vertiport Location Optimization for a Middle-Mile Package Delivery Framework: Case Study in the South Holland Region

Victor Petit,*

Delft University of Technology, Delft, The Netherlands

Abstract

With the rapidly increasing pace of urbanization and high demand for efficient modes of transport, the Urban Air Mobility (UAM) market has seen a remarkable growth in the past years. This is especially the case for the transportation of goods. Using UAM for cargo operations is likely through operating on Middle-Mile Delivery (MMD) missions to transport cargo between facilities or distribution centers in an operator's network. The efficiency and practicality of such a network are largely affected by the selection of strategic positions for vertiports. As vertiport location optimization is underexplored in current scientific research this paper aims to fill this research gap by developing and analysing a multi-objective optimization model for the placement of vertiports for a middle-mile package delivery system, considering capacity, available land space, safety and noise impact factors. We develop a novel Multi-Objective Multiple Allocation Capacitated p-Hub Coverage Problem framework for an MMD UAM network and test it using the South Holland region as a case study. Notably, the model can easily be converted to other cities. First, to reduce computational efforts, the K-means clustering algorithm is proposed. This is used to divide 6625 zones into a number of K clusters, with each cluster representing a vertiport candidate location. Furthermore, we present a multi-objective Tabu Search based heuristic optimization algorithm to solve the optimization problem. The impact of different factors such as number of clusters, number of vertiports, drone range, maximum safety distance, turn around time and the utilization of existing heliports is assessed.The presented model provides decision-makers with the ability to assess the suitability of a region for the implementation of a UAM MMD system and aids in the identification of potential good locations to set up vertiports. We demonstrate that an increase in the number of vertiports leads to a higher attainable demand coverage, however, this results in a steep drop-off in terms of safety and noise nuisance performance. Furthermore, the results show that an increase in drone range, maximum safety distance or a decrease in turn around time allow for overall better performing vertiport networks. Finally, while the incorporation of heliports in the UAM networks bears large budgetary benefits, the performance in terms of demand coverage, safety and noise nuisance is not optimal.

1 Introduction

The ever-increasing pace of urbanization and the high demand for efficient transportation options have spurred cities into a phase where traditional transportation methods are being redefined. One promising innovation that offers a high potential value is Urban Air Mobility (UAM), which offers transportation options for both passengers and cargo. The momentum in this field is demonstrated by initiatives such as Uber Elevate [1] and Amazon Prime Air [2]. In addition to this, companies such as Zipline have already utilized small Unmanned Aerial Vehicles (sUAV) for the transportation of goods [3].

Currently, existing research focuses on the transportation of people in the form of on-demand transportation or so-called air taxis [4, 5]. In contrast, far less research has been done into the delivery of goods [6]. Furthermore, papers that do consider this business model mainly focus on a last-mile delivery using sUAV, which refers to the segment of the delivery from the final distribution centre or warehouse to the destination of the package. In contrast, very little research exists on the concept of Middle-Mile Delivery (MMD). MMD refers to the delivery segment of the logistics chain between two nodes in an operator's network. For example, the segment of transport from a large warehouse to a more centrally located distribution centre. MMD is an interesting use case for UAM as it has the potential to improve rapid delivery, relieve road congestions and improve accessibility. Furthermore, using drones for MMD could also result in a reduction in operating costs as they do not require manned operations. This research will therefore focus on an MMD concept.

*Msc Student, Sustainable Air Transport, Faculty of Aerospace Engineering, Delft University of Technology

Regardless of the application, the setup of a UAM network imposes a decision-making problem on the positioning of airports for aircraft that take off and land vertically, commonly referred to as vertiports. This is a vital part of setting up a UAM network as the positioning of vertiports can have a large influence on the practicality and efficiency of the system. Moreover, placing vertiports in an urban area is largely affected and constrained by public opinion. According to a study performed by EASA, the main public concerns are safety, (cyber)security, environmental impact and noise pollution[7]. Of these concerns, safety and noise can be taken up in the decision-making process of where to place vertiports as they are highly related to the area surrounding the vertiport. For safety, this entails looking into safety distances and potential hazards that a location poses for drone operations. For noise, it is preferred to place vertiports at locations that already generate high amounts of noise to reduce nuisance. This idea was first proposed by Antcliff et al.[8] suggesting that highways and main roads of the city could function as noise absorption zones caused by the propulsion of the vehicles.

To aid in the decision-making process of placing vertiports for a UAM MMD delivery concept, this work proposes an optimization model that integrates three key metrics: demand satisfaction, safety, and noise. The model serves as a innovative framework to perform an initial analysis on the suitability of setting up an MMD UAM network in any urban environment. As the solution space for the posed problem will be very large, it is proposed to use a meta-heuristic algorithm to efficiently search said solution space. The framework that is proposed for this research builds on the framework of Gunady et al.[6] and the work of German et al.[9] and aims to fill gaps in the existing literature by providing a multi-objective optimization model, considering multiple origin locations (e.g. warehouses) and safety metrics. Furthermore, while the Tabu Search (TS) algorithm has been shown to perform very well for facility location problems as compared to other meta-heuristics such as the Genetic Algorithm (GA) and Simulated Annealing (SA) [10], TS has not been used in a UAM context. Therefore, this work introduces a Tabu Search based heuristic algorithm that can be used for solving multi-objective vertiport location optimization problems. This translates to the following research objective: **To develop and analyze an optimization model for the placement of vertiports for a middle-mile package delivery system, considering capacity, safety and noise impact factors.** The proposed framework is applied to the South Holland region to test it in a use case.

The remainder of this paper is structured as follows. First, section 2 gives an overview of the current state-of-the-art in vertiport location optimization. This is then followed by section 3 which describes the methodology. In section 4, a case study for the South Holland district is presented. This is followed by section 5, which describes the experimental setup. The results are then presented and discussed in section 6 and section 7 respectively. Finally, the conclusions and recommendations are given in section 8.

2 Literature Review

This section aims to present the current state-of-the-art considering vertiport positioning techniques and optimization methods. Vertiport positioning currently is performed in three ways in existing literature. This being through the use of Geographical Information Systems (GIS), the K-means clustering algorithm or by performing vertiport location optimization in an objective-based optimization.

GIS are systems that can be used to capture, analyze and visualize data in a spatial context. In vertiport positioning context, GIS are used to find and select suitable locations for the construction of vertiports. In literature, it has been used to assess factors such as socio-economic variables, points of interest and existing heliports. Fadhill [11] depicted regional suitable areas for vertiports in Munich and Los Angeles subject to constraints on restricted flight zones, military areas and schools. Similarly, Gonzalez [12] uses socio-economic factors in combination with a rooftop footprint and flatness analysis to determine suitable vertiport locations. Kim and Yoon [13] perform a feasibility analysis for UAM applications based on population density and airspace restrictions in San Francisco and New York. Finally, Brunelli et al. [14] create a digital twin of the city of Bologna and use building height, type and obstacle clearances to asses location suitability. While literature using the GIS approach provides great insights into location or region suitability of vertiports, no information can be provided on the UAM network performance as a whole or the application objective efficiency (e.g. demand coverage, cost minimization, travel time minimization).

The second method used in literature for vertiport positioning is the K-means clustering algorithm as described by Schütze et al.[15]. The algorithm aims to group data points into a number of K clusters by minimizing the average squared Euclidean distance between cluster centres and the respective data points. In UAM context, this means that the distance between potential vertiport locations and the origin or destination is minimized for a network with an amount of K vertiports. Due to the nature of this algorithm, it is often used for the optimization of on-demand air mobility networks. Lim and Hwang [16] use the K-means algorithm to choose the

appropriate number of vertiports and their locations based on travel time savings for an on-demand mobility network in the city of Seoul. This is done with the assumption that the closest centroid to the starting and destination points are the arrival and departure points. The downside of using the K-means clustering algorithm is that it starts out with a random initial solution, which has a large influence on the quality of the outcome [17]. Therefore, Rajendran and Zack [18] propose a multimodal transportation based warm start technique, in which they feed an initial solution to the K-means algorithm based on the determined fitness of locations. Similarly, Sinha and Rajendran [19] propose a multi-criteria warm start technique based on socio-economic factors. Although, the K-means algorithm is at the base of some works that provide meaningful insights in vertiport location optimization for air taxi services, it lacks the ability to effectively optimize for objectives other than distance. Consequently, in literature, it is mostly used to identify potentially suitable and favourable vertiport locations for an air taxi network.

Finally, the third vertiport positioning method used in literature is objective based optimization. Generally, Vertiport Location Optimization (VLO) is posed as a type of Hub Location Problem (HLP), which consist of locating hub facilities and designing hub networks so as to optimize a cost- or service-based objective. The first mathematical formulation of an HLP was posed by Campbell [20] which has been adapted for VLO a number of times [21, 22]. Generally there are three types of HLPs. These are the p-hub median problem, the p-hub center problem and the p-hub coverage problem, with the difference being the optimization objective. The median problem aims to minimize the total transportation cost (monetary, time, energy, etc.). The center problem is defined by a Mini-Max criterion which contains the objective to minimize the maximum cost of origin destination pairs in terms of money, time or distance. Finally, the coverage problem tries to maximize the coverage of a network. Due to the fact that the MMD UAM network effectiveness should be assessed, the p-hub coverage problem is the most appropriate type of HLP for the problem at hand. Furthermore, HLPs are also defined by characteristics such as the inclusion of capacity constraints on hubs or flows and whether each destination is allocated to one hub (single allocation) or multiple hubs (multiple allocation).

Similar to the K-means approach, objective based optimization has mainly been used for assessing the benefits of air taxi networks [5, 23, 21, 22]. Holden and Goel [1] propose a clustering algorithm to cluster demand points into candidate vertiport locations, after which facility location algorithm is used to maximize trip coverage. Rath and Chow [22] optimize a vertiport network for demand coverage of air-taxi's formulating it as a ridership maximization problem. While these works pose interesting insights in the general field of vertiport location optimization, they are all focused on the transport of people while considering a single objective. To scale HLPs to larger sizes and use it for an MMD concept, the aforementioned methods should be utilized and integrated into a single model considering multiple objectives.

Therefore, this work proposes to use a combination of all three methods to develop a model that is capable of optimizing and analyzing a UAM network, considering placement of vertiports for middle-mile package delivery whilst considering vertiport capacity, available land space and safety and noise impact factors. Where GIS will be used to analyze zonal characteristics, the K-means algorithm will be used to slim down the solution space and finally, the problem will be solved using a multi-objective Tabu Search based heuristic algorithm to be able to capture Pareto fronts. This framework adds to the existing state-of-the-art in a several ways. It combines a number of existing methods which are then applied to a new concept, being vertiport location optimization for MMD using UAM, which is studied very little in existing literature. It therefore aims to innovate in terms of application. To be more specific, the framework adds to the existing state-of-the-art as it is the first multi-objective vertiport optimization model for MMD. In addition it is also the first framework to consider multiple origin points, vertiport capacity, safety risks and noise nuisance for optimizing vertiport locations in a UAM network for MMD.

3 Methodology

In this section, a vertiport location optimization framework for a middle-mile delivery concept is introduced. First, a brief description of the concept of operations is given in section 3.1. Second, the mathematical model that is implemented is described in section 3.2. Third, section 3.3 provides an overview of the processes that are used in the framework. Next, section 3.4 explains the K-means clustering algorithm and the warm start technique. This is then followed by a description of the demand request allocation algorithm in section 3.5. Finally, the section is concluded by a description of the Tabu Search heuristic algorithm used to find the Pareto fronts in section 3.6.

3.1 Concept of operations and assumptions

To provide a clear overview of the intended system, this section briefly describes the concept of operations that is used to set up a framework. As mentioned, the selected application is a middle-mile delivery system for parcels in an urban environment. In the proposed framework, drones fly with a number of packages from the origin warehouse to a vertiport close to the destination zone of the packages. At the vertiport, the drone lands, is unloaded, and either the battery is swapped or the drone is charged. After this, the drone immediately flies back to its origin warehouse. The vertiport then serves as a distribution centre where packages are temporarily stored. Furthermore, the following assumptions are made:

- The last-mile delivery of the packages that are temporarily stored at a vertiport is done by either courier or self-pickup.
- Warehouses are suitable locations for vertiports. Therefore, drones can directly depart from the warehouse locations.
- Warehouses are assumed to be able to store the entire fleet of drones operating.
- No limit is set on the fleet size of drones.
- At most one vertiport can be placed in each of the zones.
- A vertiport is able to cover an entire zone.
- The geographical centroid of each of the zones, represents the vertiport candidate location accurately enough to be used for any distance calculations.

3.2 Mathematical model

To translate the proposed framework into an optimization problem, a mathematical model is developed. Consistent with existing literature, the problem is defined as a type of Hub Location Problem. The mathematical model provided is based on the works of Maleki et al.[24] and Nickel et al.[25]. The developed mathematical model contains multiple objectives and introduces capacity constraints on the vertiports. Furthermore, as the first objective is to minimize the demand that cannot be served (maximizing the coverage), it is categorized as a p-Hub coverage problem. Finally, due to the fact that multiple vertiports can be used to serve a single destination, it is modelled as an HLP with multiple allocation. Therefore, the complete mathematical model can be categorized as a Multi-Objective Multiple Allocation Capacitated p-Hub Coverage Problem.

3.2.1 Sets and parameters

The mathematical model contains the a number of sets, decision variables and parameters. These are presented below:

Sets

- N: The set of all nodes containing zones and warehouses
- K: The set of selected vertiport locations
- T: The set of vertiport types
- D: The set of origin-destination combinations

Decision variables

- z_k^t: A binary variable which assumes the value of 1 if a hub of type t is located in zone k.
- R_{ij}^k: A continuous variable which can take any value between 0 and 1 representing the fraction of demand shipped from node i to node j routed through a vertiport in zone k

Parameters

- W_{ij}: The demand from origin node i to destination node j
- SH_k: Safety score of vertiport location zone k related to the maximum height of buildings
- SM_k: Safety score of vertiport location zone k related to the mean height of buildings
- SP_k: Safety score of vertiport location zone k related to the population density
- N_k: The noise score of vertiport location zone k related to the maximum speed of cars
- p: The number of vertiports to be located
- v_{ij}^k: A binary variable assuming the value of 1 if a vertiport in zone k is able the cover the journey from origin i to destination j
- Γ_t: The capacity of a vertiport of type t
- s^t: the infrastructural space required for a vertiport of type t
- I_k: The infrastructural space available in zone k
- d: Distance to the closest vertiport or existing heliport
- d_{min}: Minimum distance to an existing heliport and between vertiports

- d_{max}: Maximum distance to an existing heliport or between vertiports to ensure safe emergency landings.
- $A^{operational}$: The aerial space needed for operating a vertiport.
- $A_k^{unrestricted}$: The aerial space available in zone k that is not affected by flight restrictions

3.2.2 Objectives

The framework is set to have three objectives, the first of which is defined by the fact that a hub covering problem is chosen. As shown in Equation 1, it aims to minimize the fraction of demand not served. This objective is chosen in order to be able to assess and reflect on the effectiveness of implementing an MMD concept in an urban environment.

$$\textbf{minimize} \quad 1 - \sum_i \sum_j \sum_k W_{ij} R_{ij}^k \tag{1}$$

The second objective, as shown in Equation 2, minimizes the safety scores of the chosen vertiport locations. This can be seen as the associated risk of implementing a network of vertiports. Three main safety impact variables are selected. The first and second safety variable to be considered relate to proximity to highrise. Placing vertiports near tall buildings raises safety concerns in terms of obstacle hazards, resulting in an enhanced collision risk during critical take-off and landing flight phases. Furthermore, tall buildings are known to disrupt airflow patterns which can create unpredictable wind and turbulence conditions with high wind speeds, which in turn poses safety risks to aircraft. For each of the zones in the network, the maximum and the mean building height are taken and the values are normalized using the min-max normalization method. This results in a maximum height safety score SH_k and a mean height safety score SM_k for each zone. The third safety variable considered relates to population density. Zones with a higher population density are less preferable due to an increased risk of casualties in emergency situations. Similar to the first two variables, the population density of each of the zones in the study area is taken and the min-max normalization method is used to normalize the values.

$$\textbf{minimize} \quad \sum_k \sum_t (SH_k + SM_k + SP_k) z_k^t \tag{2}$$

Finally, the third objective, as given by Equation 3, tries to minimize the nuisance caused by the additional noise that would be generated if a set of k vertiports were to be accepted as a network. For this, the highest maximum speed in a zone is used. This stems from the suggestion that highways and main roads of a city already generate high amounts of noise. Therefore, the additional noise caused by the presence of a vertiport will cause less nuisance [8]. The highest maximum speed is chosen as opposed to the mean due to the fact that most zones also contain a lot of small roads with a very low maximum speed. If the mean were to be considered, there may be zones containing a highway that generates a lot of noise, however, this gets cancelled out by the presence of a large amount of very small roads. Meanwhile, the zone could be a very good vertiport location in terms of noise due to the presence of this large highway. The noise impact variable is also normalized using the min-max normalization method.

$$\textbf{minimize} \quad \sum_k \sum_t N_k z_k^t \tag{3}$$

3.2.3 Constraints

To complete the framework, the main constraints are given in Equations 4-11. Starting of with the first constraint, shown in Equation 4, this constraint ensures that the model selects precisely p amount of vertiports. The second constraint, given by Equation 5, relates to coverage capability. The constraint ensures that a demand flow from node i to node j, can only be routed through a vertiport in zone k if the drone has enough range to fly from node i to the vertiport in zone k and the last-mile distance from the vertiport in zone k to destination j is not too large. The limit on the last-mile distance is also constrained to prevent packages from ending up too far from the their destination, to the point where there is no use in transporting it using a drone. Next, the third constraint, given by Equation 6 ensures that no more flow is routed through the vertiport in zone k than the capacity that it has. The fourth constraint, given by Equation 7 states that a vertiport of type t can only be positioned in a zone if there is enough infrastructural space. Furthermore, the fifth constraint, visible in Equation 8, sets safety distance limits and ensures that a vertiport has a minimum distance to the nearest vertiport and heliport to avoid collision risks. Moreover, it also ensures a maximum distance to the nearest vertiport or heliport, to account for emergency landings if necessary. The sixth constraint, given by Equation 9, ensures that vertiports can only be positioned in zones where the area that is not restricted by no-fly zones is large enough to accommodate for the necessary for flight operations. The constraint given by Equation 10 makes sure that the fraction of demand shipped from node i to j through a vertiport in zone k

can take any value between 0 and 1. Finally, the constraint shown in Equation 11 defines the variables v_{ij}^k and z_k^t to be of binary type. Where v_{ij}^k represents whether a demand request from origin i to destination j can be routed through a vertiport in zone k and z_k^t represents whether a vertiport of type t is placed in zone k.

$$\sum_t \sum_k z_k^t = p \tag{4}$$

$$R_{ij}^k \leq \sum_t \sum_k v_{ij}^k z_k^t \quad , \forall i, j \in N \ \& \ \forall k \in K \tag{5}$$

$$\sum_i \sum_j W_{ij} R_{ij}^k \leq \sum_t \Gamma_t z_k^t \quad , \forall k \in K \tag{6}$$

$$\sum_t z_k^t S^t \leq I_k \quad , \forall k \in K \tag{7}$$

$$d_{min} \leq \sum_t z_k^t d \leq d_{max} \quad , \forall k \in K \tag{8}$$

$$\sum_t z_k^t A_{operational} \leq A_{unrestricted}^k \quad , \forall k \in K \tag{9}$$

$$0 \leq R_{ij}^k \leq 1 \tag{10}$$

$$v_{ij}^k, z_k^t \in \{0, 1\} \tag{11}$$

3.3 Framework overview

Figure 1 shows an overview of the different steps within the framework to determine optimal vertiport locations. The figure shows the necessary inputs for the model, being the zone division, zonal statistics and demand data. Furthermore, the main steps of the framework to get to the desired outputs are also given.

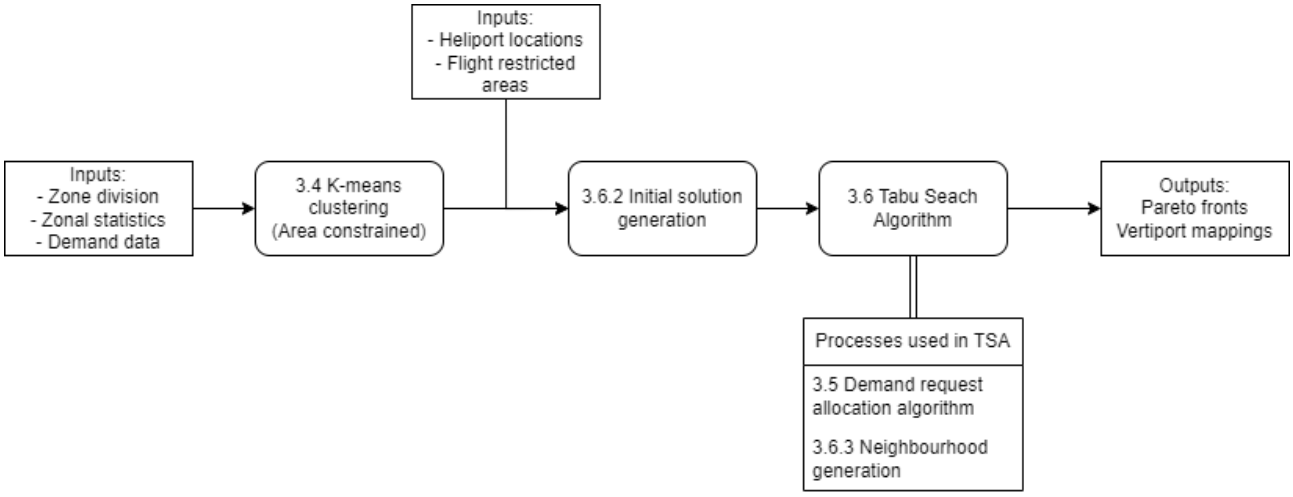

Figure 1: Overview of the vertiport location optimization framework

3.4 K-means clustering algorithm

As HLP problems are generally NP-hard in nature, a clustering algorithm is used to reduce the solution space size. For this, the K-means algorithm is chosen due to its heavy presence in existing literature as discussed in section 2. The K-means algorithm, as first described by Schütze et al. [15], aims to cluster a set of data points into a prespecified K amount of clusters. The different clusters are identified by minimizing the average squared Euclidean distance, also known as the residual square sum of squares (RSS) , between cluster centres and the respective data points. A cluster centre is defined as the mean or centroid μ of cluster ω. The equations to calculate the centroids and the RSS are given by Equation 12 and Equation 13 respectively.

$$\vec{\mu}(\omega) = \frac{1}{|\omega|} \sum_{\vec{x} \in \omega} \vec{x} \tag{12}$$

$$RSS = \sum_{k=1}^{K} \sum_{\vec{x} \in \omega_k} |\vec{x} - \vec{\mu}(\omega_k)|^2 \tag{13}$$

The algorithm starts out with a random selection of the initial centroids as a seed solution. The algorithm then moves the centroids around in space to minimize the RSS iteratvely. In each iteration, the data points are first reassigned to the cluster with the closest centroid, after which the the location of the centroids is

recomputed. A visual representation of the process is shown in Figure 2. This is repeated until the centroids do not change between iterations, indicating that the algorithm has stabilized. To prevent the algorithm from running indefinitely, a second algorithm termination criterion of 1000 iterations is set.

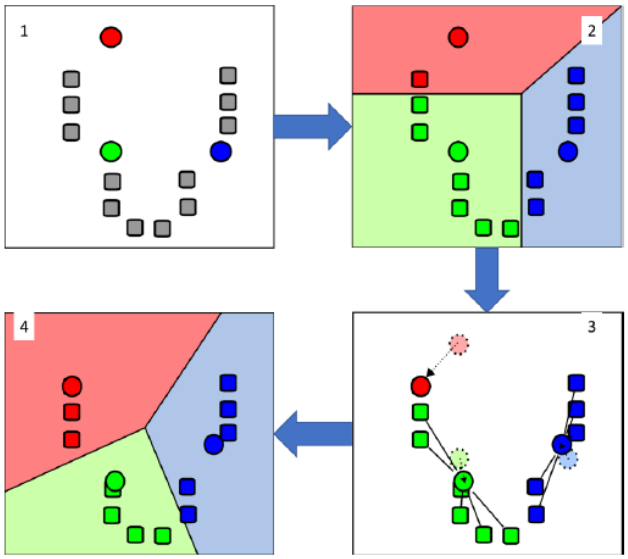

Figure 2: Visual representation of the K-means algorithm in four steps [23]:
1) Initial solution 2) Cluster assignment 3) Recomputation of centroids 4) Reassignment of clusters

3.4.1 Area constraint

As a single vertiport is assumed to cover an entire zone, there is a necessity to set an area constraint on the cluster size in the algorithm. This relates to the fact that with a larger cluster size, one loses a level of detail of the area. For example, for a cluster of six zones that all have a very large area, the assumption that a single vertiport is able to cover that entire cluster does not hold. It is therefore assumed that a cluster may have a maximum area of 100 km^2 such that it maximally covers an area of 10x10 kilometres. This ensures that the last-mile distance within a single zone does not become too large. In addition to this, whereas the centroid of a zone is used for the vertiport location in any distance calculations, this might not be the case in reality. The vertiport can be placed anywhere inside the zone. Therefore if the area of a zone becomes too large, there could be a misconception on the necessary range for drones to reach the vertiport.

3.4.2 Warm start solution

A drawback to the K-means algorithm is that it starts out with a random initial solution, which has a large influence on the quality of the outcome [17]. It is therefore suggested to implement the warm start technique. This entices inputting an initial solution of good quality as a starting point. In the chosen capacity constrained MMD network context, each vertiport has a maximum capacity of packages that can be handled throughout the day. As a result, areas containing a high demand require a greater amount of vertiports to allocate this demand. Therefore, it is chosen to input the K locations with the highest demand as a warm start solution for the K-means algorithm. This will result in a higher amount of clusters centred around areas with high demand, allowing for the possibility of placing more vertiports in those areas.

3.4.3 Clustering score factors

In the clustering process, each of the identified zones and their respective characteristics are added to a cluster. To assign a new score or to compute the metrics for the new clusters, several decisions are made. An overview of the zonal characteristics and the approach for clustering is shown in Table 1. In terms of demand, the origin-destination pairs are adjusted to fit the new clustered zones. Although the origin locations stay the same, destinations are now inside a cluster, resulting in a reduction of origin-destination pairs. For the safety score, three characteristics are clustered. These are the maximum building height, the mean height and the population density. For the maximum height, the absolute maximum height of the new zone is used as this characteristic is meant to look at the peak value. For the mean height, the mean of all zones within the cluster is taken. Furthermore, the population density is recalculated for the new zones. In terms of noise, the maximum car speeds of the zones are averaged and set as the value for the new cluster. This is done to compensate for situations where a cluster contains zones with highways as well as zones with residential areas, which are

on opposing ends of the spectrum in terms of noise nuisance. The flight restrictions, which are introduced in the model as unrestricted flight areas, are recalculated for the clusters. Finally, for the available infrastructure space, the highest category of the zones in a cluster is chosen.

Table 1: Zone characteristics clustering approach

Characteristic	**Clustering type**
Demand	Assign demand from zones to according cluster
Safety - Maximum Height	Find maximum height of all zones and assign to cluster
Safety - Mean Height	Average the mean height of all zones and assign to cluster
Safety - Population Density	Recalculate population density for new clusters
Noise - Maximum car speed	Find the average of the maximum car speed of zones and assign to cluster
Unrestricted flight area	Recalculate unrestricted flight area for new cluster
Infrastructure space	Find highest category of infastructure space and assign to cluster

3.4.4 Adapted algorithm

The resulting K-means algorithm with the aforementioned adaptations due to the considered application is shown in algorithm 1.

Algorithm 1 Adapted K-means algorithm

Input: Set of all zones Z (zone_number, centroid $\vec{x_z}$, demand), Number of clusters (K)
Output: Cluster assignment label (ω_z) for each of the zones, Set of zones assigned to cluster k (ω_k),
Set of cluster centroids ($\vec{\mu}$)
Function:
Initial centroids $\vec{\mu}$ = K nodes with largest demand
while Stopping criterion is not met **do**
  for z = 1 to Z **do**
    Assign closest cluster to zone $\omega_z = argmin|\vec{\mu} - \vec{x_z}|$
    for k = 1 to K **do**
      Calculate cluster areas A
    while any A_k **in** $A > 100km^2$
      Move centroids of clusters with too large area towards point in cluster closest to average area of cluster
      $\mu_k^{\vec{new}} = 0.5(\mu_k^{\vec{old}} + \vec{x_{avg}})$
      Assign closest cluster to zone $\omega_z = argmin|\vec{\mu} - \vec{x_z}|$
      Recompute cluster areas A
    for k = 1 to K **do**
      Recompute centroids $\vec{\mu_k} = \frac{1}{|\omega_k|} \sum_{\vec{x_z} \in \omega_k} \vec{x_z}$

3.5 Demand request allocation algorithm

There are two factors that influence the demand objective score as presented in Equation 1 in section 3.2.2. These are the set of vertiports that is selected as a solution and the allocation of demand requests. To be able to compute the demand objective score of a given solution, the given demand requests, consisting of an origin-destination pair and the parcel demand, need to be assigned to a vertiport. The allocation strategy chosen for the proposed framework is to select the closest vertiport to the destination zone, that lies within the selected drone flight range of the origin warehouse, subjected to capacity constraints. This is done under the assumption that it is preferred to use the flight mode of transport as much as possible. This assumption is in line with the goal of the MMD concept to relieve road congestion and improve rapid delivery. The demand request allocation algorithm that is developed, following this assumption, is shown in Figure 3. The algorithm takes the selected vertiports (VPs), their types (for capacity) and the demand requests as inputs and outputs the associated percentage of demand served.

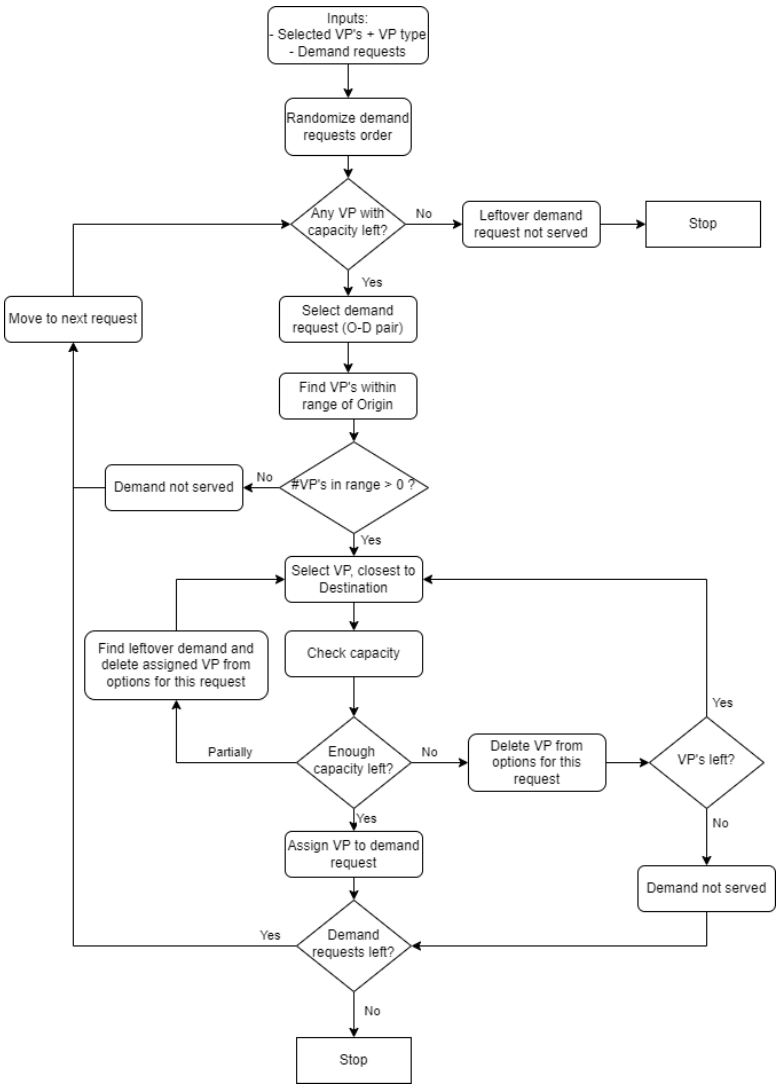

Figure 3: Demand request allocation algorithm

3.6 Tabu Search Algorithm

Due to the high complexity of the problem and its large solution space, it is not possible to try all possible solutions. Therefore, the solution space should be searched in an efficient manner to find a near-optimal Pareto front. Following the identified research gaps, a Multi-Objective Tabu Search Algorithm (TSA) that can be used for the proposed framework is developed. The TSA that is used, is based on the work of Jaeggi et al. [26]. First, a description of the memories that the algorithm uses is given. Next, an algorithm to find an initial feasible solution is presented. This is followed by the set-up of the neighbourhood structure. Finally, the section concludes with a description of the different moves that the algorithm can perform in the solution space and an overview of the entire algorithm.

3.6.1 Algorithm memories

To capture the Pareto front and efficiently explore the solution space, the algorithm works with three types of memories. These are the Short Term Memory (STM), the Medium Term Memory (MTM) and the Intensification Memory (IM). The STM stores the points that are visited by the algorithm and may not be revisited, commonly referred to as the tabu list. The MTM stores the optimal solutions that are found and is used to restart the search, following a diversification that yields no good solutions. Finally, the IM is used to store optimal or near optimal solutions, that are not selected to be the new current solution at the end of an iteration step. Furthermore, a local iteration counter i_{local} is used to define the algorithm's ability to intensify, diversify or restart the search.

3.6.2 Initial solution generation

Due to the amount of constraints that are taken up in the model, a feasible solution is not simply found by selecting a random set of p vertiports and checking whether or not it results in a feasible network. Therefore, an algorithm to find a feasible initial solution is proposed. This is shown in Figure 4. The algorithm aims to construct a feasible set of vertiports by first randomly selecting a vertiport that is in the maximum safety distance range of a heliport, after which candidate vertiports are selected and only added if they adhere to the constraints. A runtime restart is added to prevent the algorithm from running infinitely in case no feasible vertiport can be added to the constructed solution. If this is the case, the solution that is constructed so far is deleted and the algorithm starts with the construction of a completely new solution.

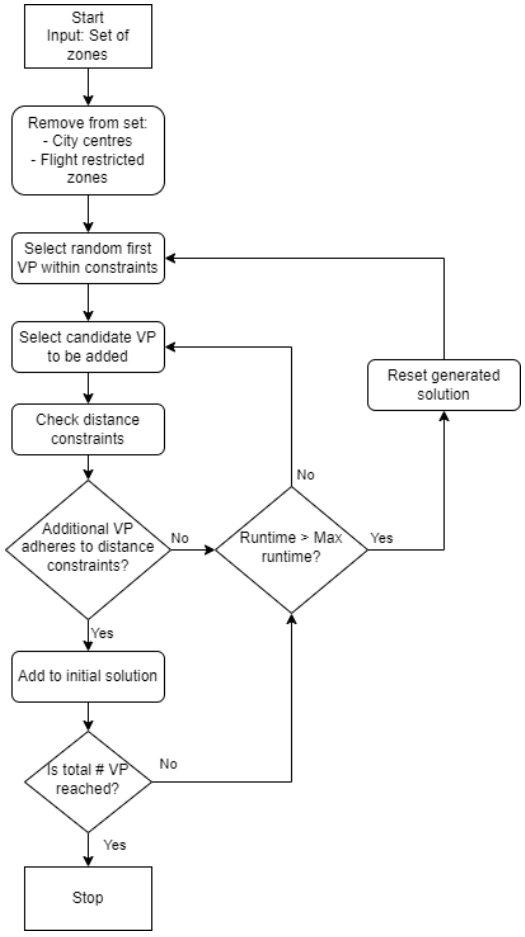

Figure 4: Initial solution generation algorithm

3.6.3 Neighbourhood structure

The proposed TSA searches the solution space by checking a set number of solutions in the neighbourhood of the current optimal solution. As, for this specific problem, a solution consists of a set of p feasible vertiport locations, the neighbourhood can be constructed by making a small adjustment to the current solution. Similar to the work of Skorin-Kapov and Skorin-Kapov [27], a neighbouring solution is defined to be any feasible solution whose set of vertiports differs in exactly one node from the set of vertiports of the current solution. Additionally, to prevent duplicate solutions, for the complete neighbourhood, a constraint is added that ensures no two solutions in the neighbourhood may consist of exactly the same set of vertiports.

3.6.4 Algorithm moves & overview

To search the solution space efficiently, the algorithm is able to perform three types of moves, being intensification, diversification and restarts. Each of these moves is performed when a user specified value of the local iteration counter i_{local} is reached. The local iteration counter is reset when a new solution is added to the MTM, indicating that the part of the solution space that is currently being exploited yields promising solutions. If no new solution is added to the MTM, the local iteration counter updates its value. The first type of move that is activated by the local iteration counter is the intensification. At each iteration, the objective scores of each of the solutions in the neighbourhood are computed. Naturally, due to the model having multiple objectives,

as shown in equations 1-3, more than one of the solutions in the neighbourhood may be Pareto equivalent. Of these found optimal solutions, one is selected to be added to the MTM and accepted as the new current solution which the algorithm moves on with. However, it is a waste to discard the other Pareto equivalent solutions. These are therefore stored in the IM and used for the intensification move. After a set amount of local search iterations yielding no better solutions or Pareto equivalent solutions as compared to the ones that are currently stored in the MTM, an intensification move is performed. This entails, randomly selecting one of the points stored in the IM and using it as the new current solution. This results in a search in an area that seemed promising at an earlier stage in the search. If the intensification yields no promising solutions, a diversification is performed. This is done to search for new promising areas in the solution space. For the diversification move, the algorithm selects a new random point in the solution space and continues to search in the neighbourhood of this new solution to escape from local optima. In the case that the diversification does not provide promising solutions after a set amount of local iterations, a restart move is performed, meaning that the algorithm returns to one of the solutions in the MTM and continues its search in that part of the solution space. Finally, if no better solutions than the current are found in the neighbourhood and the local iteration counter does not trigger an intensification, diversification or restart, one of the neighbourhood solutions is randomly selected as the next current solution. This is referred to as a downhill move which helps to escape local optima.

To provide a clear overview, a flowchart diagram of the used adapted multi-objective TS algorithm is shown in Figure 5.

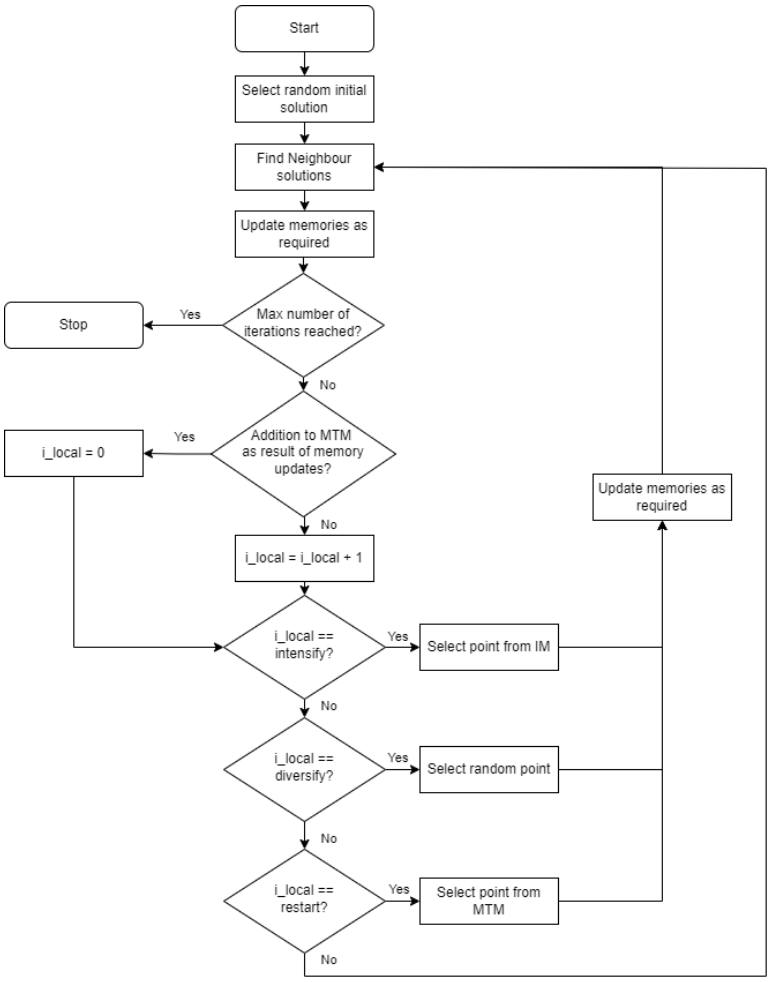

Figure 5: Adapted Multi-Objective Tabu Search Algorithm [26]

4 Case Description: South Holland region

After the description of the methodology, this section introduces the use case that is selected for this study. This is done so by a description of the study area, a description of the data that was collected and used for the model and any adaptations in the model that have to be introduced as a result of the selected study area.

For this case study, the South Holland region was chosen for several reasons. First of all, with about 3.8 million inhabitants, the province of South Holland has the largest population of all provinces in the Netherlands. Naturally, this results in a high demand for packages making it an interesting region to implement an MMD system in. Furthermore, South Holland presents a complex urban environment that contains both large cities with tall buildings as well as flatter areas of land and industrial areas such as the Maasvlakte. Moreover, the port of Rotterdam is working on the implementation of a U-space airspace [28], enhancing the interest of an MMD concept using UAM in the area of Rotterdam. Finally, data on the demand for packages is readily available in the South Holland region through the release of the Mass-GT model [29]. The Mass-GT data contains a division of the study area into a number of 6625 zones. Furthermore, the data contains 29 warehouses from several parcel delivery operators in the Netherlands. The combined demand of all warehouses is 242866 packages for a single day in 2016, which are divided up into an amount of 30168 origin-destination pairs with each their own demand value.

The selected case study imposes several constraints on the model, the first of which is the introduction of flight restrictions. The Dutch government has a set of restricted flight zones for the usage of drones. This is an aspect that should be considered when selecting suitable locations for vertiports. One major flight restricted area is caused by the presence of Rotterdam The Hague Airport (RTHA). Within the control zone of the airport, no drone flight is permitted. As this control zone covers most of the South Holland region containing high demand, it is assumed that arrangements can be made with RTHA to permit drone flight within this zone. Nevertheless, the South Holland region also contains restricted flight zones due to the presence of vital infrastructure and existing heliports. These flight restrictions are taken up in the model, constraining the feasible solution space.

A second constraint that the area of study introduces is the available infrastructure space. For this, a basic assessment is made of each of the 6625 zones using aerial pictures. The resulting estimated area is categorized into four categories being: no space, a small amount of space, a large amount of space and a very large amount of space. This is, in turn, used for capacity estimations. A further explanation of the spatial analysis is given in Part III, Supporting Work, Chapter 2.

The final additional constraint to the model relates to the presence of the city centre of Rotterdam and the city centre of The Hague, which are the two most populous cities in the province of South Holland. The constant presence of a large amount of people in these two city centres causes an increase in the risk of casualties in case of emergencies. Therefore, these areas are deemed as not being suitable for the placement of vertiports and introduce a constraint to the model.

5 Experimental Setup

In this section, the experimental setup for our case study is described. The case, as described by section 4, is used as a base for the experiments. First, the independent variables and control variables are defined accompanied by the rationale. This is followed by a description of the six experiments that are performed.

5.1 Independent Variables

As a setup for the experiments, the following independent variables are selected and varied during the experiments:

- **Cluster amount K**: The number of clusters that are used in the K-means algorithm. Three different amounts of clusters are used, being 500, 1000 and 2000.
- **Amount of vertiports**: The exact number of vertiports that are placed to construct the UAM network. Four different vertiport amounts are used, being 10, 25, 50 and 100.
- **Drone range**: The range that the used drones are able to fly from a warehouse to the destination vertiport. Four different drone ranges are used, being 20, 30, 40, and 50 kilometres
- **Maximum safety distance**: The maximum distance between vertiports or between a vertiport and an existing heliport to accommodate for diversions in emergency situations. Four maximum safety distances are used, being 5, 10, 15 and 20 kilometres.
- **Turn around time (TAT)**: The turn around time of a drone landing at a vertiport dropping of its payload and recharging or swapping batteries. Four values of TAT are considered, being 5, 10, 15 and 20 minutes.

5.2 Base settings and control variables

For the experimental setup, the base scenario and several control variables are defined. The base settings of the independent variables are shown in Table 2. The drone range is based on the Draganfly Heavy Lift cargo drone which has a range of 30 kilometres and a maximum payload of 30 kg. This drone is chosen as it is readily available and has a relatively high payload capacity. In terms of flight range, the drone has a medium performance as compared to other drones with lower payload capacities. While there are drones that can fly for around 60 kilometers such as the Blowfish A2G [30], these drones offer far lower payload capacities which might not be optimal for an MMD concept. Furthermore, for the Turn Around Time (TAT), the worst-case scenario is assumed resulting from found values for eVTOL-based operations in existing literature [31]. This resulted in a TAT of 20 minutes. Furthermore, it should be noted that the same initial solution is taken for all experiments. As the initial solution determines the starting point in the solution space, each experiment is then set to start searching at the same location. This is done to negate the effects of sensitivity of the framework to the initial solution.

Table 2: Base settings used for experiments

Input	**Value**
Number of clusters K	1000
Number of vertiports p	25
Drone range	30 [km]
Maximum Safety Distance	10 [km]
TAT	20 [min]

Next to the base settings of the independent variables, several control variables are defined for the model. In Table 3, the physical control variables and their respective values are shown. The minimum safety distance is based on the approach/departure surface specified by the heliport design and prototype vertiport design specifications of EASA [32, 33]. Similarly, the minimal available airspace is also based on these specifications, which state that both the approach and the departure surfaces need to be 1220 metres long and have a width of 152 metres, therefore, resulting in a total needed area of 0.37088 $[km^2]$. Furthermore, an average package weight of 2.5 $[kg]$ is assumed resulting in a drone capacity of 12 packages. Moreover, the hours of operations of the UAM network are assumed to be the same as regular working hours, being from 9:00 to 17:00. Following these assumptions capacity estimations were made for the vertiports. These estimations are based on the amount of drones a vertiport is able to handle throughout the span of one day. As a drone is set to have a capacity of 12 packages, the capacity of a vertiport is determined by multiplying the maximum amount of drones a vertiport can handle by the drone capacity. For small, medium and large vertiports, the vertiports are assumed to be consisting of 1, 4 and 16 pads respectively. This results in the capacities as shown in Table 3. As quite some of these control variables are based on assumptions, ideally, the values of these should also be varied. However, due to time restrictions, they are set as control variables as the chosen independent variables are deemed to be of more interest.

Finally, Table 4 shows the control variables related to the TS algorithm. The neighbourhood size determines the amount of solutions that are generated and tested at each iteration. An increase in the neighbourhood size results in searching a larger part of the solution space. While this seems beneficial, the neighbourhood size is limited by the computational power that is available. The STM size is set to be three times the size of the neighbourhood, to prevent the algorithm from returning to recently visited points for at least three iterations. This is done to ensure that the algorithm keeps exploring new parts of the solution space. Furthermore, each of the experiments is run for 4000 iterations due to computational limitations. The combination of 4000 iterations with a neighbourhood size of 50 results in testing 200.000 solutions. This is deemed to be sufficient to result in reasonable quality of results to identify relations between the independent variables and the model objectives as the results tend to stabilize when further increasing the number of iterations. Running the model with 6000 iterations showed no significant differences in terms of the solutions and relations found. Further details on this decision are given in Part III, Supporting Work, Chapter 3. Finally, i_{local} intensify, diversify and restart describe at which value of the local iteration counter i_{local} the algorithm performs an intensification, diversification or restart move.

Table 3: physical control variables

Input	Value
Minimum Safety Distance	2440 $[m]$
Maximum Last Mile Distance	10 $[km]$
Minimal available airspace	0.37088 $[km^2]$
Maximum cluster area	100 $[km^2]$
Max drone payload	30 $[kg]$
Drone capacity	12 packages
Vertiport working hours	9:00 - 17:00
Capacity of small vertiport Γ_{small}	288 packages/day
Capacity of medium vertiport Γ_{medium}	1152 packages/day
Capacity of large vertiport Γ_{large}	4608 packages/day

Table 4: Tabu Search Algorithm control variables

Input	Value
Neighbourhood size	50
STM size	150
Number of TS iterations	4000
Value of local iteration counter i_{local} for intensification	10
Value of local iteration counter i_{local} for diversification	15
Value of local iteration counter i_{local} for restart	50

5.3 Experiment A: Amount of clusters K

The first experiment relates to the selection of the amount of clusters K in the K-means algorithm. Varying the amount of clusters in the K-means algorithm has the benefit of being able to make a trade-off between detail and computational efficiency. As the HLP that is considered has a very large solution space compared to other HLP problems, it is computationally beneficial to reduce this solution space by simplifying the problem in order to get faster results. However, reducing the number of clusters comes at the cost of losing detail with respect to selecting suitable zones, as a single vertiport is then considered to cover a larger area of land. As a result, the ability to select a very specific area as vertiport location is lost. It is expected that this will also lead to a decrease in safety and noise performance as these factors are now rated over a larger area. Therefore, detail is also lost in the fact that the algorithm is not able to pick very specific areas that perform particularly well in terms of safety and noise nuisance. In terms of demand, while this is also clustered, due to the warm start solution most areas containing high demand will still have a large number of zones present and therefore candidate vertiport locations. It is therefore expected, that varying the amount of clusters will not have a large impact on the demand that can be served. This first experiment aims to select a suitable amount of clusters by making a trade-off between the detail (the highest level of detail is preferred) and the computation time that it takes to run an experiment for the set level of clusters. This is tested using 500, 1000 and 2000 clusters. The results are presented in section 6.1. The following hypotheses are set.

- H_{A1}: An increase in the amount of clusters will have a negligible effect on the demand that can be served.
- H_{A2}: An increase in the amount of clusters will improve safety scoring.
- H_{A3}: An increase in the amount of clusters will improve noise scoring.
- H_{A4}: An increase in the amount of clusters will result in an increase in computation time.

5.4 Experiment B: Amount of Vertiports

The second experiment relates to the selection of the amount of vertiports that are placed to construct the UAM network. While the proposed framework does not consider the cost of operating or building vertiports, in reality, this factor will have a large influence on the implementation of the network. For a larger number of vertiports, the construction and operating costs will be higher. A useful insight that the proposed framework may provide is therefore to look at the relation between the amount of vertiports that are placed and the demand that could be served with such a network. This can help with the decision of whether or not it is worth to implement an MMD UAM network with a select amount of vertiports. Furthermore, having to place a larger amount of vertiports, will also influence the noise and safety scores as the model might have to resort to placing vertiports in zones that do not perform well in terms of safety and noise. Therefore, it is expected that an increase in vertiports will result in worse performing networks in terms of safety and noise. Finally, it is expected that an increase in the amount of vertiports will increase the computation time due to the fact that this results in a more complex network with a larger number of options to allocate demand requests. The influence of the vertiport amount on these factors is tested using 10, 25, 50 and 100 vertiports. The results of this second experiment are presented in section 6.2. The following hypotheses are tested.

- H_{B1}: An increase in the amount of vertiports will increase the demand that can be served.
- H_{B2}: An increase in the amount of vertiports will worsen safety scoring.
- H_{B3}: An increase in the amount of vertiports will worsen noise scoring.
- H_{B3}: An increase in the amount of vertiports will raise the computation time.

5.5 Experiment C: Drone range

The third experiment takes the drone range as the variable of interest. For the base scenario, the draganfly heavy lift drone is used. This drone has a range of 30 km. The effectiveness of a UAM network is largely

influenced by the drone range as with a smaller drone range, less remote areas can be reached and vertiports will have to be placed closer to the origin locations. Therefore, it is expected that a higher demand coverage can be obtained for an increase in drone range. Additionally, lower drone ranges restrict the model from finding locations that are more suitable in terms of safety and noise. As a result, it is expected that increasing the drone range will lead to improved solutions in terms of safety and noise. While the base scenario takes an existing drone, future innovations will likely lead to the ability to use drones with higher ranges. The aim of this experiment is therefore to see the effect of an enhanced range on vertiport placement. Furthermore, a lower value of range is also tested to see the influence of selecting a drone with a smaller range, which might be cheaper. For the experiment, four values of drone range will be tested, being 20, 30, 40 and 50 [km]. The results of the experiment are presented in section 6.3 and the following hypotheses will be tested.

- H_{C1}: An increase in the range that drones can fly will increase the overall demand that can be served.
- H_{C2}: An increase in the range that drones can fly will improve the safety scoring.
- H_{C3}: An increase in the range that drones can fly will improve the noise scoring.
- H_{C4}: An increase in the range that drones can fly will have a negligible impact on the computation time.

5.6 Experiment D: Maximum Safety Distance

The maximum safety distance between vertiports is of the essence to provide safe diversion possibilities in case of emergencies. With safety being the main public concern when it comes to implementing a UAM network [7], this metric is of great interest. While a minimum safety distance between vertiports can be concluded from the vertiport design specification prototype [33], there is no given maximum safety distance. As it is expected that regulations on the maximum safety distance will be set for the design of a UAM network, it is of interest to analyze the effect that this distance has on the network. Having a lower maximum safety distance is expected to result in a denser network of vertiports, which in turn could have a negative effect on the demand served, noise and safety score. In terms of model performance, a lower safety distance results in a more constrained problem, making the solution space smaller which might result in more computation time due to the fact that it is harder to construct feasible solutions. The effects of varying the maximum safety distance are tested for four distances, being 5, 10, 15 and 20 [km]. The results of the experiment are presented in section 6.4 where the following hypotheses will be tested.

- H_{D1}: An increase in maximum safety distance will increase the demand that can be served.
- H_{D2}: An increase in maximum safety distance will improve safety scoring.
- H_{D3}: An increase in maximum safety distance will improve noise scoring
- H_{D4}: An increase in maximum safety distance will decrease the computation time.

5.7 Experiment E: Turn Around Time

The fifth experiment relates to the TAT of drones after arrival at the destination vertiport. This mainly affects the vertiport's maximum capacity and therefore the demand that can be served. This is of interest as it provides insights into the added benefits of optimizing ground processes. This could aid in decision-making on investments to improve ground operations at vertiports. For the experiment, four different values of TAT were taken, being 5, 10, 15 and 20 minutes respectively. The results are presented in section 6.5 where the following hypotheses are tested.

- H_{E1}: An increase in turn around time will decrease the demand that can be served.
- H_{E2}: An increase in turn around time will have a negligible impact on safety scoring.
- H_{E3}: An increase in turn around time will have a negligible impact on noise scoring.
- H_{E4}: An increase turn around time will have a negligible impact on the computation time.

5.8 Experiment F: Utilizing existing heliports

The final experiment aims to assess utilizing the infrastructure of existing heliports as vertiports. Using pre-existing heliports has the benefit that only minor changes would have to be made to accommodate for drone operations [34]. As a result, the initial setup costs for implementing a UAM network are less which is generally preferable. This sparks the interest to research the effects of establishing the five heliports in the study area as a base for the vertiport network and only accepting solutions in which all five of these heliports are used as vertiports. The aim of this experiment is therefore to research this influence. It should be noted that the utilization of a heliport as a vertiport results in a large amount of drone movements as compared to only helicopter operations. The addition of drone operations will cause additional noise nuisance and safety concerns. Therefore, it is chosen to use the scoring factors of the areas in which the heliports are situated to assess the fitness of these locations as vertiports. As the heliports might not be optimal locations in terms of the model

objective scores and constrain potential optimal solutions, it is expected that the implementation has a negative impact on all three objective scores. This leads to the following hypotheses.

- H_{F1}: Using existing heliports as a setup for the vertiport network will have an impact on the demand that can be served.
- H_{F2}: Using existing heliports as a setup for the vertiport network will have an impact on the safety scores.
- H_{F3}: Using existing heliports as a setup for the vertiport network will have an impact noise scores.
- H_{F4}: The impact of using existing heliports as a setup for the vertiport network will decrease as the number of vertiports increases.

6 Results

This section aims to present the results that are acquired for the experiments that are described in section 5 and to evaluate the effects of varying conditions on the proposed MMD delivery framework. The section is divided into six subsections with each one presenting the results of a single experiment.

6.1 Experiment A: Amount of clusters K

The aim of the first experiment is to select a suitable amount of clusters K to group the total of 6625 zones into. This breaks down to a trade-off between the computation time that is required versus the level of detail that is used for the optimization. It was found that the resulting Pareto fronts are very similar in behaviour, however, they are shifted with respect to safety and noise. This is best illustrated by plotting the Pareto fronts considering noise and safety as shown in Figure 6. It becomes evident that there is a correlation between the amount of clusters and the noise and safety scores that are obtained. Generally speaking, a higher number of clusters causes better safety and noise scores, resulting in a downward left shift of the Pareto front. This trend could be attributed to the fact that a lower amount of clusters results in more generalized noise and safety scores for each zone. This means that there will be fewer zones scoring very well on these factors and that the average noise and safety score for zones is higher.

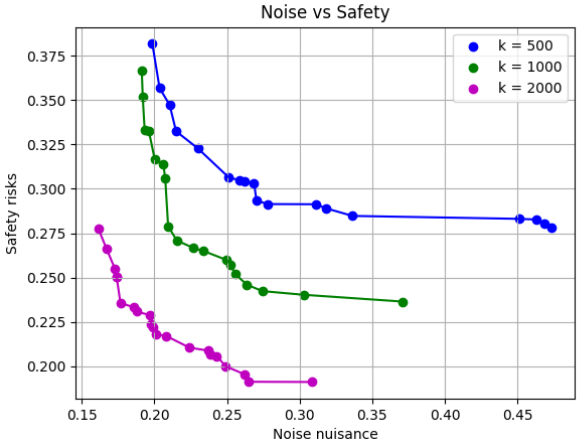

Figure 6: Paretofronts of Experiment A only considering Safety and Noise

Figure 7 shows boxplots of all objective values that are stored in the Pareto front for the demand, safety and noise objectives respectively. It is observed that the found demand scores behave somewhat similarly in the sense that the best found value of demand is the same for all three values of K. In contrast, the worst accepted demand value differs throughout the different cluster amounts which is a result of the difference in obtained safety and noise scores. From boxplot b, it can be deduced that the amount of clusters strongly affects the optimal safety scores found in the Pareto front. While a similar relation can be argued for the noise scores, the strength of this relation seems to be less as compared to the safety objective. This can be explained by the fact that the safety score consists of three factors that are generalized while only one factor is considered for the noise scoring. As as result, the clustering process will have a larger effect on the safety scores.

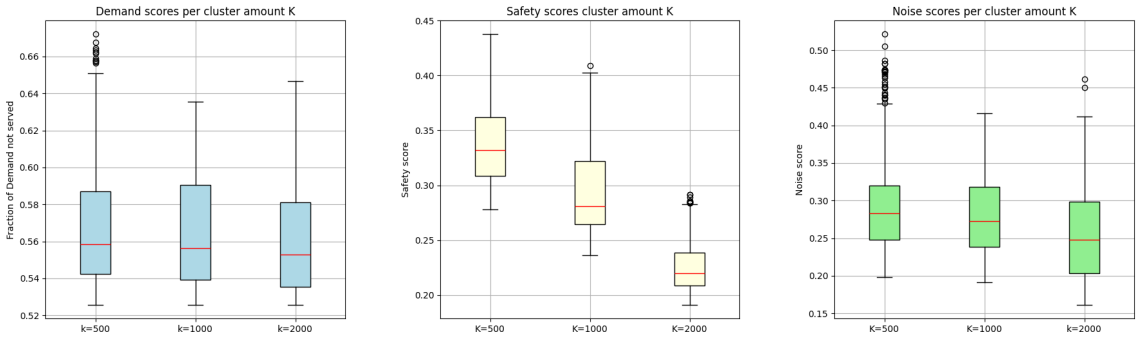

(a) (b) (c)

Figure 7: Boxplot of collected objective score from the Pareto front: (a) Fraction of demand not served (b) Safety (c) Noise

To assess the hypotheses H_{A1}, H_{A2} and H_{A3} the Kruksal Wallis significance test is used for determining whether or not there is a significant difference in the scores found for the three objectives. The p-values that are found are shown in Table 5. With a significance level of $\alpha = 0.05$, it is found that there is a significant difference in all three categories. Therefore, H_{A1} is rejected, and H_{A2} and H_{A3} are both accepted. It should be noted that while there is a significant difference in the demand scores that are found, the optimal demand values for all three values of K are equal, indicating that the difference is mainly caused due to Pareto equivalent solutions that perform better in either the safety or noise objectives.

Table 5: Kruksal Wallis significance test p-values

Objective:	**Demand**	**Safety**	**Noise**
p-value	4.88 E-3	2.38 E-188	3.65 E-16

In terms of computation time, it can be seen in Figure 8, that a higher number of clusters results in significantly larger computation times. It is found that for an amount of 2000 clusters, the computation time it takes to run an experiment is just short of 15 hours, whereas it takes 4.4 hours to run an experiment with 500 clusters. Ideally, to obtain maximum detail, experiments should be run with the highest number of clusters possible. However, as this work mainly serves as a proof of concept, it is chosen to use 1000 clusters due to time restrictions. Due to the evident relation between the number of clusters and the computation time, H_{A4} is accepted.

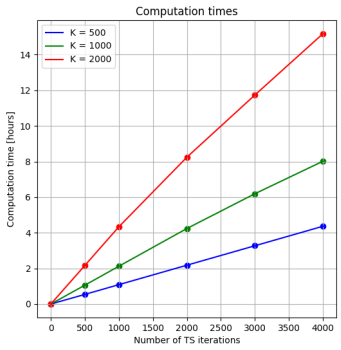

Figure 8: Computation times as a function of of iterations

6.2 Experiment B: Amount of Vertiports

As described in section 5.4, the second experiment relates to the impact of changing the amount of vertiports with respect to the objective scores as well as the computational effort. The resulting Pareto fronts that are found are shown in Figure 9. Furthermore, the best score found per objective can be seen in Table 6. From the obtained results it becomes evident that there is a strong relation between the amount of vertiports and the demand served. Whereas, with a total of 10 vertiports, 81% of all package demand can not be served, this total decreases drastically as more vertiports are placed, with the system not being able to serve only 9.8% of

all package requests when using 100 vertiports. This result is as expected since, naturally, a network containing more vertiports will be able to reach more areas and has a higher total capacity. Furthermore, it is observed that the best solutions in terms of safety risks and noise nuisance, degrade linearly with an increase in demand coverage as caused by the increase in the number of vertiports. One interesting result that can be seen in the Pareto fronts is that, with an increase in vertiports, the model tends to find more Pareto equivalent solutions that score very well in terms of demand, however, a lot worse in safety and noise. This is indicated by the upward right shift of the Pareto front as the number of vertiports increases. An explanation for these results could be that, with an increase in vertiports, the model is forced to pick some locations that perform worse in terms of these objectives. In combination with the fact that the increase in vertiports opens up the model to finding more solutions that score very well in terms of demand, this results in an expansion of the Pareto front towards networks that have a high percentage of demand served. In general, the zones that are selected often in solutions for a smaller amount of vertiports, are also selected often when increasing the amount of vertiports. Therefore, the increase of vertiport results in an expansion from existing networks that are found for a small amount of vertiports and not necessarily finding completely different solutions. In addition, it is found that the zones that are often are centered around areas that contain a particularly high demand, being the South East, North East and near large cities.

Table 6: Best scores per objective

	Best score found per objective		
	Demand not served	**Safety risks**	**Noise nuisance**
10 VP's	81.0 %	0.134	0.087
25 VP's	52.6 %	0.236	0.191
50 VP's	17.7 %	0.310	0.262
100 VP's	9.8 %	0.354	0.320

Table 7: Computation time per vertiport amount

	Computation time [s]
10 VP's	25337
25 VP's	25968
50 VP's	27113
100 VP's	28232

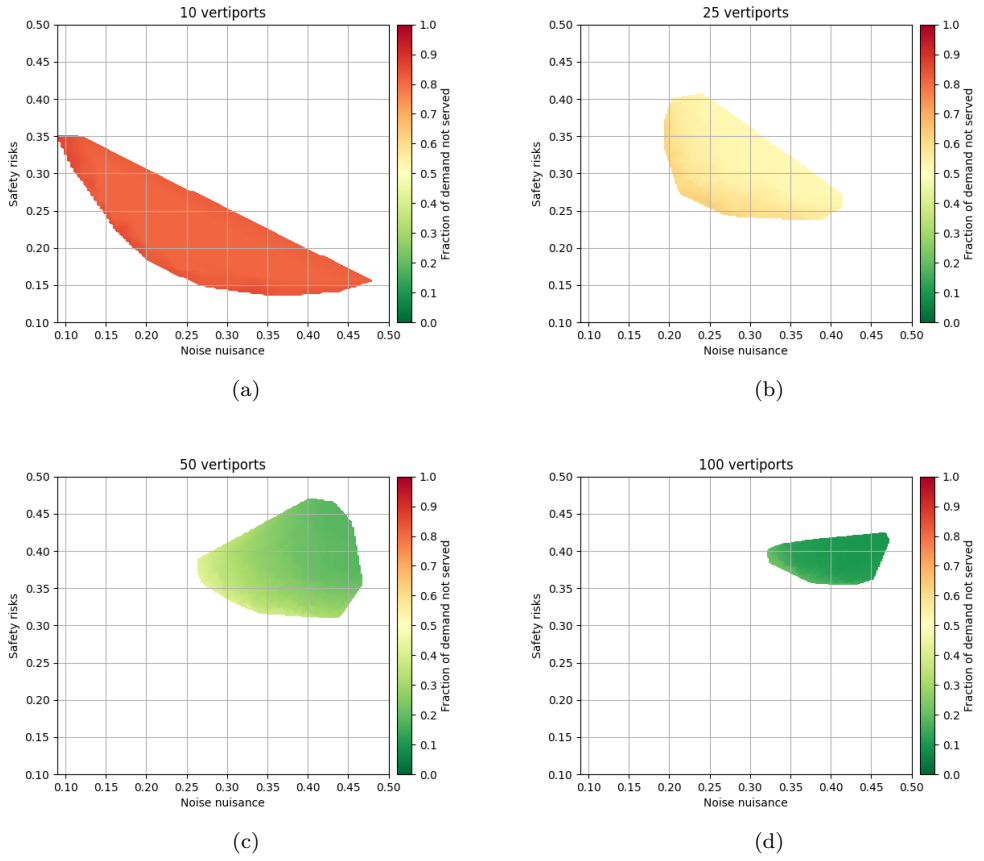

Figure 9: Pareto front considering a UAM network with: (a) 10 VPs (b) 25 VPs (c) 50 VPs (d) 100 VPs

When plotting the Pareto fronts while only considering noise and safety objectives, such as shown in Figure 10, the drop-off for noise and demand scores with an increased amount of vertiports can be seen even more evidently. Next to the negative correlation between the amount of vertiports and safety and noise scores, it is also visible that the Nadir points on the Pareto front, which are the two outer points, move towards each other as the

number of vertiports increases. This indicates a reduction in variability between the found solutions in terms of noise and safety scores. This is a logical result as an increased amount of vertiports results in a smaller solution space and noise and safety scores that are naturally closer together.

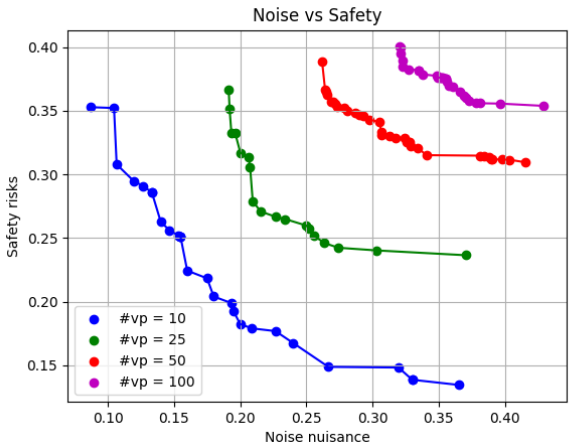

Figure 10: Paretofronts of Experiment B only considering Safety and Noise

Finally, Table 7 shows the computation time necessary to run the algorithm for 4000 iterations for each of the vertiport amounts. It is observed that the computation time has a positive relation to the amount of vertiports with the smallest amount of vertiports taking about 7 hours and the largest amount 7.8 hours. While this is acceptable for the set number of 4000 iterations, it is important to note that computation time increases linearly with the number of iterations. Therefore, when extending the program runtime to obtain better solutions, the increased computation time should be taken into account.

To strengthen our claims and either reject or accept the set hypotheses in section 6.2, a Kruksal Wallis statistical test is performed with a significance level of $\alpha = 0.05$ on each of the sets of objective values found. As the found objective scores are so far apart, this resulted in a p-value of 0 for the demand, safety and noise objectives. Therefore, hypotheses H_{B1}, H_{B2} and H_{B3} are all accepted. As the significance of the increase in computation time is very much dependent on the available runtime and set amount of iterations, hypothesis H_{B4} is neither accepted nor rejected.

6.3 Experiment C: Drone Range

The third experiment, as described by section 5.5, relates to the range that a drone is able to fly from a warehouse to the destination vertiport. This is a one-way distance as it is assumed that the drone either receives a battery swap or is recharged at the destination vertiport. Figure 11 shows the Pareto fronts that are found for variable drone ranges. It is observed that a lower drone range generally results in a higher spread of the objective scores for given solutions. This indicates that for a smaller range, a harder decision has to be made on what objective is seen as most important when selecting a set of vertiports as the trade-off between objective scores is steeper. While there is not so much of a difference in the best values found for each separate objective, the model is able to find a better combination of objective scores if the range is larger. Furthermore, there is a general downward left shift of the Pareto front as the range increases, indicating that better safety and noise scores can be obtained for larger ranges. Both of these results make sense as a larger range relieves model constraints. This results in the potential for better performing UAM networks.

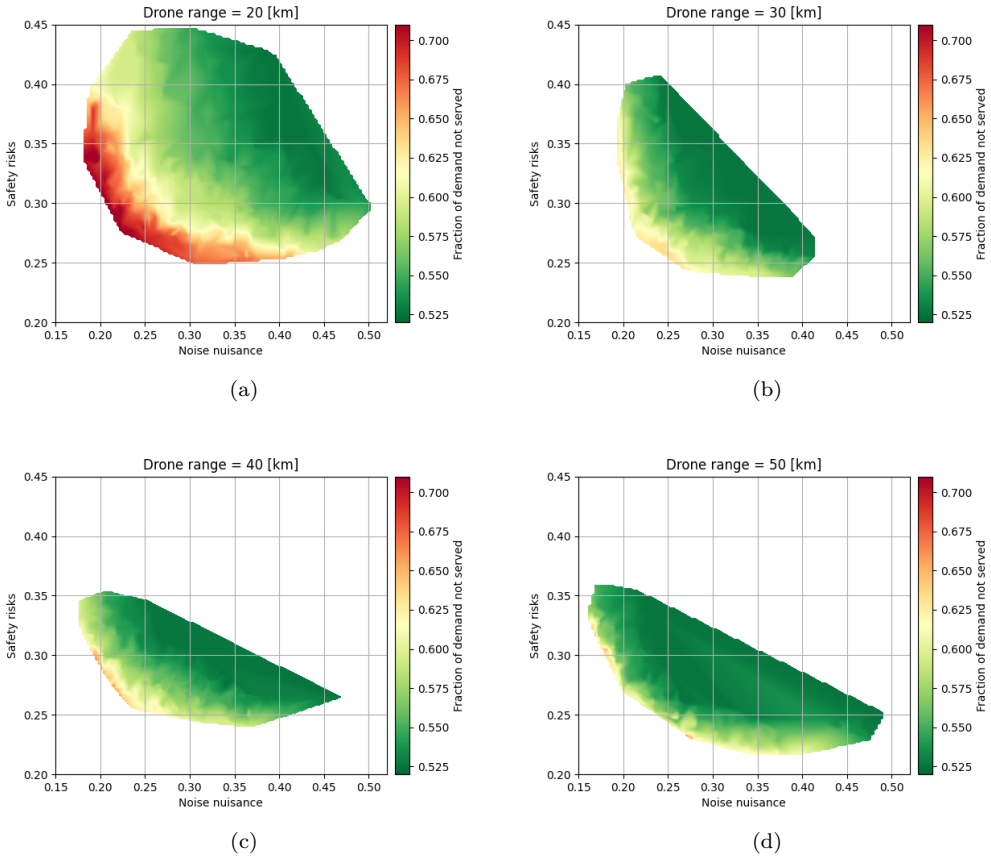

Figure 11: Pareto front considering a UAM network with drone range: (a) 20 [km] (b) 30 [km] (c) 40 [km] (d) 50 [km]

Figure 12 shows the boxplots of the obtained objective scores for Experiment C. Similar to the results obtained from the Pareto fronts in Figure 11, it can be seen that there are clear improvements in all scores as the range increases. An interesting fact is found using the Mann-Whitney U statistical test with a significance level of $\alpha = 0.05$. The Mann-Whitney U test is used to prove statistically significant differences between two datasets. It is found that, while there is no significant difference between the demand scores found for the ranges of 40 and 50 kilometres, there are significant differences between the safety and noise scores for these ranges. This indicates that increasing the range beyond 40 [km] does not necessarily increase demand scores however it does result in networks that overall score better on noise and safety.

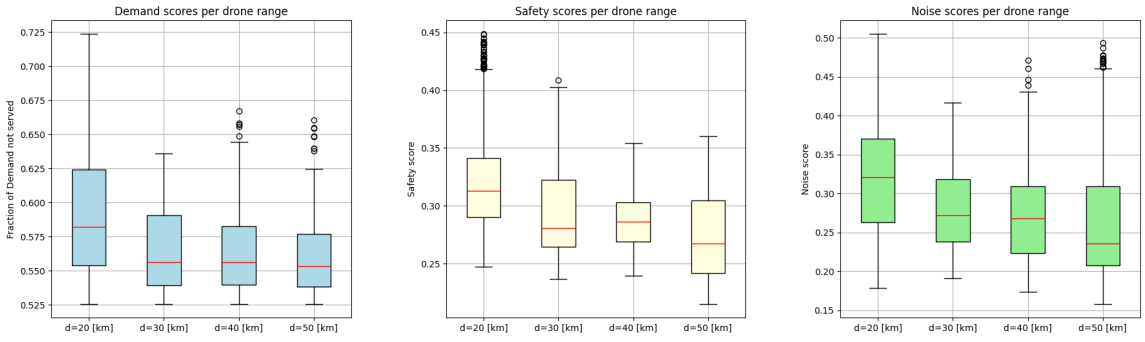

Figure 12: Boxplot of collected objective scores from the Pareto front: (a) Fraction of demand not served (b) Safety (c) Noise

To support the claims to either accept or reject hypotheses H_{C1}, H_{C2} and H_{C3}, a Kruksal Wallis significance test was performed with a significance level $\alpha = 0.05$. The resulting p-values are shown in Table 8. As all of

the p-values are below the selected significance level, the impact of varying the drone range is significant for all three objectives. Therefore, hypotheses H_{C1}, H_{C2} and H_{C3} are all accepted.

The computation time that it takes for each of the experiments to run is shown in Table 9. It is observed that there is no clear relation between computation time and the set drone range, as the maximum difference, being 30 minutes, occurs between the two middle values of the range variable. As this difference is relatively small compared to the overall runtimes,it is chosen to accept hypothesis H_{C4}.

Table 8: Kruksal Wallis significance test p-values

Objective:	**Demand**	**Safety**	**Noise**
p-value	2.58 E-35	3.60 E-73	2.65 E-49

Table 9: Computation times per range setting

Range [km]	**Computation time [s]**
20	26374
30	27292
40	25512
50	26573

6.4 Experiment D: Maximum Safety Distance

As described in section 5.6, experiment D aims to find the relation between the maximum safety distance and the objective scores. The resulting Pareto fronts are shown in Figure 13. From a visual analysis, it can be seen that, while the best demand scores are similar for all four settings, there is a slight increase in terms of safety and noise for some of the solutions found when increasing the maximum safety distance. This is indicated by the downward left extension of the Pareto front. It should be noted that while the best scores found per objective do improve, there is no clear improvement in terms of safety and noise for the entire Pareto front. This is best illustrated by Figure 14, which shows the Pareto fronts while just considering safety and noise scores. It can be seen that, in the most extreme case with a maximum safety distance of only 5 kilometres, overall, the solutions that were found perform worse in both safety and noise as it is shifted upward right. In contrast, for the other three distances, there is no overall improvement of the Pareto front in terms of the safety and noise objectives. Nevertheless, the best values for the individual objectives, indicated by the Nadir points, do show some improvements when increasing the maximum safety distance. This results in having to make a more impactful decision on preference between objective scores when selecting a set of vertiports to implement as the trade-off is steeper.

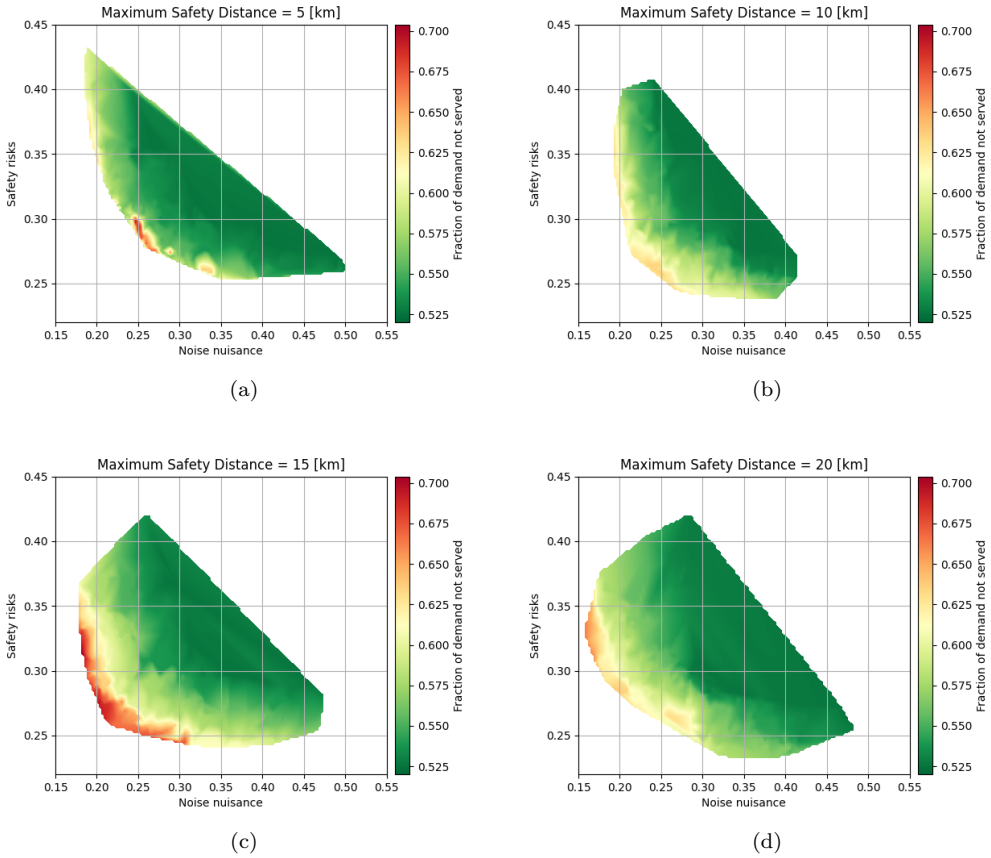

Figure 13: Pareto front considering a UAM network with maximum safety distance: (a) 5 [km] (b) 10 [km] (c) 15 [km] (d) 20 [km]

An interesting result becomes apparent when analyzing the boxplots of the demand objective scores as shown in Figure 15. It is observed that an increase in maximum safety distance does not necessarily increase the demand that can be served as all best demand scores are roughly the same. However, worse demand scores are accepted by the model more often as viable solutions due to the improvements in safety and noise scores. As a result, no clear conclusion can be made on the influence of the varying maximum safety distance on the demand that can be served.

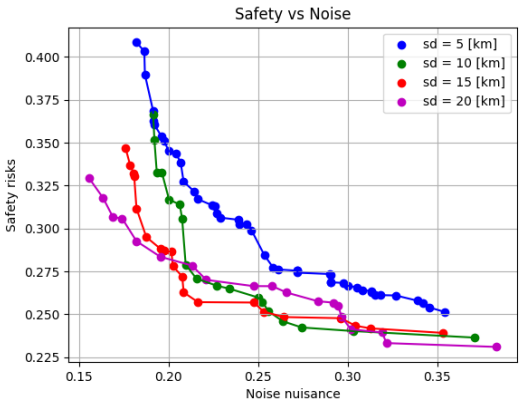

Figure 14: Paretofronts of Experiment D only considering Safety and Noise

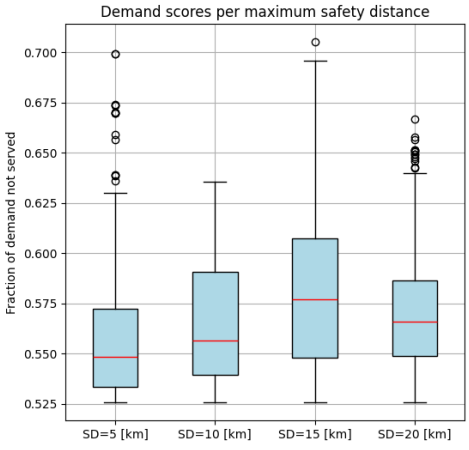

Figure 15: Boxplot of collected demand objective scores from the Pareto front (fraction of demand not served)

To evaluate whether varying the maximum safety distance significantly influences the objective scores, the Kruksal Wallis significance test is performed with significance level $\alpha = 0.05$. The resulting p-values can be found in

Table 10. It is concluded that the maximum safety distance does have a significant impact on all three of the objective scores. While the impact is significant, this can mainly be attributed to the fact that the model is able to find better scores for individual objectives and not necessarily a combination of the objectives. From the obtained results, it is not possible to accept hypothesis H_{D1} as no improvements of the demand objective are found with the increase of the maximum safety distance. Moreover, the obtained best solutions in terms of demand show very similar demand scores. The lack of improvement in demand scores could be a consequence of capacity limitations of the UAM network. Therefore hypothesis H_{D1} is also not rejected. For safety and noise, while the overall Pareto front does not necessarily shift, a significant improvement in best safety and noise scores was observed as a result of increasing the maximum safety distance. Therefore, hypotheses H_{D2} and H_{D3} are accepted.

In terms of computation times, a decrease is observed with an increasing maximum safety distance, as shown in Table 11. This is a logical result as increasing the variable results in a constraint relief, making it easier to construct feasible solutions. Therefore hypothesis H_{D4} is accepted.

Table 10: Kruksal Wallis significance test p-values

Objective:	**Demand**	**Safety**	**Noise**
p-value	2.14 E-23	2.23 E-11	0.04

Table 11: Computation times per maximum safety distance setting

Safety Distance [km]	**Computation time [s]**
5	28220
10	27853
15	27752
20	24732

6.5 Experiment E: Turn Around Time

Experiment E aims to assess the relation between a varying TAT and the objective scores as well as the computation time. The resulting Pareto fronts of the experiment as described in section 5.7 are shown in Figure 16. What is most noticeable is that the Pareto fronts do not significantly change positions as a result of varying the TAT. It is observed that the Pareto front extends in an upward right fashion as the TAT decreases. This could be attributed to the fact that, with a lower TAT, better demand scores can be obtained, resulting in the acceptance of worse safety and noise scores. Furthermore, a logical finding is that the demand score increases drastically with a decrease in TAT.

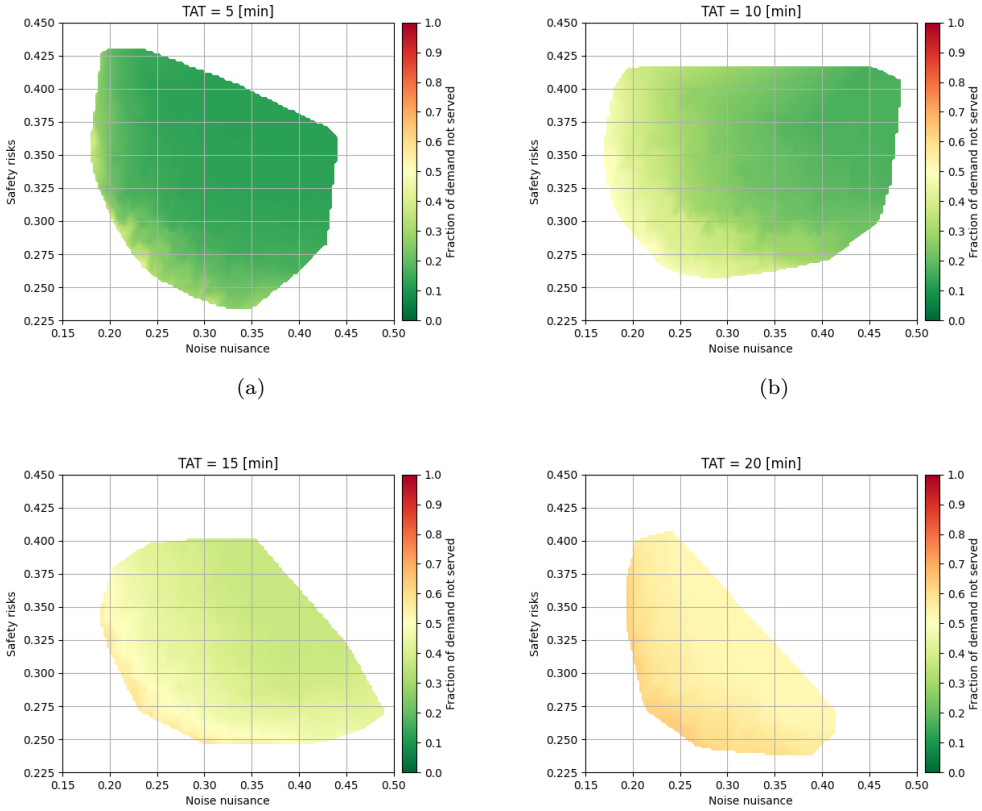

Figure 16: Pareto front considering a UAM network with TAT of: (a) 5 [min] (b) 10 [min] (c) 15 [min] (d) 20 [min]

The findings drawn from the Pareto fronts are confirmed by the boxplots shown in Figure 17. It can be seen that for a higher TAT the fraction of demand that is not served increases significantly, not only in best obtained value but also in median. Therefore hypothesis H_{E1} is accepted. Furthermore, from the boxplots it is found that the noise and safety scores do not have a strong reaction to the TAT variable as the found solutions contain quite similar scores. The Kruksal Wallis test with significance level $\alpha = 0.05$ results in p-values of $3.26E-26$ and 0.01 for collected safety and noise scores respectively. This would indicate a significant difference in the solution scores that are found, which can be attributed to the acceptance of more solutions that score particularly well on demand but not necessarily for noise and safety. Therefore, hypotheses H_{E2} and H_{E3} can not definitively be accepted but they are also not rejected.

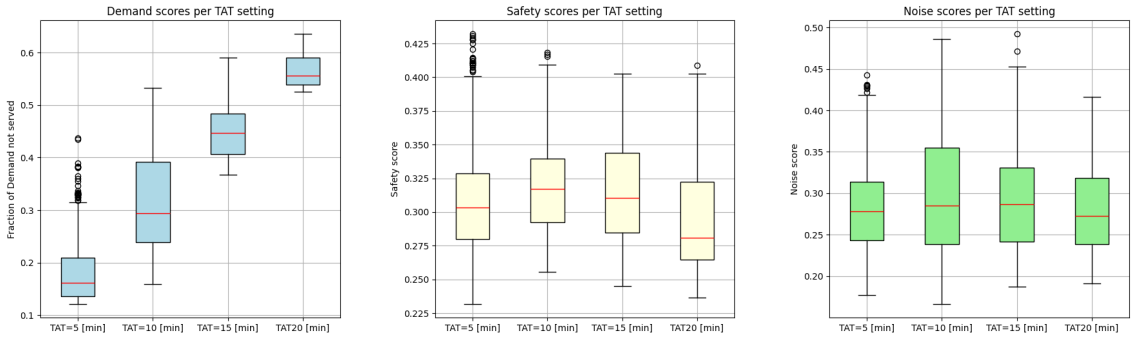

Figure 17: Boxplot of collected objective scores from the Pareto front: (a) Fraction of demand not served (b) Safety (c) Noise

Finally, Table 12 shows the computation time for each of the TAT settings. It is observed that the difference

between the longest run and the shortest run, being the runs with a TAT of 20 minutes and 5 minutes respectively, is only 12 minutes. As the total runtimes are around 7 hours, it is assumed that this difference has no significant influence on the computation time. As this would not affect modelling decisions for longer runs, due to the difference being relatively small, it is chosen to accept H_{E4}.

Table 12: Computation times per maximum safety distance setting

TAT [min]	**Computation time [s]**
5	25405
10	25231
15	25833
20	25952

6.6 Experiment F: Existing heliport utilization

The aim of experiment F, as described in section 5.8, is to assess the impact of utilizing the five existing heliports in the area of study by using them as the first setup of the UAM network. Every solution that is found and evaluated, therefore, contains all five heliports as selected vertiports. As the locations of heliports might not be optimal in terms of the three model objectives, it is expected that the resulting Pareto fronts generally consist of worse scores. This relation is evident in terms of safety and noise performance as can be seen in Figure 18. The figure shows the Pareto fronts considering the safety and noise objectives for three amount of vertiports with and without heliport utilization. It is observed that irrespective of the number of vertiports in the network, the utilization of heliports results in worse noise and safety performance. Furthermore, the figure demonstrates that the impact of utilizing existing heliports decreases as the number of vertiports increases. This is indicated by the two Pareto fronts moving closer together.

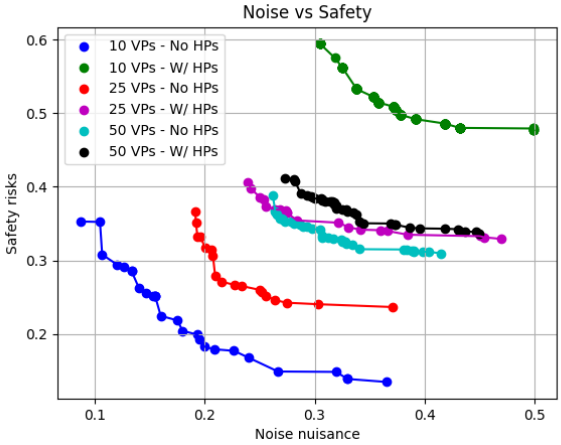

Figure 18: Pareto fronts for several scenarios considering only noise and safety

These findings are confirmed by the boxplots showing the collected scores per optimization objective in Figure 19. Similar to the Pareto fronts, it is observed that the utilization of heliports causes a worse performance in all three objectives. As a result it is chosen to accept H_{F1}, H_{F2} and H_{F3}. Furthermore, it is clearly visible that the impact of utilizing heliports decreases as the number of vertiports increases. For reference, the difference in the best demand that can be served for a vertiport network of size ten is 7.9% while this difference reduces to 0.4% for a network of size 50. Additionally, for the scenario with 10 vertiports where heliports are utilized, it can be seen that a very small range of solution objective scores is obtained. This is due to the fact that this scenario is highly constrained. As only five extra vertiport locations are chosen next to the heliports, while all 10 vertiports have to adhere to the maximum safety distance, the framework is forced to pick one location near each of the existing heliports. This results in quite few different performing solutions. This effect becomes a lot smaller if the number of vertiports is increased. It is therefore chosen to accept H_{F4}.

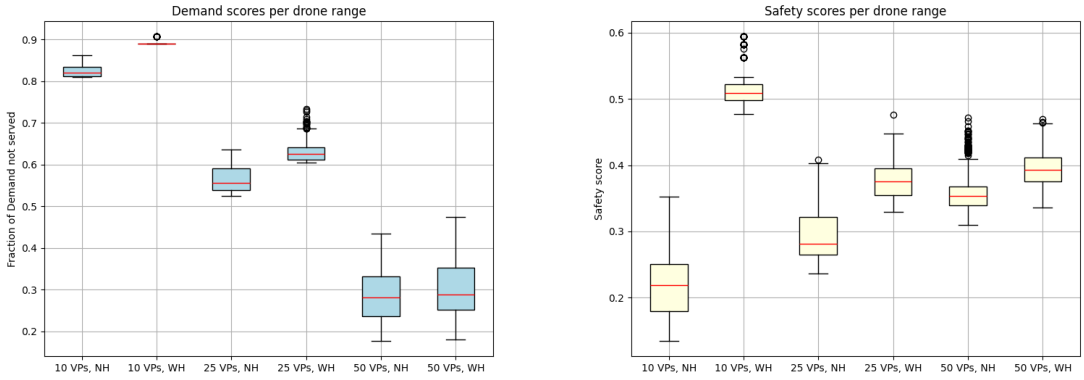

(a)

(b)

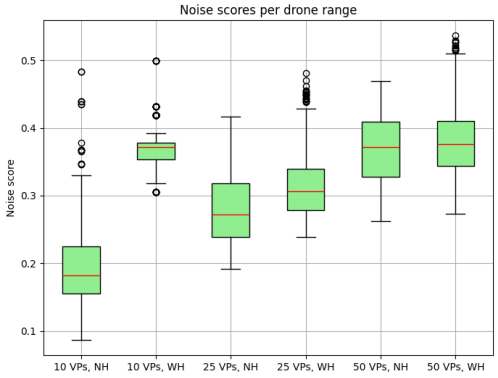

(c)

Figure 19: Boxplot of collected objective scores from the Pareto front: (a) Fraction of demand not served (b) Safety (c) Noise

7 Discussion

This section is aimed at discussing the developed framework and its implementation. Through the performed experiments, it was demonstrated that the framework is able to identify several relations between a number of independent variables and Key Performance Indicators (KPIs), being network demand coverage, safety risks, noise nuisance and computational effort. The results show that there is often an opposing balance between responding to demand and acceptable noise and safety levels. Moreover, the tool can be used for any city or region for which the necessary data can be acquired.

The section is divided into three subsections. First, the implementation of the framework for decision-makers and its use is discussed in section 7.1. This is followed by a discussion of how the model is affected by some of the assumptions that were made in section 7.2. Finally, the section is concluded by discussing the limitations of the developed framework in section 7.3.

7.1 Implementation

The developed framework offers a number of possibilities to help in the design of a UAM network and the decision-making process of vertiport positioning. One of the possibilities that the developed framework offers is to assess whether or not a certain urban area is suitable for the implementation of an MMD network using UAM. This can be done through the analysis of the Pareto front that is created for a specifically chosen set of input parameters. Users can easily input the number of vertiports, drone characteristics, safety distances, ground efficiency processes (in terms of turn around time) and whether or not existing heliports are used. The framework then outputs the acquired Pareto front from which several insights can be obtained, for example, to see if there are solutions that perform well in terms of demand coverage, safety risks and noise nuisance.

An area can be seen as particularly suitable if it adheres to some minimum demand coverage while offering networks that contain low safety risks and little noise nuisance.

Furthermore, the framework allows companies to identify potential vertiport networks and aids in decision-making on investments. For example, the maximum attainable demand coverage is easily identified for a set of input parameters. This gives decision-makers an immediate impression of the effectiveness of implementing a vertiport network for MMD with the desired inputs. This can then be used for decisions on whether to invest in building a higher amount of vertiports, increasing ground efficiency processes or selecting a better performing drone. Network tuning can then be done using the identified relations between the independent variables and KPIs as a guideline. In addition, the Pareto front offers companies the ability to determine preferences in the three objectives. It allows users, to make their own trade-off between the three objectives and select a solution that is acceptable for their needs. The framework then outputs the network of vertiports corresponding to the selected solution.

7.2 Assumptions

It should be noted that there are a number of assumptions that could have an influence on the frameworks' performance and the solutions that are found. First of all, for the performed experiments, 4000 iterations of the Tabu Search algorithm were performed. In each of these iterations, 50 solutions were checked, resulting in a total of 200.000 possible solutions being tested, which is in the order of 10^5. If a total of 25 vertiports are selected out of 1000 locations (as is the case for the base scenario), the solution space is roughly of the size 10^{50}. Due to the large amount of constraints that are introduced in the framework, the feasible solution space will be a lot smaller. Nevertheless, we are still only checking a relatively small portion of the total amount of solutions. Therefore, it can not be guaranteed that the absolute optimal solutions are obtained and in real-life applications, it should be considered to run the model for a larger amount of iterations to obtain results of higher quality. Additionally, this phenomenon also causes the framework to have some sensitivity to the initial solution that is inputted. In general, it is recommended to run the framework for as many iterations as possible with a large neighbourhood, subject to limitations on time and computational power, in order to negate these effects. Additionally, it should be noted that the framework assumes the geographical centroid of a zone to be the location of the vertiport. This location is therefore used for any distance constraints and calculations. As the maximum area of a zone is set to be of size 100 km^2, the real location of the vertiport could differ from the centroid by a few kilometres, depending on the shape of the zone. As this might affect parameters such as the necessary drone range, this phenomenon should be considered when selecting vertiport locations and the drone type.

7.3 Limitations

Finally, while the framework is able to provide interesting insights into vertiport positioning, there are some limitations to the model that should be noted. The first limitation is the high amount of unknowns about the implementation of UAM for MMD. For example, the capacity estimations that are made for a vertiport are quite basic due to limited available knowledge on drone operations for MMD. Furthermore, the identified relations between the independent variables and KPIs are based on estimated drone characteristics. As innovation within the heavy lift drone market occurs, drone characteristics might change significantly. In addition, future regulations on vertiport placement are currently not all known. The regulations that were implemented are based on the prototype design specifications of vertiports as published by EASA [33]. This is still subject to change. While these unknowns, introduce some uncertainty in the obtained results, the framework can easily be adapted to changes by simply changing input parameters or adding constraints in case of regulation adaptations. Other limitations of this framework consist of its ability to measure other network performance indicators than demand coverage. For example, the framework is not able to assess the effects of cumulative noise or give a quantification of travel time savings. These are recommended as extensions to the framework to perform more complex analyses on general network performance. The final limitation of the framework to be discussed is the considerably long runtime for exhaustive searching. As mentioned, searching a larger part of the solution space could result in the discovery of better performing networks. The downside of this is that the computational time increases linearly with the amount of tabu search iterations. This is a phenomenon to take note of in the case that there are time limitations on a project for which this framework is used.

8 Conclusions & Recommendations

This paper presented a Multi-Objective Multiple Allocation Capacitated p-Hub Coverage Problem optimization model for the positioning of vertiports in a parcel delivery system where drones are used for the middle-mile segment of the transportation process. In the considered framework, parcels are transported from 29 warehouses to centrally placed vertiports that function as distribution centres. We proposed a Tabu Search based heuristic approach to solving the optimization problem due to the large size and complexity. Furthermore, an area constrained version of the K-means algorithm was presented to scale down the solution space and decrease computational efforts. The model serves as a basic framework to perform first analyses on the implementation of a Middle-Mile Delivery (MMD) Urban Air Mobility (UAM) network by identifying optimal locations for vertiports. The South Holland region was selected as a use case, however, the model is easily adapted to other areas.

The framework's ability to gain insight into the following decisions and the relations to the different objectives were demonstrated. First, the framework provides the options to assess the vertiport networks considering various amount of vertiports. It was found that investing in a larger amount of vertiports enhances a network's demand coverage while introducing more safety risks and noise nuisance. Secondly, the work provides information on the effects of selecting different types of drones. We demonstrated that investing in better performing drones, with a larger range, allows for networks that perform better in terms of demand coverage, safety risks and noise nuisance. Although the type of drone is largely determined by an operator's budgetary considerations and current technology, this work shows that investments in the innovation of drones can yield large benefits. Thirdly, introducing a maximum safety distance between vertiports or vertiports and existing heliports to allow for safe diversions in case of emergencies was demonstrated to result in a steeper trade-off between the three objectives when selecting a viable network. This leaves decision-makers with a harder decision on preference between demand coverage, safety risks and noise nuisance. Moreover, we demonstrated the benefits of increasing the efficiency of ground operations. For example, it was found that the demand coverage can be increased from 55 % to 85 % by decreasing the turn around time from 20 minutes to 5 minutes. Finally, this study evaluated the effects of utilizing existing heliport infrastructure on network performance. Existing heliports are likely to be used as vertiports in the future as this offers large budgetary benefits due to the high similarity between heliport and vertiport infrastructure [34]. Nevertheless, this study showed that the utilization of heliports reduces the network's performance in terms of demand coverage, safety risks and noise nuisance. Additionally, it was demonstrated that this effect decreases as the amount of vertiports in the network increases.

Overall, the developed model provides a first basis for additional research to build upon as, currently, there exist no multi-objective models for a UAM MMD system considering multiple warehouses. Furthermore, the model can aid in the analysis of potential vertiport networks for decision-makers. The framework offers the possibility to assess the suitability of a region for the implementation of a UAM network for MMD. In addition, decision-makers can use the framework to decide upon investments and tune network performance. Furthermore, since the framework does not contain bias or preference towards any of the three objectives, it offers the ability for users to determine these preferences themselves and perform a trade-off. In terms of future improvements, first of all, it is recommended to extend the framework by including fleet size limitations, warehouse capacities and budgetary constraint. These are factors that are not taken up in the developed framework but will play a large part in actual network development. Secondly, the framework could benefit from the introduction of more advanced safety and noise metrics. For example, for noise nuisance, the model can be extended to consider the effects of cumulative noise. Furthermore, it is recommended to implement a more advanced capacity model when more statistics on vertiport ground operations become known as this largely influences network performance. Finally, the demand request allocation algorithm could be extended to optimize for energy or time efficient routing.

References

[1] J. Holden and N. Goel, "Uber elevate: Fast-forwarding to a future of on-demand urban air transportation," Uber, Tech. Rep., 2016.

[2] Amazon, "How amazon is building its drone delivery system," https://www.aboutamazon.com/news/transportation/how-amazon-is-building-its-drone-delivery-system, accessed: 2024-04-10.

[3] Zipline, "About zipline," https://www.flyzipline.com/about/, accessed: 2023-09-27.

[4] M. Brunelli, C. C. Ditta, and M. N. Postorino, "New infrastructures for urban air mobility systems: A systematic review on vertiport location and capacity," *Journal of Air Transport Management*, vol. 112, p. 102460, 2023.

[5] J. E. Macias, C. Khalife, J. Slim, and P. Angeloudis, "An integrated vertiport placement model considering vehicle sizing and queuing: A case study in london," *Journal of Air Transport Management*, vol. 113, p. 102486, 2023.

[6] N. Gunady, B. E. Sells, S. R. Patel, H. Chao, D. A. DeLaurentis, and W. A. Crossley, "Evaluating future electrified uam-enabled middle-mile cargo delivery operations," in *AIAA AVIATION 2022 Forum*, 2022, p. 3756.

[7] European Union Aviation Safety Agency (EASA), "Study on the societal acceptance of urbain air mobility in europe," EASA, Tech. Rep., 2021.

[8] K. R. Antcliff, M. D. Moore, and K. H. Goodrich, "Silicon valley as an early adopter for on-demand civil vtol operations," in *16th AIAA Aviation Technology, Integration, and Operations Conference*, 2016, p. 3466.

[9] B. German, M. Daskilewicz, T. K. Hamilton, and M. M. Warren, "Cargo delivery in by passenger evtol aircraft: A case study in the san francisco bay area," in *2018 AIAA Aerospace Sciences Meeting*, 2018, p. 2006.

[10] M. A. Arostegui Jr, *An empirical comparison of tabu search, simulated annealing, and genetic algorithms for facilities location problems.* University of Houston, 1997.

[11] D. N. Fadhil, "A gis-based analysis for selecting ground infrastructure locations for urban air mobility," *Masters Thesis, Technical University of Munich*, vol. 31, 2018.

[12] C. J. D. Gonzales, "Rooftop-place suitability analysis for urban air mobility hubs: A gis and neural network approach (doctoral dissertation)," Ph.D. dissertation, Universitat Jaume I, 2020.

[13] N. Kim and Y. Yoon, "Regionalization for urban air mobility application with analyses of 3d urban space and geodemography in san francisco and new york," *Procedia Computer Science*, vol. 184, pp. 388–395, 2021.

[14] M. Brunelli, C. C. Ditta, and M. N. Postorino, "A framework to develop urban aerial networks by using a digital twin approach," *Drones*, vol. 6, no. 12, p. 387, 2022.

[15] H. Schütze, C. D. Manning, and P. Raghavan, *Introduction to information retrieval.* Cambridge University Press Cambridge, 2008, vol. 39.

[16] E. Lim and H. Hwang, "The selection of vertiport location for on-demand mobility and its application to seoul metro area," *International Journal of Aeronautical and Space Sciences*, vol. 20, pp. 260–272, 2019.

[17] G. Usman, U. Ahmad, and M. Ahmad, "Improved k-means clustering algorithm by getting initial cenroids," *World Applied Sciences Journal*, vol. 27, no. 4, pp. 543–551, 2013.

[18] S. Rajendran and J. Zack, "Insights on strategic air taxi network infrastructure locations using an iterative constrained clustering approach," *Transportation Research Part E: Logistics and Transportation Review*, vol. 128, pp. 470–505, 2019.

[19] A. A. Sinha and S. Rajendran, "A novel two-phase location analytics model for determining operating station locations of emerging air taxi services," *Decision Analytics Journal*, vol. 2, p. 100013, 2022.

[20] J. F. Campbell, "Integer programming formulations of discrete hub location problems," *European journal of operational research*, vol. 72, no. 2, pp. 387–405, 1994.

[21] H. Shin, T. Lee, and H. Lee, "Skyport location problem for urban air mobility system," *Computers & Operations Research*, vol. 138, p. 105611, 2022.

[22] S. Rath and J. Y. J. Chow, "Air taxi skyport location problem with single-allocation choice-constrained elastic demand for airport access," *Journal of Air Transport Management*, vol. 105, p. 102294, 2022.

[23] L. Wei, C. Y. Justin, and D. N. Mavris, "Optimal placement of airparks for stol urban and suburban air mobility," in *AIAA Scitech 2020 Forum*, 2020, p. 0976.

[24] M. Maleki, N. Majlesinasab, and A. K. Sinha, "An efficient model for the multiple allocation hub maximal covering problem," *Optimization Methods and Software*, vol. 38, no. 5, pp. 1009–1030, 2023.

[25] S. Nickel, H. Karimi, and M. Bashiri, "Capacitated single allocation p-hub covering problem in multi-modal network using tabu search," *International Journal of Engineering*, vol. 29, no. 6, pp. 797–808, 2016.

[26] D. M. Jaeggi, G. T. Parks, T. Kipouros, and P. J. Clarkson, "The development of a multi-objective tabu search algorithm for continuous optimisation problems," *European Journal of Operational Research*, vol. 185, no. 3, pp. 1192–1212, 2008.

[27] D. Skorin-Kapov and J. Skorin-Kapov, "On tabu search for the location of interacting hub facilities," *Location Science*, vol. 1, no. 3, p. 61, 1995.

[28] Port of Rotterdam, "Drone port of rotterdam: U-space airspace prototype whitepaper," 2023, accessed: 2023-10-17.

[29] M. de Bok and L. Tavasszy, "An empirical agent-based simulation system for urban goods transport (mass-gt)," *Procedia computer science*, vol. 130, pp. 126–133, 2018.

[30] Z. UAS, "Ziyan uas products, blowfish a2g," https://www.ziyanuav.com/en/list/306.html, accessed: 2023-10-26.

[31] L. Preis, A. Amirzada, and M. Hornung, "Ground operation on vertiports–introduction of an agent-based simulation framework," in *AIAA Scitech 2021 Forum*, 2021, p. 1898.

[32] European Union Aviation Safety Agency (EASA), "Cs-hpt-dsn issue 1," EASA, Tech. Rep., 2019.

[33] "Prototype technical design specifications for vertiportsc," EASA, Tech. Rep., 2021.

[34] U. Northeast, "Advanced air mobility (aam) vertiport automation trade study," 2020.

II

Literature Study
previously graded under AE4020

1

Introduction

The ever-increasing pace of urbanization and the high demand for efficient transportation alternatives have propelled cities into an era where the existing and traditional modes of transportation are being redefined. An ecxiting and promising mode of transportation is Urban Air Mobility (UAM). UAM can be employed for the transportation of people in the form of air taxis or the transportation of goods. Uber has been planning the introduction of on-demand UAM [55] and are working with Joby Aviation, who are planning to launch the production of electric Vertical Take-Off and Landing (eVTOLs) aircraft capable of transporting passengers in 2020 [4]. In terms of transportation of goods, several companies have been employing small Unmanned Aerial Vehicles (sUAV) for quite some time, such as zipline [113].

Whether it is for the transportation of passengers or goods, for the implementation of UAM, so-called vertiports have to be built. A vertiport is an airport that supports the operation of VTOL aircraft. This imposes a decision-making problem on the strategic positioning of these vertiports. This is a vital part of setting up a UAM network in which many considerations have to be taken into account. Factors such as safety, noise pollution, visual pollution, infrastructure space, cost of land, and societal impact are all examples of elements that could influence the decision-making process of locating these vertiports. Furthermore, an optimization tool for locating vertiports could aid in the decision-making process. This literature study therefore aims to scope out the existing scientific knowledge on vertiport location optimization tools and models and tries to identify what this thesis can add to existing research.

The setup of the literature study is as follows. It is divided into 8 chapters. First, chapter 2 gives some background information on UAM and goes into the several applications that UAM has after which a use case is selected and rationale is provided. It also contains information on the drones that could be used for the selected application. Next, chapter 3 aims to discuss several characteristics of vertiports itself as well as discuss some of the model metrics and considerations that are associated with the placement of a vertiport. This is followed by an analysis of the Rotterdam area regarding flight restrictions, infrastructural implications and price of land and a demand analysis in chapter 4. This is followed by chapter 5 that describes the different methods used in literature for assessing the suitability of locations for vertiports as well as location optimization methods and algorithms. Next, chapter 6 gives a short description of the proposed system and the requirements that follow from the information provided in the previous chapters. Furthermore, it also lists the assumptions that might be made for the development of a vertiport location optimization model. The research proposal which includes the research gaps, research objectives and research question is then presented in chapter 7. Finally, the conclusion of this literature study is given in chapter 8.

2

Urban Air Mobility background and application

The Urban Air Mobility (UAM) industry is a relatively new and emerging industry that could have a big effect on the transportation of both passengers and cargo within urban areas. UAM is broadly defined as a spectrum of new aviation capabilities serving densely populated areas with a variety of public commercial services [17]. A large enabler of these UAM services is all-electric and hybrid-electric vertical takeoff and landing (eVTOL) aircraft. This chapter will elaborate on the several applications and services of UAM to provide the background information that is necessary for this thesis. The aim is to provide a scope of the current landscape of UAM.

First, section 2.1 will describe the different applications of UAM and provide reasoning for the selected use case. Second, section 2.2 will discuss the different types of unmanned aerial systems (UAS) or drones that are currently being used and could be of interest to this thesis.

2.1. UAM applications

UAM offers a revolution in the transport and logistics industry. With the increase in population as well as urbanization, traditional transportation systems are being stretched to their limits. UAM offers a solution to leading challenges such as congestion, pollution, and restricted mobility. The main applications of UAM can be split into two categories, the first of which is passenger transport and the second is the transport of goods. The transportation of goods can, in turn, be divided into cargo transportation and package delivery. Next to these main two applications, there are several others such as emergency services, public safety and law enforcement, news reporting, infrastructure inspection, and aerial photography.

2.1.1. Passenger

UAM offers an exciting possibility to reduce road traffic congestion in dense urban areas through the use of so-called air taxis. The main benefit of UAM services as compared to current passenger transport is that it has the potential to reduce commuting times for long-distance trips in highly congested areas [55]. There are several companies currently working on the concept of air taxis. Uber published a whitepaper on the concept of on-demand urban air transportation in 2016 [55]. Uber then decided to partner up with Joby Aviation on this. Joby Aviation is one of the leading companies in the development and production of eVTOLs and has launched their production of these aircraft in 2023 [4]. Next to Joby Aviation, there are several other companies working on the development of eVTOL air taxis such as Volocopter [104], Voltaero [105], Lilium [64] and Jaunt [59].

Several studies on the market for air taxis studies suggest that the market will significantly grow in the years to come with governments and aviation companies investing large amounts of money into the development of eVTOLs and air taxi services [57],[85]. North America is expected to be the most dominating player in this market due to the high consumer demand that is anticipated there. Furthermore, it is expected that during the initial stages of operation, the industry will mainly be focusing on piloted air taxis as opposed to UAS. To

have unmanned aircraft flying in densely populated areas, there must be a robust fail-safe system. Next to that, the public will have to trust autonomously flying vehicles, which might prove difficult as safety is the number one public concern according to a study performed by the European Aviation Safety Agency (EASA) in 2021 [15].

2.1.2. Delivery of goods

The second use case for UAM is the delivery and transportation of goods. With e-commerce rapidly growing, the need for efficient, swift, and environmentally friendly delivery solutions becomes ever more important. UAM offers a compelling alternative to the currently used ground-based methods. Due to the fact that delivery or cargo drones are not affected by traffic congestion, there is a large potential to reduce delivery times significantly in an environmentally friendly manner. There are several operational concepts to be considered when examining the possibility of using UAM for the transportation of goods. These are middle-mile cargo transportation, last-mile delivery and hyper-local delivery.

Last-mile delivery

Last-mile delivery is the delivery of packages from local distribution hubs to the final destination. Current last-mile delivery options are human-driven delivery fans, cargo bikes, and self-service, where the receiver of the package comes to a centralized pick-up point to collect their package. UAM offers rapid last-mile delivery through the use of small Unmanned Aerial Systems (sUAS). There are several advantages of using sUAS for this:

- **Faster and cheaper delivery**
  Due to the fact that drones are able to fly over obstacles, avoid congestion and take a shorter route than ground-based vehicles, packages can be delivered faster. Furthermore, fuel and labour costs can be reduced, resulting in cheaper delivery.

- **Better accessibility and flexibility** sUAS can reach areas that are difficult or impossible to access such as disaster zones or rural areas. For example, Zipline is a company that uses sUAS to deliver blood and medical products to clinics in Africa [113].

- **Sustainability**
  The usage of sUAS can lead to an increase in the sustainability of delivery companies. Electric drones produce very little to no emissions during operation. This is a heavy contrast to gas or diesel-powered delivery vehicles. The reduction in emissions helps to combat air pollution and has less impact on the greenhouse effect. Furthermore, drones have a lower impact on existing infrastructure as drones do not add to congestion and do not make use of roads, which reduces degradation [6].

Next to having a drone fly from a distribution centre to the package destination and back, there is also another option for using drones in last-mile delivery services. This would be through the use of a drone-truck delivery system. A truck carrying multiple drones would then drive to a designated area where it launches multiple drones for the final part of the delivery. The drones drop off the package and return to the truck which then drives back to the distribution centre [19].

Finally, it is important to note that despite the benefits, using sUAS for last-mile delivery also faces challenges. This includes safety concerns of the public as with all UAM concepts but there are also heavy limitations on payload capacity and range.

Cargo (middle-mile delivery)

Cargo transportation is a very interesting application of UAM. Many papers that discuss the delivery of goods focus on the concept of Last-mile delivery through the use of sUAS. However, a very likely application of UAM is the so-called middle-mile delivery. This refers to the segment in the delivery process between two nodes in the operators' network. For instance, this could be the transport of goods from a warehouse to a strategically placed vertiport that serves as a distribution centre. Another example can be seen in Figure 2.1. The figure presents a model for implementing middle-mile delivery using UAS in a supply chain. The package is transported from the origin hub to the origin airport and from the destination airport to the destination hub using UAM.

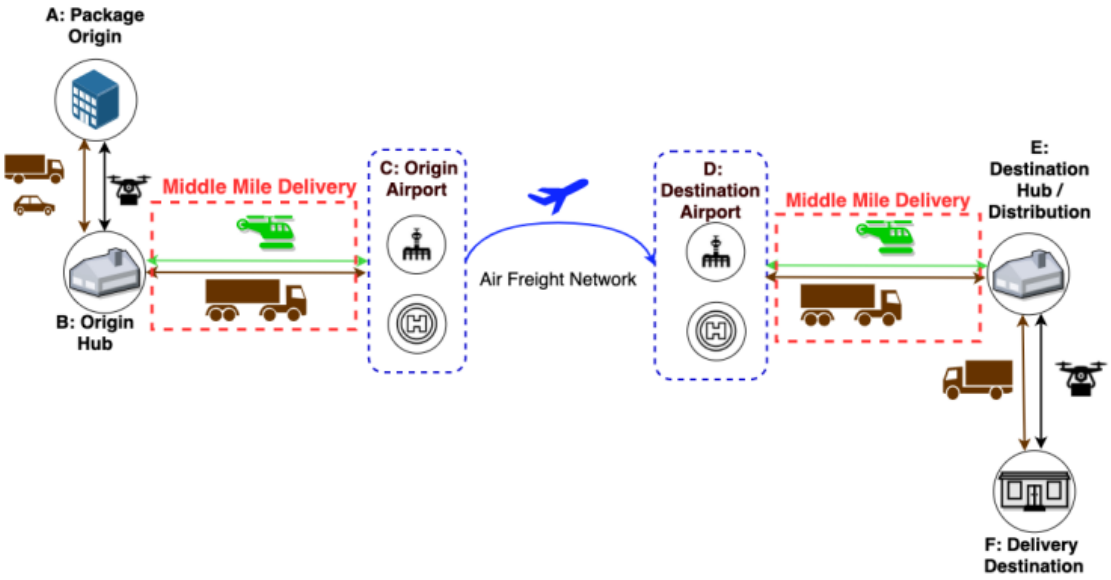

Figure 2.1: Supply chain that utilises UAS for middle mile delivery [38]

Hyper-local delivery

Hyper-local delivery focuses on the delivery of food and retail items of local stores only. This differs from last-mile delivery in the aspect that last-mile delivery mainly focuses on the delivery of retail items of large corporations. This type of delivery is often done by third-party delivery companies such as Uber Eats, Just Eat Takeaway and Deliveroo. Since the product to be transported is of a specific nature, fast delivery is required. For example, food should be delivered fresh and warm to the customer. Since the delivery distance and time are often relatively short, it could be interesting to employ sUAS for hyper-local delivery. Currently, bike or scooter couriers are often used for hyper-local delivery, which results in high labour costs for these types of companies. One of the biggest challenges of hyper-local delivery is fleet management. This is due to the fact that the exact demand of items to be delivered at any time is unknown upfront. As a result the size of the fleet often does not match the demand. A solution could therefore be to use drones for this as there are very little costs when a drone is not operating.

2.1.3. Other use cases

Next to these two main applications, there are several other applications such as using UAM for emergency services. UAM could significantly improve emergency response times. UAS could transport medical emergency personnel or equipment to an accident site or patients to the hospital. An example would be the ambulance drone that TU Delft is developing [12], which is able to deliver an Automated Defibrillator to people suffering a cardiac arrest. A second example of drones for emergency services is firefighting drones such as the ones used by Skydio [95]. These UAS are equipped with thermal imaging equipment to detect and capture the radiation that is emitted by fires.

Next to emergency services UAM aircraft can also be used for infrastructure inspection and maintenance. This application of UAM is currently already widely in use. An example of this is the Dutch company RSP [90], which uses drones for land surveying, drone mapping, identification of asbestos and structural inspections.

Lastly, the final application to be discussed is public safety and law enforcement. The first aspect that comes to mind when using UAM for law enforcement is surveillance. This is a controversial topic as using drones for surveillance conflicts with public opinion on the right to privacy. Drones can also assist in law enforcement. Agencies can use UAM for enhanced situational awareness and rapid deployment. One such drone is being produced by Elistair [18], which is designed for defense, homeland security, and civil organizations.

2.1.4. Selected use case

As discussed previously, there are quite a few applications of UAM to be considered. The two main applications of interest are the transport of persons and the transport of goods. For this thesis, the latter one was selected due to several reasons:

1. **Regulations** - Since there will be no people aboard the cargo UAVs, there might be fewer regulatory hurdles regarding safety concerns that are associated with cargo transportation. This can result in a faster path to certification and hence a faster deployment of UAM cargo operations.

2. **Demand for Rapid Delivery** - In today's day and age, there is a growing demand for faster and more efficient delivery of goods, particularly in urban areas. UAM offers a solution to address this need as it can provide rapid, point-to-point cargo delivery as opposed to delivery or cargo trucks which move at a much slower pace and are subject to congestion and other ground-based hindrances.

3. **Maturity** - There are already multiple drones out there that are capable of transporting goods and several companies have been using drones for the delivery of goods [113].

4. **Demand data** - The data for estimating parcel delivery demand is readily available for the area of Rotterdam through the release of the Mass-GT model. This will be elaborated upon in chapter 4.

5. **Existing Research** - Considerably less research has been done on the use of UAM in the context of delivery of goods which makes it more interesting to research for this thesis as it leaves more room for contribution to literature.

6. **Complexity** - From a research point of view, the transport of goods is a more interesting study case due to the challenges that it incorporates, such as the estimated high number of simultaneous operating vehicles. Additionally, another challenge lies in the fact that delivery demand matches residential areas where it is difficult to put a vertiport. Finally, it might be of more interest to consider drones with a lower energy capacity, in which case the vertiport location becomes an even more pressing issue.

In terms of delivery of goods, there is still the distinction between last-mile and middle-mile delivery. For this thesis, middle-mile delivery was deemed most interesting to research as the implementation of middle-mile delivery has been researched quite little, while the benefits to the public are potentially large.

2.2. Drone types

Now that the use case has been established, this narrows down the scope in terms of drone types that can be used. For middle-mile cargo operations, generally, larger drones with higher capacities are preferred. This will result in fewer flight legs having to be flown and hence a less crowded airspace. It is assumed that sUAS are mainly used for last-mile parcel delivery and are not feasible for cargo operations as they are able to carry too little payload. Furthermore, there are few papers available in literature discussing larger cargo drones. One study performed its own sizing of eVTOL aircraft [50] based on mission specifics and requirements. The basis of their sizing approach comes from another study on the reduction of cost for eVTOL operations [37]. A different study by Gunady et al. [38] bases its drone capabilities on another study by Howard et al. [39] (Class 6 semi) and a UPS press release stating capabilities of to-be-bought VTOL aircraft under development by Beta Technologies [101]. What is interesting is that estimations have been made on the direct operating cost of these vehicles, which is rarely found in other literature.

Table 2.1: Drone capabilities as used by Gunady et al. [38]

Parameter	Class 6 semi	"Beta like" UAM Vehicle
Direct operating cost	$2 per mile	$550 per flight hr
Payload (lbs)	20,000	2,000
Nonstop Max range	660 mi	250 mi

To get a more complete image on the available options for drone cargo operations, some of the drones that are currently available and will become available in the near future were scoped out. These cargo drones and their operational capabilities can be seen in Table 2.2. When looking at the properties in the table it becomes apparent that there are quite some differences. A lot of the drones that are readily available for cargo

operations tend to have lower payload capacity. However, companies are currently developing drones with higher payload capacity and range and endurance capabilities. Examples of this are the Pipistrel Nuuva V300 and the Flargo Heavy lift drone. When comparing Table 2.1 and Table 2.2 with each other it becomes apparent that payload capacity and max range estimations are quite a bit higher than the expected capabilities drones that are actually in development.

Table 2.2: Drone capabilities

Company	**Drone**	**Payload [kg]**	**Weight [kg]**	**Range [km]**	**Endurance [min]**	**Max speed [km/h]**
Wave Aerospace	X-5B Huntress [2]	22.5	22.5	-	60	49
	Falcon II LE [1]	9	11	-	60	32
Velos Rotors	Velos V3 [88]	15.8	8.5	-	80	120
Draganfly	Heavy lift drone [13]	30.4	0	30	55	0
Ziyan UAS	Blowfish A2G [99]	12	13.8	62.5	60	100
	Blowfish A3 [100]	12	13.8	62.5	60	100
Gadfin	Spirit X [49]	150	-	200	-	150
Pipistrel	Nuuva V200 [79]	20	100	typical: 250 max: 1000	720	100
	Nuuva V300 [79]	460	1700	typical: 300 max: 2500	720	220
Flargo	Heavy lift drone [48]	680	-	880	240	220

3

Vertiport characteristics and model metrics

In the process of determining the optimal location of vertiports for middle-mile cargo operations, there are many aspects to be taken into account. One of these aspects is the characteristics of vertiports as they can have a large impact on the positioning process. This chapter therefore aims to discuss several of these characteristics that could have an impact on deciding where to place vertiports.

The chapter starts with section 3.1 that describes the topology of vertiports and the design choices that could be made. This is then elaborated upon in section 3.2, which discusses literature regarding the capacity of vertiports. In section 3.3, energy storage and the effect of charging times is discussed. This is then followed by section 3.4, which discusses what factors influence the societal impact of placing vertiports. This is then elaborated upon in the following sections, with section 3.5 discussing noise pollution. This is followed by section 3.6 which describes visual pollution. Finally, section 3.7 discusses safety considerations that could be taken into account in the design of a UAM network and positioning of vertiports.

3.1. Vertiport topology

As the concept of vertiports and VTOL aircraft is relatively new there are very few regulations imposed on the design. EASA has released a "prototype technical specifications for the design of vertiports" in 2022 [14]. Due to the lack of regulations, most studies on vertiport design are based on heliport regulations[32] as provided by the Federal Aviation Administration (FAA) [45] and the International Civil Aviation Organization (ICAO) [56]. This is due to the high similarities in the ground infrastructure of heliports and vertiports. The most important dimension for the design of vertiports is the dimension "D", as shown in Figure 3.1, which is the diameter of the smallest circle enclosing the VTOL aircraft projection on a horizontal plane, while the aircraft is in the take-off or landing configuration, with rotor(s) turning [14]. This determines the dimensions of the main elements of the vertiport and will therefore have a large impact on the size of the vertiport.

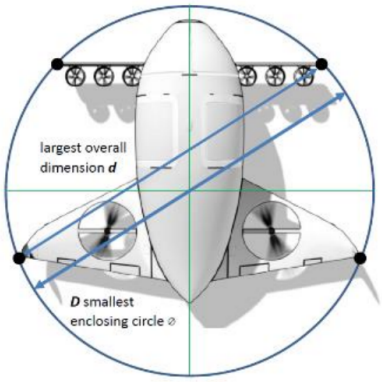

Figure 3.1: Dimension "D" [14]

There are three main elements to the layout of a vertiport, namely pads, gates, and stand. Pads are places where VTOLs can take-off and land. In terms of regulations, there are some associated areas with the pads. First of all, there is the Touchdown and Lift-Off Area (TLOF). The TLOF should have the minium dimensions of either $0.83D$ or $1D$ depending on wether the pad is elevated or not [14]. Furthermore, the TLOF is surrounded by the Final Approach and Take-Off area (FATO). The FATO should provide an area free of obstacles (except for essential objects which because of their function are located on it), and of sufficient size and shape to ensure containment of every part of the design VTOL-capable aircraft in the final phase of the approach and at the commencement of the take-off in accordance with the intended procedures [14]. The FATO can be either square or circular but it is required to have a minimum dimension of $1.5D$. Finally, the FATO is surrounded by a Safety Area (SA) which is added to compensate for manoeuvring errors under challenging environmental conditions. The design criteria of the FATO and the SA are shown in Figure 3.2.

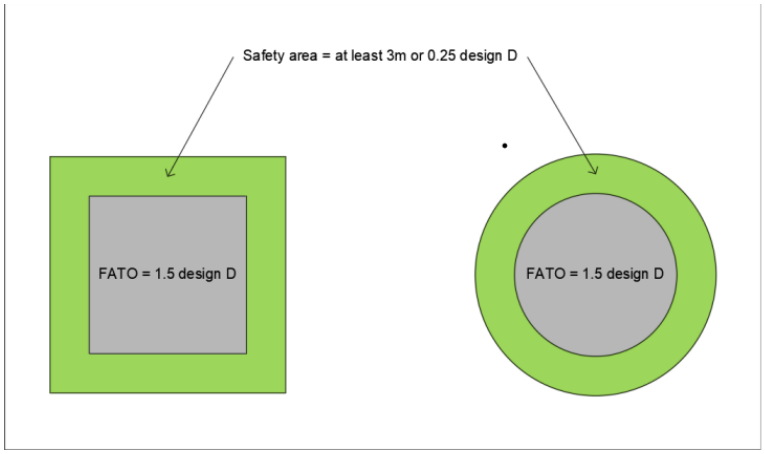

Figure 3.2: FATO and SA design criteria [14]

The second main element of vertiport topology are gates, which are sites where either cargo or passengers can be picked up and dropped off by eVTOLS. Finally, the third element is stands, which are parking places for the aircraft when they are not being used. These three elements are usually connected to each other through the use of taxiways.

There are also several layouts of vertiports considered in vertiport design literature. For example, [103] and [80] consider layouts that are used in current heliport designs. These are the satellite, pier, and linear layout as shown in Figure 3.3. Furthermore, more complex layouts have also been discussed such as the ones discussed by [112] who take a squared vertiport layout approach where the pads are situated in each corner shown in Figure 3.4.

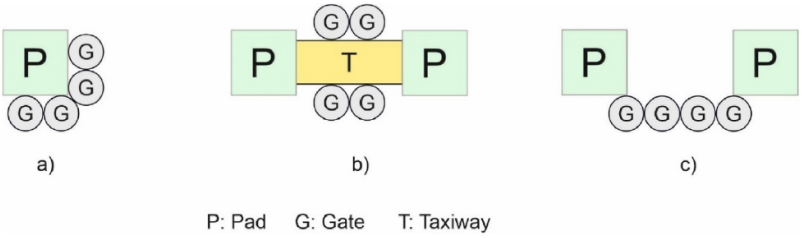

Figure 3.3: Example of vertiport layouts: a) Satellite, b) Pier, c) Linear [32]

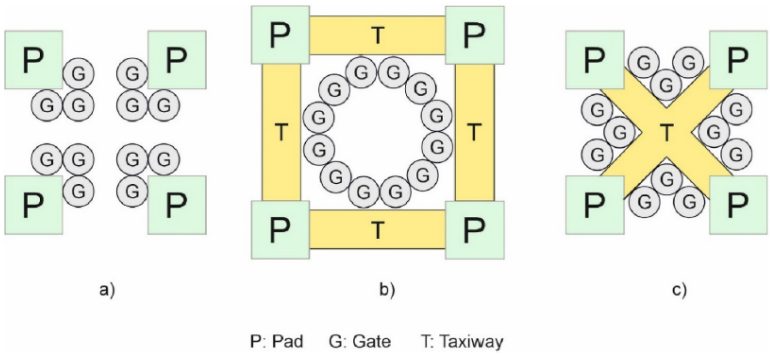

Figure 3.4: Examples of squared vertiport layouts with 3 gates for each TLOF: a) Disconnected, b) Perimetral, c) Central [32]

To summarize, the layout and size of vertiports can differ according to the properties that are necessary for their application. For example, the need for a higher capacity will lead to a larger size of the vertiport. Furthermore, the selection of a bigger drone will result in having to design with a bigger dimension "D", which, in turn also results in larger area usage of the vertiport. This is something to take into account when modelling the capacity and selecting locations for vertiports.

3.2. Capacity

Vertiport capacity and throughput have been studied multiple times in literature. As capacity characteristics are heavily dependent on the vertiport size and layout, estimating the capacity becomes a research topic of its own. Multiple approaches have been used to research vertiport capacity. Several researchers have used a Discrete Event Simulation (DES) to estimate vertiport characteristics based on design choices [47, 87, 93]. Others have used Agent-Based Simulations [81] or Integer Programming methods to determine vertiport layout and capacity [3, 28, 77, 80, 103]. As the vertiport design problem, on which the capacity is heavily reliant, is a whole separate problem from vertiport location optimization it is assumed to be out of the scope of this thesis. Nevertheless, the capacity of vertiports of several sizes can be estimated using findings from literature. An overview of literature discussing vertiport capacity can be found in Table 3.1. The table contains information on take-off and landing operating times, surface times and the resulting capacity as found in existing research. This could be used to make estimations on the turnaround times of drones and vertiport capacity. One should note that almost all papers discussing capacity are in the context of passenger transport (air taxis). As a consequence of this, only certain findings from these papers can be used in the context of this thesis. Therefore, assumptions on the several processes such as the time it takes to load and unload an aircraft will have to be made.

Table 3.1: Vertiport capacity characteristics

Author(s)	Application	Take off/ Landing operating time	Surface time	Capacity
Ahn and Hwang (2022) [3]	Passenger	60s	15s taxiing time + 300s turnaround time	80 passenger/h for each TLOF pad with 4 gates
Feldhoff and Soares Roque (2021) [47]	Passenger	180s	1800s (30 min) battery loading + 60s taxi time	9.6 movements/h
Goodrich and Barmore (2018) [54]	Passenger	72s	-	Strongly dependent on number of TLOF and gates
Guerreiro et al. (2020) [33]	Passenger	60s	From 120s (minimum) to 900s (15 min) (average)	No more than 38 operations per hour
Preis et al. (2021) [28]	Passenger	From 30s to 90s depending on vehicle	60s, 300s or 1200s (20min) depending on the operation	60 to 780 movements/h depending on the layout and dimensions
Vascik and Hansman (2019) [103]	Passenger	From 15s to 90s	Turnaround time 30600s Taxi time 590s	Strongly dependent by the number of gates per TLOF
Zelinski (2020) [112]	Passenger	60s	480s (8 min) spent at the gates + average taxi time depending on the layout	Strongly dependent on the layout configurations
Rimjha and Trani (2021) [87]	Passenger	60 - 90s	Taxi time 60s 10 minutes spent at the gates	Configs: [pads/stalls] [1/8] 41 movements/h [2/16] 52 movements/h [3/24] 86 momvements/h
Scheiger, Knabe and Korn (2021) [93]	Passenger	66 - 75s	600s	
Preis and Hornung (2022) [81]	Passenger	Varied between 60s, 90s, 120s and 150s	Varied between 2 to 5 minutes	
Zeng et al. (2020) [44]	Package delivery	-	-	316.3 million orders over 7 droneport Does not state capacity of a droneport but rather the capacity of their system
Park and Kim (2022) [77]	Passenger			80 AC per hour
Preis (2022) [80]	Passenger	-	-	Throughput heavily dependant on vertiport design and layout

3.3. Energy storage

In the usage of eVTOLs, charging and battery monitoring is an important aspect that will have influence on both the performance of drones and the throughput capacity of a vertiport. For smaller drones, it could be

assumed that one is able to switch the battery at a vertiport when it is observed that the State of Charge (SOC) is not high enough to carry out the next mission. However, with middle-mile delivery, generally, larger drones will be needed that require more energy storage. Therefore, it cannot be assumed that batteries can be replaced while stationary at a vertiport. There are several strategies that can be used for charging an eVTOL for a certain mission. The most common ones are:

- 100% SOC
- 80% SOC
- mission-based% SOC

Where the mission-based strategy involves charging until the SOC is high enough to carry out the desired mission. According to a study by Vossen [106], both the 80% SOC and the mission-based strategy outperform the 100% SOC strategy yielding less environmental impact, lower financial cost and a higher flying efficiency. When comparing the mission-based strategy with the 80% SOC strategy, they perform comparably. Charging eVTOLs to their maximum state of charge is therefore not desirable. This could, in turn, also affect the throughput rate and capacity of a vertiport itself as less charging time might be needed. While energy storage is a factor that influences drone performance and vertiport capacity heavily it is not often considered in the development of UAM networks and especially not in the decision-making process of placing vertiports. It could therefore be interesting to incorporate charging times and in-flight energy discharge rates in a vertiport location optimization model.

3.4. Societal impact

Societal impact is a metric that is heavily influenced by the other metrics that were mentioned earlier such as noise, visual pollution and safety. In 2021, EASA published a study on societal acceptance of UAM in Europe [15]. The main concerns identified from this study are safety, security and environmental impact. These are based on air taxis as well as drone delivery concepts. When focusing on the concerns based on drone delivery only, some changes are visible as shown in Figure 3.5. For clarity, security refers to incidents caused by harmful deliberate or intentional actions, such as cyber-attacks or the failure of mobile networks, while safety refers to incidents caused by technical or human failures. The main takeaway from this is that safety is the most important metric to be considered to reduce the societal impact. Noise pollution and visual pollution are considered to be less important metrics.

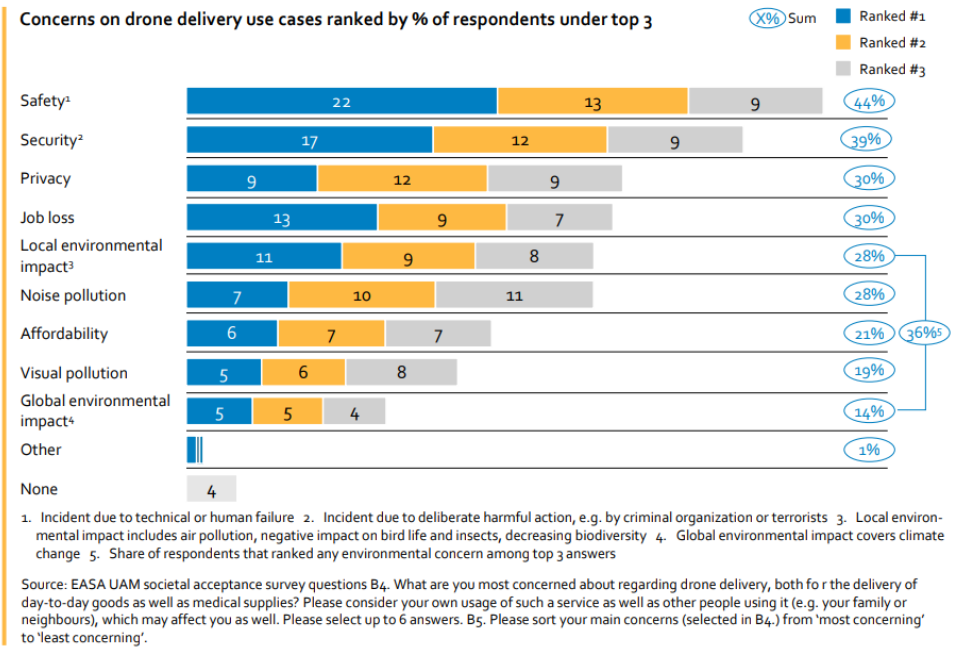

Figure 3.5: Top concerns of implementing delivery drones in Europe [15]

3.5. Noise

Another factor to be taken into account when deciding upon a vertiport location is the nuisance caused by the noise of eVTOL operations. Several noise modelling tools for eVTOL operations around a vertiport have been developed [21, 98]. Nevertheless, noise is, together with security, one of the most underrepresented topics in the body of scientific research vertiport positioning, but also in regulatory guidelines and vertiport design proposals [92].

Metric types that are used for airports and hence could be interesting for vertiports to assess noise levels throughout a day are the day-night average level L_{dn} and the day-evening-night average level L_{den} measured in dBA, which is the A-weighted sound pressure level. These metrics evaluate the noise at different times of the day and assign different penalties for events that cause noise during the day, evening or night. As the day-night average level does not make a distinction between day and evening operations, the time slots and associated penalties will be different from the day-evening-night average level. An overview of the penalties is given in Table 3.2. The resulting equations used to calculate L_{dn} and L_{den} are then given by Equation 3.1 and Equation 3.2 respectively.

Table 3.2: L_{dn} and L_{den} timeslots and associated penalties

	Ldn	**Lden**
Day	07:00 - 22:00 (+0 dB)	07:00 - 19:00 (+0 dB)
Evening	N/A	19:00 - 22:00 (+5 dB)
Night	22:00 - 07: 00 (+10 dB)	22:00 - 07:00 (+10 dB)

$$L_{dn} = 10log\left[\frac{1}{24}\left(15\cdot 10^{\frac{L_d}{10}} + 9\cdot 10^{\frac{(L_n+10)}{10}}\right)\right] \tag{3.1}$$

$$L_{den} = 10log\left[\frac{1}{24}\left(12\cdot 10^{\frac{L_d}{10}} + 3\cdot 10^{\frac{L_e+5}{10}} + 9\cdot 10^{\frac{L_n+10}{10}}\right)\right] \tag{3.2}$$

Where L_d is the average sound level during the day, L_e is the average sound level during the evening and L_n is the average sound level during the night. Only one paper was found that incorporates noise metrics in assessing a UAM network. Jeong et al. [24] use the day-evening-night average level to assess how much of the population of Seoul metropolitan area will be highly annoyed by their proposed UAM network. For this, they used a curve fitting function of the Schultz curve which is used to calculate the number of residents negatively affected by noise. The curve fitting function for the Schultz curve is shown in Equation 3.3[91].

$$\text{Highly annoyed,\%} = \frac{100}{1+e^{11.13-0.141L_{dn}}} \tag{3.3}$$

The L_{dn} value is approximated to be the same as L_{den} as Brink et al. [30] stated that the difference in noise levels between the two is small. However, Miedema and Oudshoorn [68] propose another curve representing the noise impact of aircraft as this impact tends to be higher as compared to other noise sources. The curve fitting functions as proposed by Miedema and Oudshoorn are shown in Equation 3.4 and Equation 3.5.

$$\text{Highly annoyed,\%} = 1.395\cdot 10^4(L_{dn}42)^3 + 4.081\cdot 10^2(L_{dn}42)^2 + 0.342(L_{dn}42) \tag{3.4}$$

$$\text{Highly annoyed,\%} = 9.199\cdot 10^5(L_{den}42)^3 + 3.932\cdot 10^2(L_{den}42)^2 + 0.2939\cdot(L_{den}42) \tag{3.5}$$

It should be noted that the noise impact is not taken into account by Jeong et al. [24] for deciding the location of vertiports, rather it is used to determine aerial routes that have a less negative impact on the resident as a result of noise pollution. Literature that does take into account noise when selecting suitable locations for vertiports mainly focuses on reducing the nuisance that it causes by selecting locations that already generate high a amount of noise [46, 53]. This idea was first proposed by Antcliff et al. [26], suggesting that highways and main roads of the city could function as noise absorption zones caused by the propulsion of the vehicles.

Summarizing, noise is an important metric to be considered when selecting vertiport locations. Nevertheless, no literature exists that includes noise metrics in location optimization. It is rather used to either select suitable places with respect to certain infrastructural elements such as cloverleaves, highways and main roads or design network flight paths that reduce noise pollution.

3.6. Visual pollution

Visual pollution is an interesting metric that is discussed very little in literature and has not been included in any studies considering the placement of vertiports. Visual pollution is defined as the negative impact an individual may experience by viewing visual pollutants and their movement [76]. Visual pollution is a subjective metric and is dependent on the observer. It can cause various health-related issues such as distraction, mood disorders, stress anxiety, overstimulation and reduced work efficiency [36]. What is most difficult about visual pollution is that it can not be measured physically but only psychologically. Therefore, it is hard to quantify the level of visual pollution. One study was found that tries to quantify the visual pollution that results from UAM networks [97]. Various factors that influence the perceived visual pollution due to UAM were identified. These are:

- **Appearance** - Observable characteristics of the UAV. Is it aesthetically pleasing?
- **Awareness** - Information (e.g. through an app) about the UAV, such as where it is going, where it comes from, what its speed is etc.
- **Distance** - Distance to the observant and altitude of the UAV.
- **Environment** - In which environment the UAV is seen. For example, if it is seen in a rural area or an urban area could result in different levels of perceived visual pollution.
- **Formation** - If the UAVs are flying in a line formation, in groups, completely scattered, etc.
- **Movement** - If the movement of the UAV or its speed has an influence on how it is perceived.
- **Number of UAVs** - How many UAVs are visible at the same time.
- **Purpose** - If the UAV is carrying cargo, passengers, or is on an Emergency Medical Services (EMS) mission.
- **Temporal component** - Factors related to the time of exposure or the number of times that a person would see the UAV.

The study conducted a survey among 227 participants from which they identified the importance of each of the factors that might contribute to visual pollution. The function to calculate visual pollution (VP) shown by Equation 3.6 was extracted from the survey results.

$$VP = \frac{3.83}{\sqrt{Dist}} + 0.97\sqrt{Num} + 20.12\sqrt{\frac{Num}{Dis}} - 0.19Purp + 0.89Info \tag{3.6}$$

Where $Dist$ is the distance from the observer to the closest UAV, Num is the number of UAVs visible, $Purp$ is the purpose of a UAV (1 if it is an EMS UAV, 0 if it is not) and $Info$ reflects if there is extra information regarding the UAV (equal to 1 if there is extra information, else 0). It was identified that the most important factors were the number of UAVs flying as well as the distance between the observer and the closest UAV. Therefore, the function could be simplified to the function given by Equation 3.7.

$$VP = 47.76\frac{Num^{0.65}}{Dist^{0.67}} + 1.37 \tag{3.7}$$

3.7. Safety

A metric that is of great interest but has been rarely incorporated in existing vertiport location optimization research is safety. For UAM systems to be incorporated in society they will have to adhere to rigorous safety standards and protocols that encompass aspects such as vehicle design, maintenance, pilot training, airspace management and infrastructure. The strategic positioning of vertiports is no exception to this. There are several aspects that could be taken into account, when determining vertiport locations, such as emergency diversion vertiports, highrise, population density, high traffic areas and parks and recreational areas.

Emergency diversion vertiports

In the case that an event forces a UAM aircraft to a precautionary or emergency landing, before reaching their destination vertiport, alternative landing sites will be required. A concept of operations by Wisk and Boeig proposes three types of alternative landing sites. These are [111]:

- **Diversion vertiports**
  Diversion vertiports are vertiports in the UAM route network that have enough capacity to accommodate off-nominal landings. These vertiports are a part of the operations in the general UAM network but will accommodate space for emergency landings.
- **Secure emergency landing zones**
  Secure emergency landing zones (ELZ) are sites along UAM routes that will support efficient UAM flight planning where vertiports are not avaible. They will provide the required services for approach and landing (e.g. position, navigation, and timing). Simply speaking, secure ELZs are specialized emergency vertiports that only serve a purpose in the case of an emergency situation and are not meant to be used in the general operations of UAM network.
- **Non-secure emergency landing zones**
  Non-secure ELZs are sites that have been surveyed and determined to be suitable for landing with minimal chances of encountering human activity on the ground. An example of this would be golf courses. These sites should be used as a last resort and diversion vertiports and secure ELZs are highly preferred for emergency landings.

In case of an emergency landing, the diversion vertiports should be picked first by the drones. In the case that it is not possible to reach a diversion vertiport, the drone should land at a secure ELZ. Only if neither of the aforementioned options is available, landing in a non-secure ELZ is permitted.

Furthermore, the prototype technical design specifications for vertiports provided by EASA [14] specifies the structure as shown in Figure 3.6 for Continued Safe Flight and Landing (CSFL). In yellow it shows a normal adequate aerodrome (heliport or vertiport), from where the VTOL can subsequently take off, which meets all D-values and has a full range of facilities and services required for the operation. In blue it shows an adequate aerodrome (heliport or vertiport), from where the VTOL may not subsequently take off, which meets all D-values but has only a minimum set of facilities and services. The emergency landing site in red corresponds to the Non-secure emergency landing zones as described earlier.

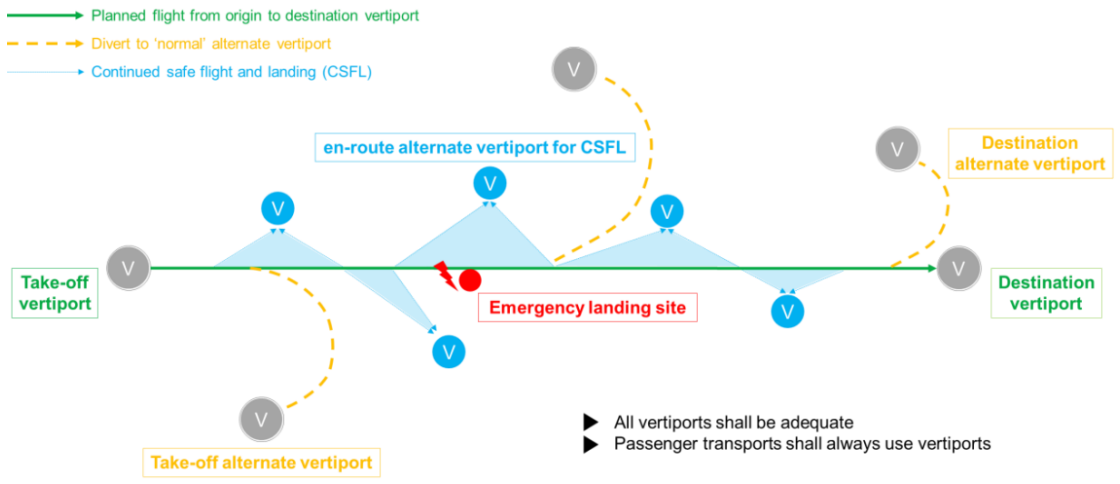

Figure 3.6: En-route alternate vertiport for CSFL [14]

Highrise

Another safety-related aspect to take into account is the proximity of high-rises in areas where vertiports will be placed. Placing vertiports near tall buildings can raise safety concerns for several reasons. First, tall buildings introduce obstacle hazards for UAM aircraft which increases the risk of collisions during landing and

takeoff. Furthermore, tall buildings are known to disrupt airflow patterns, creating unpredictable wind and turbulence conditions. This poses safety risks to aircraft during critical flight phases. Proximity to high-rises also introduces a reduced manoeuvring space for the UAM aircraft which could potentially lead to unsafe flight paths and restricted emergency escape options. It is, therefore, in the interest of safety, not preferred to place vertiport in the vicinity of tall buildings.

Data on the locations of high-rises is readily available through the "Actueel Hoogtebestand Nederland" (AHN) [71]. This is a digital map containing the current data on buildings and heights in the Netherlands. The AHN contains detailed and precise height data with an average of ten height measurements per squared metre. This data can be used to identify locations of highrise for the safety analysis.

Population density

Placing vertiports in densely populated areas might not be preferable when considering safety. Quite logically, having the vertiport located in an area with a lot of people increases the risk of casualties in emergency situations. It might therefore be preferable to avoid densely populated areas when locating vertiports. Population data of the Netherlands is openly accessible per municipality [107].

High traffic areas, parks and recreational areas

Similar to population density, areas with a high amount of traffic are also less preferable for locating vertiport in terms of safety. Although these locations are highly suitable when looking at it from a noise perspective, in terms of safety, they introduce a higher risk of casualties in case of emergencies. High-traffic areas include highways, city centres and main roads. Similarly, parks and recreational areas are interesting for the placement of vertiports in terms of space, however, as there will be a lot of people in the vicinity of these areas it again introduces higher safety risks and concerns.

4

Rotterdam area and demand analysis

To apply the problem of vertiport location optimization to a case study, the Rotterdam area was chosen. Rotterdam is one of the largest cities of the Netherlands with a population of over 600,000 people. As it is an environment with a large population, naturally the demand for packages is relatively high as compared to areas that are populated with low density. Therefore, it is interesting to apply the vertiport location optimization problem in the context of middle-mile cargo operations in this area. Furthermore, parcel delivery demand data is available for the area of Rotterdam through the release of the Mass-GT model as will be discussed in section 4.4. This chapter aims to describe the Rotterdam area and the associated metrics to take into account when placing vertiports in this area. The chapter is structured as follows. First, section 4.1 will elaborate on the flight restrictions and no-fly zones that are in place for drones in the Rotterdam area. Next, section 4.2 discusses the metric of available infrastructure space. The costs associated with purchasing land to build a vertiport in Rotterdam are discussed in section 4.3. Finally, the way demand can be modelled and how data on this can be acquired is discussed in section 4.4.

4.1. Flight restrictions

In the determination process of optimal locations for vertiports, several aspects have to be taken into account. One particular essential aspect is the presence of flight-restricted areas within the given region. Even though drones are physically capable of manoeuvring through the entire city, this might not be preferred due to several concerns. These concerns are related to privacy, safety, environmental aspects and nuisance. Consequently, the need to circumvent these flight-restricted zones leads to alterations in the flight routes between certain combinations of warehouses and vertiports. In the context of Rotterdam, there are several flight-restricted areas to be identified. Figure 4.1 shows a map with flight restrictions for drones in the area of Rotterdam as acquired from [86]. Two of the main points of attention are the restrictions caused by Rotterdam The Hague Airport (RTHA) and the Port of Rotterdam. These will be discussed in the following sections. Furthermore, the impact of the city centre and vital infrastructure and protected areas is also discussed.

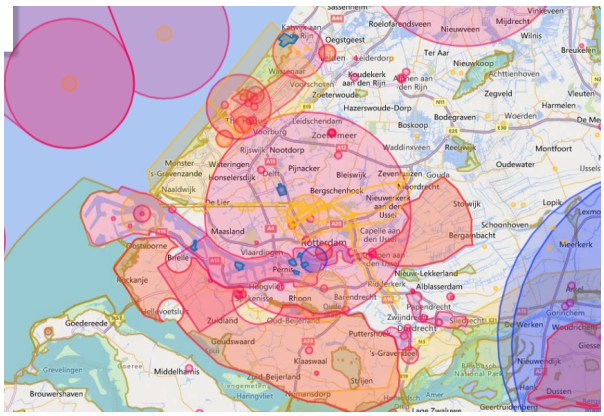

Figure 4.1: Flight restriction zones for drones in the area of Rotterdam [86]

Rotterdam The Hague Airport

RTHA is situated in the North of Rotterdam and has heavy implications for the no-fly zones, situated in Rotterdam. The Control Zone (CTR) of RTHA covers the city of Rotterdam in its entirety. This is a controlled airspace, where local air traffic control manages clearances, instruction and communications with air traffic. There are two prerequisites for conducting drone flight within the CTR[86]:

- 1. A permit must be granted by the Inspectorate for the Environment and Transport (ILT)
- 2. Clearance by Luchtverkeerleiding Nederland (LVNL)

Even when these two conditions are satisfied, the prescribed maximum altitude within the CTR of Rotterdam is 120 meters [86], which is in line with the maximum altitude for UAS as specified by EASA [16]. It is assumed that with the permit for ILT and clearance by LVNL drone operation within the airspace of Rotterdam is feasible.

Port of Rotterdam

A second area, causing restricted flight access is the port of Rotterdam situated in the South. Currently, the entire port of Rotterdam and industrial area is a no-fly zone for drone operations. However, the Port of Rotterdam is working together with the Ministry of Infrastructure and Water Management (I&W), ILT and the Ministry of Defence to create a U-space airspace prototype [72], which is a Unmanned Traffic Management system(UTM). The Port of Rotterdam expects the first vertiports to be installed in 2024 for testing and demonstration. Furthermore, they expect the first commercial flight of air taxis to be executed as soon as 2026. This illustrates that the Port of Rotterdam is very willing to cooperate in innovative processes involving drone operations. It is therefore assumed that the Port of Rotterdam has no impact on the flight routes for cargo drones and is a viable option for locating vertiports.

City centre

The city centre of the municipality of Rotterdam is a densely populated urban area. Although there are no official flight restrictions, there is a high amount of people present in the city centre at all times (traffic, stores, housing). As a result of this, there are high safety risks associated with flying over or locating a vertiport in the city centre. In order to compensate for these safety risks the city centre of Rotterdam could be treated as a no-fly zone and the optimization method should prohibit the placement of vertiports in the city centre. To give an idea of how large the area is, Figure 4.2 shows the city centre as defined by Google Maps.

Figure 4.2: City centre of Rotterdam as defined by Google Maps

Vital infrastructure and protected areas

Finally, there are several no-fly zones visible in Figure 4.1 that are a consequence of the location of vital infrastructure and protected areas [86]. These zones should be taken into account when placing vertiports as they should not be located inside these zones. Furthermore, placing vertiports in close proximity to these zones could limit the routes that a drone is able to take to land at the vertiport. Therefore, vertiport should also not be located near these zones.

4.2. Available (infrastructure) space

Assessment of the available infrastructure space is an interesting metric to take into account as it might prove a UAM network to be infeasible in the case that no vertiports could be placed in the area where they are recommended to be located. Furthermore, space availability does not refer simply to the area occupied by the vertiport infrastructure, but also to a suitable volume around it for allowing safe landing and take-off manoeuvres [31]. Assessing the available space in large areas such as the study area for this thesis is a complex and time-intensive task. Available space is also dependent on the size of the vertiports considered. In the context of on-demand mobility such as air taxis, smaller vertiports could be enough. In this case, it might be interesting to look at rooftop availability such as the work by Delgado Gonzales [53]. In cargo operations, placing vertiports on rooftops might be less preferable as more space is required and the cargo would have to be transported from the rooftop to ground level, introducing more logistic processes. Another study created a digital twin of the city of Bologna to asses different socio-economic variables as well as infrastructure space and rooftop suitability for vertiport placement [31]. This was done through the use of a Geographic Information System on which will be elaborated more in chapter 5.

What could be of interest for cities that consist of a lot of water such as Rotterdam, is to look at the option to locate vertiports on water. As mentioned in section 4.1, the port of Rotterdam is looking into the creation of a U-space airspace. With this in mind, placing vertiports on water instead of on land could be perceived as a saver option due to the lower risk of casualties in case of emergencies. This is especially interesting for bodies of water near high traffic and highly populated areas where, in terms of safety, it is not optimal to place a vertiport in that area itself as the vertiport could then be positioned close to an area with a potentially high demand.

4.3. Price of land

In the process of locating vertiports, it is beneficial for the developer to minimize costs. Therefore, it might be of interest to incorporate cost factors in the optimization model. A cost factor that is directly related to the location of a vertiport is the price of land. There is currently no literature that has been published that incorporates this metric in the decision-making process for vertiport positioning. Nevertheless, this metric could be of interest when considering the development and particularly financing side of the problem. A way of estimating the price of land could be to look at the price per squared meter of housing in the area of interest. Data should be available on the housing market and thus the price per squared meter of the Netherlands, for example, the company Walter Living [66] offers a map with information on the housing prices per municipality in Rotterdam itself and the surrounding area. Generally speaking, it can be seen that the price of land decreases as the distance from the centre of Rotterdam increases. This relationship could be used to make estimations on the price of land in the case that there is not enough data available.

4.4. Demand modelling

The parcel demand in the area of Rotterdam is an important metric to be modelled in order to determine the optimal locations of vertiports. A Multi-Agent Simulation System for Goods and Transport (Mass-GT) was developed by the TU Delft to assist decision-makers with the impact assessment of city logistic developments and policies [10]. The Mass-GT model was developed in Python and adopts the open source philosophy, inviting external users to make use of existing versions of the model and contribute to the further development of the model. Furthermore, the model incorporates four different types of stakeholders, being producers, customers, carriers, and local administrators. These stakeholders emerge from four different markets which are the commodity, logistics services, transport, and infrastructure markets. An extensive dataset with freight vehicle trip diary data was used to develop data-based simulation solutions and calibrate logistical choice models. This data was retrieved from the Central Bureau of Statistics (CBS) Netherlands. What is particularly

useful for this thesis is the data that the Mass-GT model uses. The data contains information about the warehouses, zones, and delivery demand.

Warehouses

The first data that can be acquired by extraction from the Mass-GT model is the location of warehouses. These locations are based on real life and are shown as orange squares in Figure 4.3. PostNL used these warehouses as distribution centres for parcel shipments. In the context of this thesis, these warehouses will be used as origin points of cargo. It is assumed that the warehouses can be used as vertiports where cargo drones can take off and land without restrictions. Cargo drones will fly from these locations to the selected vertiport locations which will in turn function as local distribution centres. Furthermore, in the scope of this thesis, it is assumed that the warehouses have an unlimited capacity for storage, charging and maintenance of the to-be-used cargo drones.

Zones and commodity demand

Other useful data that can be acquired from the Mass-GT model are the zones and the commodity demand associated with these zones. Figure 4.3 does not only show warehouse locations, but it also shows a division of the Rotterdam areas into zones. This can be seen in Figure 4.4 where parcel schedules are illustrated with arrows originating in the warehouse and ending at the destination zone. With this information, Origin-Destination (O-D) pairs can be constructed for the demand model. The Mass-GT model also contains data on the commodity demand for each of these zones. As this provides data on commodity flows from warehouses to delivery zones and the amounts this is very relevant for the scope of this thesis. This information will be used to model the demand throughout the area of Rotterdam.

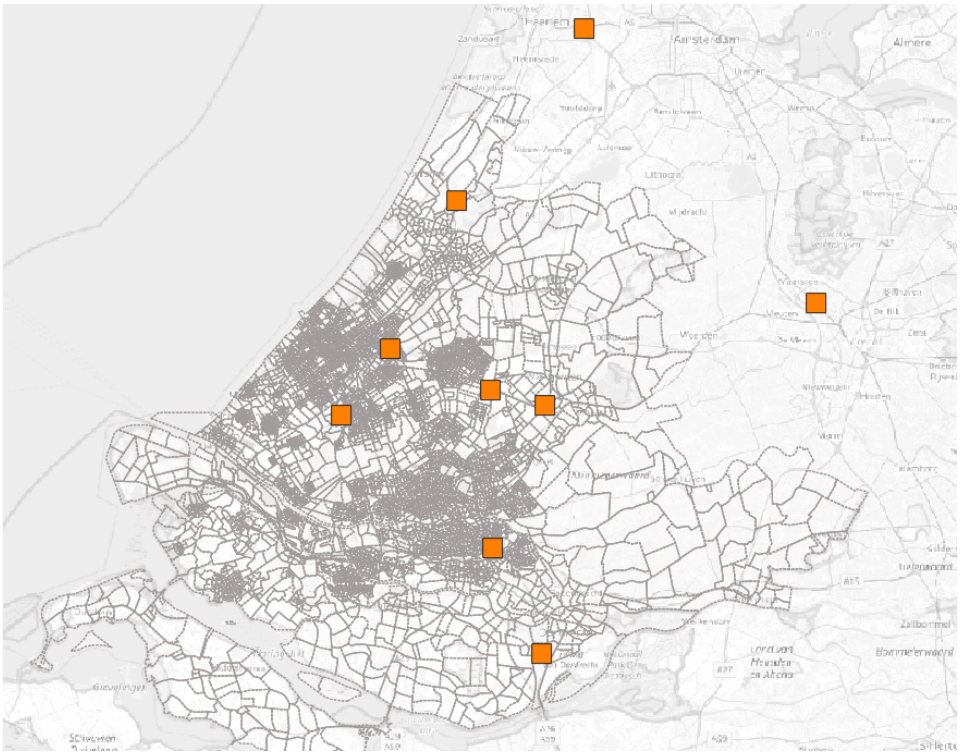

Figure 4.3: Warehouse locations extracted from the MASS-GT [10] model in QGIS [96]

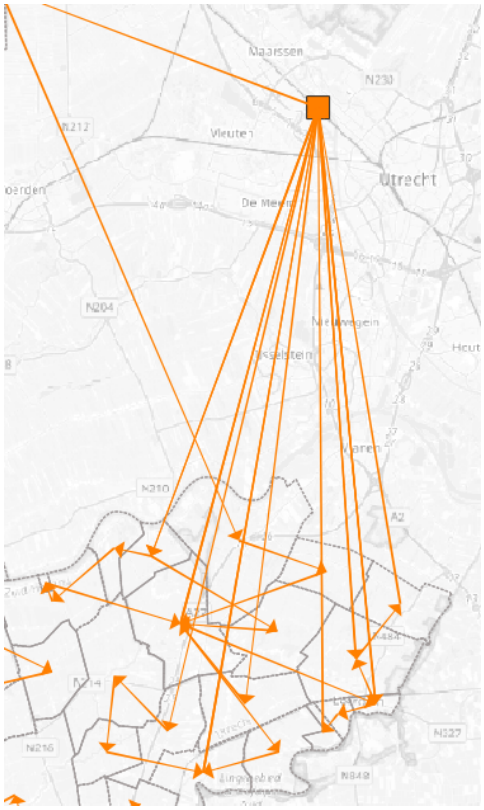

Figure 4.4: Example zones and parcel shipments extracted from the MASS-GT [10] model in QGIS [96]

5

Location selection and optimization methods

As there are several methods and techniques that can be used to assess the suitability and optimize the location of vertiports, this chapter will elaborate on some of these methods. The aim of this chapter is to map out the possible methods and algorithms that can be used to tackle the location optimization problem. First, section 5.1 describes the usage of Geographic Information Systems to assess the suitability of vertiport locations. Next, section 5.2 gives a description of the K-means algorithm that is often used to either select vertiport locations or reduce the solution space. This is then followed by section 5.3, describing the process of objective-based optimization and how the selection of vertiport locations is often optimized in literature. Finally, the chapter concludes with section 5.4 discussing several solution methods that could be used for the optimization. A trade-off between these solution methods is also included.

5.1. Geographic Information Systems

Geographic Information Systems (GIS) are used in literature to select suitable locations for vertiports. This differs from the k-means algorithm and objective optimization methods since it is not focused on optimizing the location but merely looking at potential options. At its core, GIS is a system that can be used to capture, store, analyze and visualize data in a spatial context. With the help of GIS, various layers of information can be integrated, often in the form of maps. This allows for the exploration of patterns, relationships and trends. An example of this is the demand data presented previously in section 4.4. While the data on demand itself is most important, GIS-based systems can help visualize the system and understand relationships or patterns.

In literature, GIS has been used to assess factors like socio-economic variables, points of interest, and existing heliports. Locational constraints have also been mapped, such as no-fly zones or noise-restricted zones. For example, Fadhill [46] assigned weights to various socio-economic factors through expert opinions and interviews. This allowed for the depiction of regional suitable areas, however, not precise vertiport locations. Other studies, like the one by Brunelli et al. [31], have applied GIS to allocate vertiports based on geographic and socio-economic data within a digital twin model of the area, identifying suitable locations, and considering factors like travel time and air routes. Additional studies have examined rooftop suitability using Lidar data and land use information. These assessments are essential for identifying viable vertiport sites in densely populated urban areas, while regulatory considerations and geofences play a crucial role in airspace allocation and safety. In summary, GIS aids in the complex task of selecting the most suitable vertiport locations for urban air mobility, taking into account a wide array of geographic and socio-economic factors while adhering to safety regulations and practical considerations. While it is very useful for selecting suitable locations, it does not make network optimization possible in terms of being able to minimize travel time or maximize satisfied demand for example. An overview of literature that uses GIS for vertiport location selection is shown in Table 5.1.

Table 5.1: Literature using GIS to find suitable vertiport locations

Author	Application	Variables	Constraints
Gonzalez (2020) [53]	On-demand mobility	Population, population density, median household incomes,	Rooftop footprint and flatness
Fadhill (2018) [46]	On-demand mobility	Population density, median income, office rent price, points of interest, major transport nodes, annual transport cost, job density, extreme commuting, existing noise	No fly zones on schools and military areas
Kim and Yoon (2021) [61]	On-demand mobility and parcel delivery	Population density on daytime and night-time	Airspace reduction caused by geofences
Brunelli et al. (2022) [31]	On-demand mobility	population density, job locations, obstacle clearance, building type	

5.2. K-means algorithm

Another type of approach to vertiport location optimization is the K-means algorithm as described by Schütze et al. [23]. This is a clustering algorithm that groups data points into a number of K clusters. The different clusters are identified by minimizing the average squared Euclidean distance between cluster centres and the respective data points. A cluster centre is defined as the mean or centroid $\vec{\mu}$ of cluster ω. The centroid can be calculated as shown in Equation 5.1.

$$\vec{\mu}(\omega) = \frac{1}{|\omega|} \sum_{\vec{x} \in \omega} \vec{x} \tag{5.1}$$

To measure how well the centroids represent the data point of their cluster, the residual sum of squares (RSS) can be calculated as shown in Equation 5.2. This is the squared distance between the centroid and each vector, summed over all vectors.

$$RSS = \sum_{k=1}^{K} \sum_{\vec{x} \in \omega_k} |\vec{x} - \vec{\mu}(\omega_k)|^2 \tag{5.2}$$

The first step in the K-means algorithm is the random selection of initial centroids called the seeds. The algorithm then moves the centroids around in space in order to minimize the RSS. This is done iteratively in two steps until a stopping criterion is met. The first step is to reassign data points to the cluster with the closest centroid and the second step is to recompute the location of the centroid based on the current data points that are assigned to its cluster. Several stopping criteria could be implemented:

- **Fixed number of iterations**
  Fixing the number of iterations limits the runtime of the algorithm. The risk of this criterion is that the quality of the clustering could be bad due to an insufficient number of iterations.

- **Assignment of data points to clusters does not change**
  This condition will produce a good quality of clustering but might result in a high runtime.

- **Centroids do not change between iterations**
  This is equivalent to the assignment of data points to clusters not changing.

- **RSS falls below a prespecified value**
  This ensures clustering of desired quality. However, this criterion should be combined with a limit on the number of iterations to ensure termination.

- **RSS decrease falls below a prespecified value**
  If the decrease in RSS between iterations is small, it indicates that the algorithm is close to convergence. Again, this criterion should be combined with a limit on the number of iterations to ensure termination.

Algorithm Algorithm 1 shows the k-means algorithm.

Algorithm 1 K-means algorithm [23]

K-MEANS ($\{\vec{x}_1, \ldots, \vec{x}_N\}$, K)
($\vec{s}_1, \vec{s}_2, \ldots, \vec{s}_K$) ← SELECTRANDOMSEEDS(t$\{\vec{x}_1, \ldots, \vec{x}_N\}$, K)
for k ← 1 **to** K
do $\vec{\mu}_k \leftarrow \vec{s}_k$
while stopping criterion has not been met
do for $k \leftarrow 1$ to K
    do $\omega_k \leftarrow \{\}$
    for $n \leftarrow 1$ **to** N
    do $j \leftarrow \arg\min_{j'} \left|\vec{\mu}_{j'} - \vec{x}_n\right|$
        $\omega_j \leftarrow \omega_j \cup \{\vec{x}_n\}$ (reassignment of vectors)
    for $k \leftarrow 1$ **to** K
    do $\vec{\mu}_k \leftarrow \frac{1}{\omega_k|} \sum_{\vec{x} \in \omega_k} \vec{x}$ (recomputation of centroids)
return $\{\vec{\mu}_1, \ldots, \vec{\mu}_K\}$

In UAM context, the K-means algorithm is very interesting as it minimizes the distance between the potential vertiport location and the O-D points. This has often been used in literature for vertiport location optimization of on-demand air mobility (air taxis) [24, 55, 65, 82, 94]. It is important to note that the number of vertiports is an input to the algorithm. This means that the traditional algorithm is unable to determine the optimal number of vertiports to be used. In order to compensate for this drawback some alterations to the K-means algorithm have been proposed. The iterative K-means algorithm allows for flexibility in the number of clusters or vertiports. The approach starts with a set number of clusters after which the number of clusters is iteratively increased until a number of constraints are satisfied [82, 94].

A second drawback to the K-means algorithm is that it initializes with a random solution. This has a significant impact on the final solution as the algorithm is not guaranteed to find the global optimum solution [102]. In order to improve the quality of the final solution some studies propose the warm start solution technique [82, 94]. The warm start solution technique provides a high-quality initial seed to the k-means algorithm that can be based on several aspects.

5.2.1. Clustering quality assesment

As mentioned before, the K-means algorithm does not guarantee the global optimum solution. Therefore, the quality of the cluster is often evaluated. Two methods for assessing the quality are the silhouette technique and the Davies-Bouldin Index.

Silhouete technique

The silhouette technique is a method that is used to quantify the quality of clusters as proposed by Rousseeuw [89]. The Silhouette technique calculates the ratio of the average distance between a certain point, i, and other data points within the same cluster to the average distance between the point, i, and all other data points in other clusters [65]. The value representing this ratio, $s(i)$, is given by Equation 5.3.

$$s(i) = \frac{b(i) - a(i)}{\max\{a(i), b(i)\}}, -1 \leq s(i) \leq 1 \tag{5.3}$$

Where $a(i)$ is the average distance from point i to all other data points in its own cluster and $b(i)$ is the minimum average distance from point i to all data points from the other clusters. The value of $s(i)$ can take any value between -1 and 1. The closer to 1, the better the quality of the clustering. A negative or small value of $s(i)$ means that the value K is either too small or too large. The silhouette technique provides accurate results, but has the drawback that it involves computing the pairwise distances between each set of data points within a cluster. This makes the silhouette technique, computationally heavy for large data sets.

Davies-bouldin Index

The Davies-Bouldin Index (DBI), as proposed by Davies and Bouldin [9], aims to determine the appropriate number of clusters within a dataset with a preferable lower value. The DBI is the ratio of the sum of inter-cluster scatter to the between-cluster separation [84]. To calculate the DBI, two components are essential to know:

- 1. The distance between the cluster centres and their assigned data points for the inner-cluster scatter.
- 2. The distance between different cluster centres for the cluster separation.

The inner cluster scatter can be calculated as shown in Equation 5.4 [94].

$$S_i = \sqrt[p]{\frac{1}{|C_i|} \sum_{X_j \in C_i} (X_j - A_i)^p} \tag{5.4}$$

Where X_j is a member of cluster C_i and A_i is the centroid of cluster C_i. As, in UAM context, the data points are geographical coordinates, the distance between data points is a spherical distance. This can be calculated as shown in Equation 5.5.

$$d_{ij} = r \times \theta_{ij} \tag{5.5}$$

Where r is the radius of the earth and θ_{ij} is the angle between point i and j. This angle can best be estimated using the haversine formula, resulting in Equation 5.6 [70].

$$d_{ij} = r \times \text{hav}^{-1}\left(\text{hav}\left(\gamma_j - \gamma_i\right) + \cos\left(\gamma_i\right) \times \cos\left(\gamma_j\right) \times \text{hav}\left(\lambda_j - \lambda_i\right)\right) \tag{5.6}$$

Where γ_i is the lattitude of point i and λ_i is the longitude of point i. This transforms Equation 5.4 into Equation 5.7.

$$S_i = \frac{1}{|C_i|} \sum_{X_j \in C_i} d_{ij} \tag{5.7}$$

To calculate the cluster separation ($B_{a,b}$) between point cluster a and b, the haversine formula can also be used. This separation can be calculated as shown in Equation 5.8.

$$B_{a,b} = r \times \text{hav}^{-1}\left(\text{hav}\left(\gamma_b - \gamma_a\right) + \cos\left(\gamma_a\right) \times \cos\left(\gamma_b\right) \times \text{hav}\left(\lambda_b - \lambda_a\right)\right) \tag{5.8}$$

For any two clusters a and b, the ratio of the sum of inter-cluster scatter to the between cluster separation ($R_{a,b}$)is then given by Equation 5.9.

$$R_{a,b} = \frac{S_a + S_b}{B_{a,b}} \tag{5.9}$$

Finally the DBI can then be calculated using Equation 5.10.

$$DBI = \frac{1}{K} \sum_{a=1}^{K} \left(\max_{a \neq b} R_{a,b}\right) \tag{5.10}$$

The advantage of the DBI, in comparison with the silhouette technique, is that the DBI requires a lot less computational power, making it more suitable for large datasets.

5.2.2. Overview

An overview of the literature that used the k-means algorithm for vertiport location optimization is given in Table 5.2. The K-means algorithm is only used in literature for on-demand mobility applications in UAM context. Nevertheless, it seems to be a very interesting method of clustering data and could very well be used for scaling down the size of the optimization problem.

Table 5.2: Overview of literature employing the k-means algorithm for vertiport location optimization

Author	Application	Approach	Solution assesment
Lim and Hwang (2019)[65]	On-demand mobility	Traditional k-means	Silhouette technique
Rajendran and Zack (2019)[82]	On-demand mobility	Iterative k-means with multimodal WS	Davies-Bouldin index
Jeong et al. (2008)[24]	On-demand mobility	Traditional k-means	Silhouette technique
Sinha and Rajendaran (2022)[94]	On-demand mobility	Iterative k-means with multicriteria WS	Davies-Bouldin index
Holden and Goel (2016)[55]	On-demand mobility	Traditional k-means	-

5.3. Objective based optimization

Objective based optimization is a powerful and versatile tool that is used often in engineering. In essence, objective based optimization tries to find an optimal solution by defining clear objectives to be achieved. The primary objective is to either maximize or minimize a certain parameter while subjecting it to certain constraints and limitations. These objectives can range from minimizing costs, maximizing revenue, and optimizing resource allocation to improving performance metrics such as efficiency, reliability, or throughput rates. A mathematical model is created with the ultimate aim of finding a set of input parameters or decision variables that lead to the best possible outcome, which is referred to as the global optimum. To find the global optimum, objective based optimization employs mathematical modelling, algorithms, and computational tools to explore the often large solution space systematically. This method has been used for vertiport location optimization multiple times in existing literature and is a promising candidate for this thesis. There are several approaches that are used in literature, which will be discussed further.

5.3.1. Hub Location Problem

In literature, vertiport location optimization is most commonly modelled as a Hub Location Problem (HLP). Classically, HLPs consist of locating hub facilities and designing hub networks so as to optimize a cost- or service-based objective. Their key feature lies in the use of transshipment, consolidation, or sorting points, called hub facilities, to connect a large number of origin-destination (O-D) pairs using a small number of links [62]. The connection to UAM context is then easily made as the vertiports will serve as hub facilities that lie in between the warehouses (origin) and the final destination of packages.

The first mathematical formulation of the HLP was formulated by O'Kelly [73]. This formulation has been used and adapted in literature for determining vertiport locations [25, 29, 43, 83, 110]. Generally, depending on the objective there are three types of the HLP [40].

- **p-hub median**
  In the p-hub median problem, the objective is to minimize the total transportation cost, where the transportation cost is usually defined as the travel distance or the travel time from origin to destination. In this type of problem, p is the number of hubs that are used. This is typically an input parameter. A difficulty with the p-hub medium problem is that is NP-hard in nature. As a result, heuristics are often used to solve this problem.

- **p-hub center**
  The p-hub centre formulation was originally proposed by Campbell [7] and is defined on the Mini-Max criterion. This criterion focuses on minimizing the maximum distance between O-D pairs. Typical applications of this type of HLP are emergency facilities.

- **p-hub covering problem**
  The p-hub covering problem tries to maximize the coverage that can be achieved by a set of p amount of hubs. The p-hub covering probelm was also originally proposed by Campbell [7] and can be further split into two problems. These are Hub set covering location problem as described by Kara and Tansel [60] and the p-Hub maximal covering location problem [108].

Next to these three main types, HLP's also have several characteristics. For example, there are two types of assignment structures. The first structure is single allocation. In single allocation each node is served by a single hub and all the incoming and outgoing flows of each node are routed through that hub. Secondly, in multiple allocation, flows can be sent and received through more than one hub [78]. Furthermore, the HLP can also be classified as either capacitated or incapacitated.

As mentioned before, for vertiport location optimization the HLP model has been used multiple times, with several papers adding different extensions to the model. One of the papers minimizes the total travel cost [43]. This includes the operational costs and the fixed costs. The paper adds to existing literature by adding collision risk cost to the HLP model. Furthermore, it applies the Reformulation Linearization Technique (RLT) [51] to linearize the objective function. Another paper that also used the HLP model proposes two alternate objectives [83] being the maximization of air taxi ridership or the maximization of revenue.

Table 5.3 gives an overview of papers that use an HLP model for vertiport location optimization, their objective, and the assumptions that were made that are of interest to the use case as selected for this thesis.

Authors	Optimization objective	Assumptions
Shin et al. (2022)[43]	Minimize total travel cost	1. Demand does not vary over time 2. Vertiport can be located at census tract 3. Euclidian distance for distance between vertiports
Rath and Chow (2022)[83]	Maximize air taxi ridership Maximize revenue	1. No infrastructure cost considered Number of vertiports is considered as the budget constraint 2. No capacity limit 3. Single allocation 4. No congestion effects considered 5. Existing helicopter landing spaces on airports serve as landing spots
Macias et al. (2023)[25]	Maximize total travel time saved	1. One vertiport per census tract
Willey and Salmon (2021)[110]	Maximize difference between travel time UAM and existing ground systems	-
Wei et al. (2020)[29]	Minimize aggregate demand-weighted distance	1. Capacity is constant for all facilities

Table 5.3: Literature using an HLP model for vertiport location optimization

5.3.2. Location allocation problem

Next to the HLP, the Location Allocation Problem (LAP) has also been used to optimize vertiport locations. LAP tries to find the optimal locations for facilities when given a set of demand nodes. The main difference between the LAP and the HLP is that the LAP does not necessarily consider the facilities to be hubs. It is also generally more used for problems that focus on the demand side and do not have set origin points such as the warehouses considered in the selected use case of this thesis. The LAP is most often used for setting up air taxi networks in UAM context as these are primarily focused on origin nodes. Origin nodes that have a high demand are often also in high demand as destinations. This aspect makes it very suitable to apply the LAP to. Furthermore, the only paper considering the LAP for delivery of goods only makes use of one warehouse which is not taken up in the optimization [50]. What is meant by this is that the locations of the vertiports are not based on the location of the warehouses, but it is purely based on the demand locations of parcels. In general, the HLP is a type of LAP with a focus on determining the location of hubs instead of all types of facilities.

5.4. Solution methods

There are several approaches proposed in literature to solve an objective based optimization problem. An overview of these approaches is shown in Figure 5.1. When an exact solution is needed for a problem, methods such as Integer Programming and Bender Decomposition can be used. In the case that better computational efficiency is needed and a close-to-optimal solution is acceptable, specifically designed heuristic algorithms or meta-heuristics can be used. The meta-heuristics that were used most in literature for the HLP are the Tabu Search, Variable Neighbourhood Search, Genetic Algorithms and Simulated Annealing.

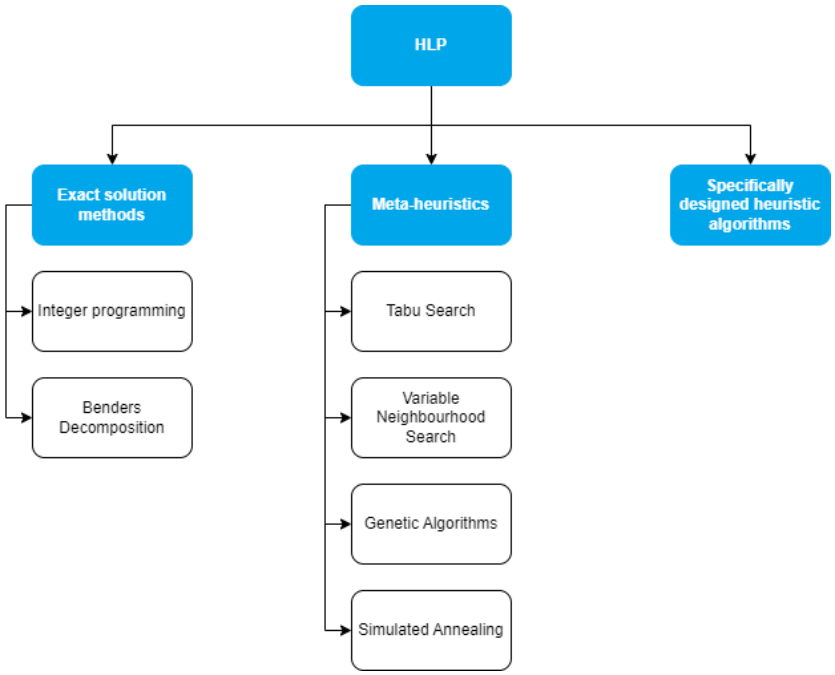

Figure 5.1: Solution methods used to solve the HLP

5.4.1. Integer Programming

Integer programming (IP) is a mathematical programming technique that can be used to solve optimisation problems. In IP problems, an objective function is set up and subjected to a set of constraints. These variables can only take on integer values. There are several types of integer programming that can be used depending on the problem at hand. Some problems require variables that do not assume integer values. This is known as Mixed Integer Programming (MIP), where only some variables can only take integer values. Furthermore, in the case that no non-linear features are used in a MIP or IP model it is classified as Mixed Integer Linear Programming (MILP) or Integer Linear Programming (ILP). The process of IP solving typically involves algorithms that explore different combinations of feasible solutions to determine the optimal solution. Techniques such as branch and bound, branch and cut are often used to solve IP problems. Moreover, there are several online IP solvers currently available for use. Examples of this are Gurobi and CPLEX, with Gurobi being the most commonly used solver found in literature for problems involving vertiport location problems. The downside of IP optimization approaches is that, although suitable for smaller HLPs, computation time can grow exponentially when considering bigger HLPs [41]. Furthermore, although commercial solver are becoming ever more sophisticated, their performance is still well below that of carefully designed custom algorithms, due to the very challenging nature of the more complex HLPs [42].

5.4.2. Benders decomposition

Some studies have used Benders Decomposition algorithm to tackle the HLP [41]. In 1962, Bender [5] proposed a partitioning method for solving mixed-variable programming problems. The approach is a relaxation algorithm for a problem, partitioning it into two simpler problems. These consist of an integer problem known as the Master Problem (MP) and the Sub Problem (SP). The MP becomes a relaxed version of the original problem with the set of integer variables and its accosted constraints. On the other hand, the SP becomes the original problem with the values of the integer variables temporarily fixed by the MP [11]. Each one of the

two simpler problems is solved iteratively, one at a time. At each iteration, a new constraint which is known as Benders cut is added to the MP, which is originated by the dual problem of the SP. This continues until the objective function value of the optimal solution to the MP is the same as that of SP. An example of the Benders decomposition algorithm as used for an uncapacitated multiple allocation HLP is shown in Algorithm Algorithm 2, where UB is defined as the upper bound and LB is the lower bound. Furthermore $z^{\star}_{MP}$ and $z^{\star}_{SP}$ refer to the optimal solutions obtained by the current MP and SP respectively. Finally, y_k is the decision variable deciding whether or not a hub is built a location k and a_k are the cost associated with building a hub at location k.

Algorithm 2 Classical Benders algorithm [11]

1 Set UB = $+\infty$, LB = 0
2 If LB = UB –> stop. Terminate, we have obtained the optimal solution of the original problem
3 Solve the MP , obtaining $z^{\star}_{MP}$ and the optimal values for the integer variables y_k
4 Set LB = $z^{\star}_{MP}$ and update y_k in a new dual problem
5 Solve the dual problem
6 Add a new Benders cut to the MP
7 If $z^{\star}_{SP} + \sum_k a_k y_k <$ UB , set UB = $z^{\star}_{SP} + \sum_k a_k y_k =$. Go to step 2

The computational efficiency of the Bender decomposition algorithm is dependent on three aspects:

- 1. The number of iterations necessary to obtain global convergence
- 2. The time needed to solve each SP at each iteration
- 3. the time and computer effort demanded at solving each MP on each iteration

It was found that the third aspect can be identified as the bottleneck as it takes a considerable amount of time to find the optimal solution of the MP at each iteration [11].

5.4.3. Meta-Heuristics

As the HLP can quickly run up computational times for exact solving methods when considering larger or more complex types, heuristic methods might be preferable. Heuristic methods are used for finding a feasible solution that is relatively close to optimal. The downside of such a solution method is that heuristics tend to be ad hoc in nature, meaning that each method is designed to fit a specific problem type rather than having a variety of applications. This problem is resolved with the introduction of meta-heuristics. This is an overarching approach that offers a general framework and strategic principles for creating a tailored heuristic method to address a specific type of problem [63]. This section aims to discuss several of these meta-heuristics, such as Tabu Search, Variable Neighbourhood Search, Genetic Algorithms and Simulated Annealing, that could be of interest to apply in the proposed problem of this thesis.

Tabu Search

The tabu search algorithm, as first proposed by Glover [52], explores promising areas to hold good solutions by rapidly eliminating unpromising areas that are classified as tabu [63]. Furthermore, it incorporates intuitive concepts to break free from local optima. A flowchart describing the tabu search algorithm is shown in Figure 5.2. The algorithm initiates with a feasible trial solution. It then explores the solution space by making small modifications or moving to neighbouring solutions. The quality of each candidate solution is assessed using an objective function. The best solution in the candidate list is cross-referenced with the existing tabu list and the optimal solution and tabu list are both updated when the candidate solution is not already in the tabu list. This continues until a certain stopping criterion is met. This could for example be a fixed amount of runtime or a fixed number of iterations without improvement of the objective value. Moreover, the algorithm will also stop when there are no feasible moves into the local neighbourhood of the trial solution.

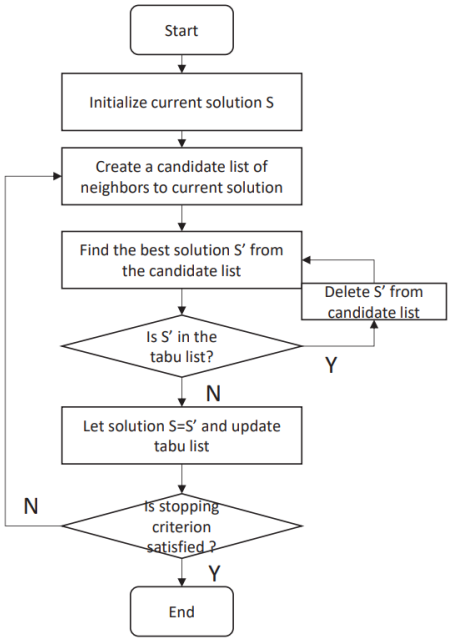

Figure 5.2: Flowchart of the tabu search algorithm

Although the tabu search algorithm has not been applied in studies considering UAM context yet, it has been used multiple times to solve the HLP [22, 58, 67]. Furthermore, tabu search is also often combined with a greedy heuristic to improve the allocation part of the nodes to hubs. Nodes are then reallocated to hubs and the reallocation that results in maximum gain is implemented. Computational findings indicate that such a local search significantly improves solution quality without immoderately increasing computation times [75].

Variable Neighbourhood Search

The Variable Neighbourhood Search (VNS) was first introduced by Mladenovic and Hansen [69]. The algorithm has been commonly applied to solve large-scale problems in recent years. In VNS, an initial solution is followed up by a sequence of local searches that are used to obtain local optima [27]. The general idea behind VNS is to combine multiple local search procedures. These are each defined by a different "neighbourhood" structure. This results in the solution space being explored more thoroughly. A neighbourhood refers to a set of solutions that are close to the current solution. VNS consists of the following steps:

- 1. Initialize with a feasible solution.
- 2. Apply local search procedures within the first neighbourhood structure to find a better solution. For this often the Variable Neighbourhood Descent (VND) method is chosen.
- 3. If the solution found in step 2 is better than the current best solution, update the current best solution.
- 4. Move to a different neighbourhood structure. This is often done using specific strategies which are selected to suit the specific problem.
- 5. Iterate steps 2-4 until a predefined stopping criterion is met. This could be a maximum number of iterations, a time limit, or a convergence condition.

VNS can escape local optima and explore a broader range of solutions by cycling through different neighbourhood structures. This potentially leads to a more globally optimal solution. Literature suggests that VNS has relatively good computational time for several types of HLP, however, due to the fact that a local search algorithm as well as several strategically chosen neighbourhood structures have to be set up, the implementation complexity and time of VNS is relatively high as compared to other meta-heuristics.

Genetic Algorithm

Another meta-heuristic to be discussed is the Genetic Algorithm (GA). A genetic algorithm is inspired by the process of natural selection and genetics. A flowchart of how a standard GA works is shown in Figure 5.3. The algorithm starts with a population consisting of feasible potential solutions which have been obtained through some heuristic method. These are often called "chromosomes" or "individuals." The fitness of each of these solutions is then evaluated through the use of a fitness value, which is the result of a fitness function. This function quantifies how well each of the solutions performs in the context of the problem. The goal of the algorithm is to either maximize or minimize the fitness value. The next step in GA is selection. Some of the existing chromosomes are chosen to become parents for the next generation, based on their fitness. This step simulates the concept of "survival of the fittest" by assigning higher probabilities of being chosen to solutions that have a better fitness. The selection step is followed by crossover. The pairs of chromosomes that are selected are combined to create new solutions. The offspring are created by utilizing genetic operators. There are several methods for crossover operators available such as single-point, two-point, k-point and arithmetical crossover [34]. Similarly, there are also several methods available for the mutation operator which is used in the next step. In the mutation step, several individuals in the population may undergo random changes, similar to the process of mutation in real-life genetics. This results in the introduction of genetic diversity into the populations, which explores new regions of space. This can help overcome local optima in the optimization process. The existing population is then often replaced by the offspring as the population size is typically kept constant. The final step is the termination of the algorithm. Termination happens when a termination criterion is satisfied, such as a predefined number of iterations, runtime or a satisfactory solution.

GAs are highly adaptable and can be applied to a wide range of optimization problems. It has been used to solve the HLP multiple times in literature, however, not in the context of UAM. GAs are particularly suited for problems with multiple local optima, where traditional optimization techniques may get stuck. The GA has the following advantages [20]: (1) it does not require continuity or differentiability on functions; (2) it may search a vast tract of feasible areas; and (3) it uses probabilistic rather than deterministic transition rules. However, it should be noted that it is important to fine-tune the algorithm parameters as well as design the fitness function carefully to achieve effective results.

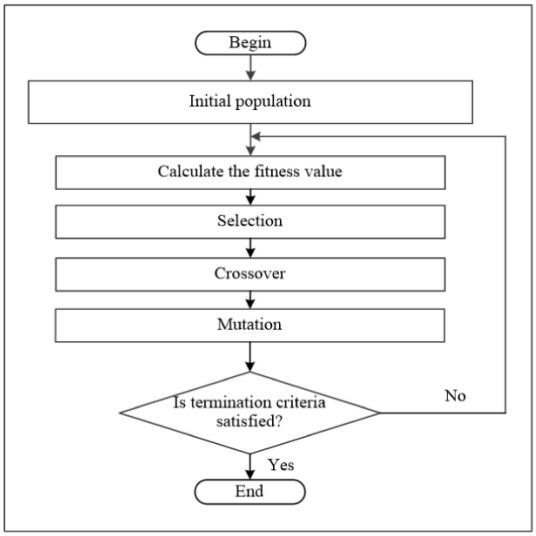

Figure 5.3: Flowchart of Genetic algorithms [34]

Simulated Annealing

The final meta-heuristic to be discussed is Simulated Annealing (SA). The SA algorithm is probabilistic based and inspired by the annealing process in metallurgy. The basic concept of SA is to explore a solution space iteratively by modifying the current solution and evaluating the quality of the new solution. This is done through the guidance of a temperature parameter that controls the probability of accepting worse solutions. As the algorithm progresses, the temperature is decreased, which results in a decrease of the likelihood that a

worse solution is accepted. This enables the algorithm to converge towards a better solution.

Figure 5.4 shows a flow diagram of the SA algorithm [8]. It starts with an initial solution to the problem and the definition of a temperature schedule that decreases over time. In each iteration, a small random change to the current solution is made to generate a neighbouring solution. The quality of the neighbouring solution is then assessed using the objective function. If the neighbouring solution is better, it is accepted as the new current solution. On the other hand, if the solution is worse, it is accepted with a probability that depends on the current temperature and how much worse the solution is as compared to the current solution. After a certain number of iteration steps the temperature is lowered according to a temperature schedule. As temperature decreases, the algorithm becomes more selective, favouring better solutions. Finally, the algorithm terminates when a preset lower temperature bound is reached.

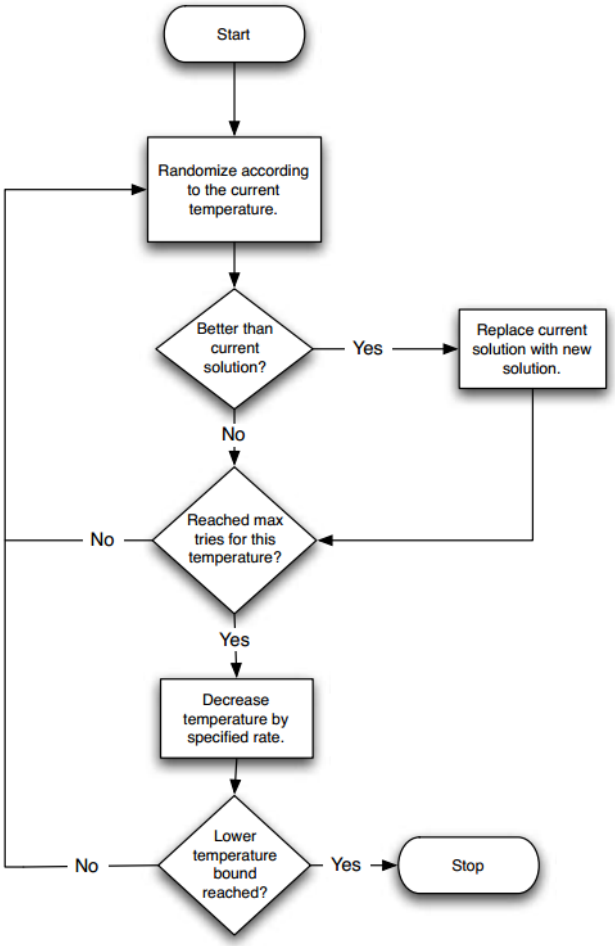

Figure 5.4: Flowchart of the Simulated Annealing algorithm [8]

5.4.4. Overview and trade-off

As described before there are several ways of solving an objective-based mathematical optimization problem. These consist of exact solving, generally done with online commercial solvers such as Gurobi and CPLEX, or heuristic-based solving. The exact solution methods that are generally used for the HLP are Integer Programming and Bender Decomposition. It was found that, in UAM context, the IP approach is always chosen in the case of exact solution methods. Furthermore, it was found that although exact solution methods provide a globally optimal solution, they do not perform well in terms of computational time and scalability. In more complex examples of the HLP, meta-heuristics can be used to find a close-to-optimal solution with considerably less computational time. It was found that in UAM context, only GA and VNS were used for the HLP, whereas tabu search also presents itself to be an interesting method for solving complex HLPs. An overview of

the literature that uses objective-based optimization in UAM context and the corresponding objectives and solution methods is shown in Table 5.4.

Table 5.4: Overview of the solution methods used for vertiport location optimization

Authors	Optimization objective	Solving method
Willey and Salmon (2021) [110]	Maximize the difference between the expected travel time on the proposed UAM network and that of the existing ground transportation network	Heuristics
Daskilewicz et al. (2018) [50]	Maximize the cumulative time saved in commuting throughout the entire network	IP
German, Dakilewicz et al. (2018) [50]	Maximize demand served, subject to a limit on how many vertiports can be constructed	IP
Macias et al. (2023)[25]	Minimize total cost of the UAM system	IP
Wu and Zhang (2021) [109]	Minimize the generalized travel cost for all users, including the costs for pure ground transportation and multimodal UAM service	IP
Rath and Chow (2022) [83]	Two separate models: 1. Maximize total air taxi ridership 2. Maximize air taxi revenue	IP
Zeng et al. (2020) [44]	Maximizing existing and potential demand coverage and area coverage and also minimizing accumulated service distance	GA
Shin et al. (2022) [43]	Minimize total cost travel cost, facility cost, and collision risk cost	GA
Chen et al. (2022) [27]	Find the most economical location for all grid cells	VNS

A table containing a trade-off between the different solution methods can be seen in Table 5.5. The trade-off is based on several criteria with assigned weighting. A weighting of either 1,2 or 3 has been assigned to each of the criteria with 3 being regarded as the most important and 1 being the least important. Similarly, methods can also score either 1,2,3 with 1 being the worst score and 3 being the best.

As mentioned, the trade-off is based on several criteria. Overcoming local optima is an important factor as the HLPs for larger networks often have a large solution space and will therefore also have many local optima. As IP and Bender Decomposition are exact solution methods, they will find the global solution, hence scoring high on this criterion. Scalability refers to the ability to expand the problem when using this solution algorithm. Computational time refers to how quickly the method is able to converge to a good solution. Implementation time refers to the estimated time it takes to implement the method in the model. This differs from implementation complexity in the fact that complexity refers to the complexity of the theory behind the solution method. Some solution methods could have Python libraries available resulting in a low implementation time while it might take more time to completely understand the strategy and theory. For example, VNS has a bad score in implementation complexity as a strategy must be chosen for varying the neighbourhoods on which the quality of the solution depends. Finally, contextual usage refers to whether or not the method has been used in the context of UAM. Methods that have not been used in UAM context while they have been used a multiple of times for other HLPs are of more interest than methods that have been used in this context a lot.

From the trade-off table it becomes apparent that tabu search, overall, scores the best. This is mainly due to the fact that HLPs are NP-hard problems making exact solution methods not ideal in terms of computational efficiency and scalability. Furthermore, the outperformance of the tabu search algorithm as compared to GA and SA is in line with the findings of Arostegui Jr. et al. [35], which states that, overall, the tabu search algorithm performs the best for facility location problems. Moreover, it should be noted that changes in the weighting, such as an equal weight for all criteria or a 1-3-9 weighting system, do not change the outcome of the trade-off. Only, in the case that computational time and implementation time and complexity do not matter, the exact solution methods score better.

Table 5.5: Solution methods trade-off table

	Weight	IP	Bender Decomposition	Tabu Search	VNS	GA	SA
Overcoming local optima	**3**	3	3	2	2	1	1
Scalability	**2**	1	1	3	2	2	3
Computational time	**2**	1	1	3	2	2	2
Implementation time	**2**	3	1	2	1	2	2
Implementation complexity	**1**	3	3	2	1	2	3
Contextual usage	**1**	1	3	3	2	2	3
Weighted sum		23	21	27	19	19	23

6

System Requirements and Assumptions

The system that is proposed to be developed entices selecting the optimal locations for vertiports when considering the usage of UAVs for middle-mile cargo delivery. This can be modelled as an HLP that considers many metrics, such as capacity, safety, regulations, and environmental impact that are related to deciding and optimizing the location. This chapter aims to list the requirements and assumptions that should be considered for the model. In section 6.1 the requirements that are set to the to-be-developed model are listed and a level of importance is assigned to them. Next, section 6.2 lists the assumptions that will be made in the development of the model. Finally, section 6.3 discusses some aspects that are considered to be out of the scope of this thesis.

6.1. Requirements

The requirements that were identified are shown in Table 6.1. The corresponding section from which the requirements stem and the level of importance are also given. For the level of importance, a score of either 1,2 or 3 is assigned with 3 being the most important and 1 representing requirements that are of least importance. In a perfect world, all requirements that were identified are met. However, there is not enough data available to correctly represent every element. Additionally, this thesis also has a set amount of time and there will not be time to include every single element. Therefore, the level of importance can be used to determine whether or not a requirement is imposed on the system.

Table 6.1: System requirements

Identifier	Category	Requirement	Section	Importance
Req-Are-001	Area	Vertiports shall be sized accordingly to the area that is available in the selected zone	3.1	1
Req-Are-002	Area	Vertiports shall be located only in areas that have enough infrastructural space available	4.2	1
Req-Cap-001	Capacity	All vertiports shall have enough capacity for the assigned amount drones throughout the day	3.2	2
Req-Cap-002	Capacity	The ELZs shall have enough capacity to accommodate for TBD emergency landings throughout the day	3.2	2
Req-Met-001	Environment	The optimization model shall try to minimize the effects of noise pollution	3.4	1
Req-Met-002	Environment	The optimization model shall try to minimize the effects of visual pollution	3.5	1
Req-Res-001	Flight restrictions	Vertiports shall not be positioned within TBD metres of RTHA	4.1	3
Req-Res-002	Flight restrictions	Vertiports shall not be positioned within TBD metres the city centre of Rotterdam	4.1	3
Req-Res-003	Flight restrictions	Vertiports shall not be positioned within TBD metres of vital infrastructure and protected areas	4.1	2
Req-Saf-001	Safety	Drones shall at all times be within TBD distance from a emergency diversion vertiport or ELZ	3.7	3
Req-Saf-002	Safety	Vertiports shall not be positioned in zones with a aggregate height of TBD metres	3.7	3
Req-Saf-003	Safety	Vertiports shall not be positioned in prohibited areas (e.g. the city centre of Rotterdam)	3.7	3
Req-Saf-004	Safety	Vertiports shall not be positioned within TBD metres from each other in order to minimize risk of collision between drones	3.7	3
Req-Veh-001	Vehicle	All vertiport locations shall be reachable within existing drone capabilities	2.2	3

6.2. Assumptions

An overview of the assumptions made for modelling the vertiport location optimization problem in Rotterdam is shown in Table 6.2.

Table 6.2: Identified assumptions

Identifier	Category	Assumption	Section
Ass-Del-001	Delivery	Usage of UAS shall only be considered for Middle-Mile Cargo operations	2.1
Ass-Dem-001	Demand	The demand data that can be extracted from the Mass-GT is assumed to be an accurate representation of the real world demand	4.4
Ass-Loc-001	Locations	Warehouses can be used as vertiports where cargo drones can take off and land without restrictions	4.4
Ass-Loc-002	Locations	Warehouses are able to house all drones in case they are not used.	4.4
Ass-Loc-003	Locations	Warehouses have an unlimited capacity for storage, charging and maintenance of the to-be-used cargo drones.	4.4
Ass-Loc-004	Locations	Each zone in the Rotterdam area can host at most one vertiport	4.4
Ass-Tsp-001	Transport	The selected drones will be able to carry cargo up to TBD kg	2.2
Ass-Tsp-002	Transport	Cargo shipments are assumed to have set dimensions and weight	2.2
Ass-Tsp-003	Transport	Drone operation within Rotterdam is feasible with a permit from ILT and clearance from LVNL	4.1
Ass-Tsp-004	Transport	The Port of Rotterdam has no impact on the flight routes for cargo drones and is a viable option for allocating vertiports	4.1
Ass-Tsp-005	Transport	Flight restricted zones that have a radius of less than TBD metres are assumed to have a negligible effect on the flight distances, flown by drones	4.1
Ass-Ver-002	Vertiport	Loading and unloading procedures for drones will take TBD time	3.2

6.3. Out-of-scope

There are some aspects that could be considered in vertiport location optimization but are considered to be out of scope for this thesis due to time limitations. First and foremost of these aspects is the vertiport design problem. As mentioned in chapter 3, the capacity of a vertiport is highly reliant on its size and layout. Ideally, a specific vertiport based on the requirements of the network and the proposed application is used to model the capacity. However, the design of vertiports is a whole separate optimization problem of its own and due to time limitations, this is considered to be out of the scope of this thesis.

Furthermore, weather conditions can also impact drone operations. This could cause delays, which could in turn affect the capacity of vertiports and the entire network. As weather conditions are an uncertainty which will require an extensive amount of time to model, it will also be assumed that this is out of the scope of this thesis.

7

Research proposal

This chapter aims to state the research proposal of this thesis. This proposal is based on the extensive background information presented in previous chapters. First, the research gaps will be identified and stated in section 7.1. Next, section 7.2 will present the research objective and finally, all research questions and their corresponding subquestions are stated in section 7.3.

7.1. Research gaps

In the current day and age, Urban Air Mobility (UAM) is an industry that is rapidly emerging and shows a great deal of promise. Its main applications are the transportation of passengers in so-called air taxis and the transportation of goods. Whereas there have been quite a few studies performed on designing UAM in the context of passenger transportation in the form of on-demand mobility, relatively few studies consider the transport of goods. Within the transportation of goods, middle-mile cargo operations seem to be a very interesting application for UAM due to its ability to rapidly distribute cargo in a sustainable way when working with electric Vertical Take-off and Landing (eVTOL) vehicles. Furthermore, UAM is not affected by traffic congestion and does also not contribute to this, relieving some of the burden on public roads. The lack of research in this area makes it interesting to look at UAM middle-mile cargo operations and how decisions on vertiport placement can be made.

When looking at existing research there are a few gaps that come to light. First of all, there is currently no existing research on UAM middle-mile cargo operations that considers multiple warehouses or origin points. In reality, setting up a UAM network for this purpose will involve multiple warehouses from which cargo will be shipped. Furthermore, it was identified that safety is one of the main concerns with the implementation of UAM. Safety concerns have a large influence on public trust and hence the societal impact of UAM. Nevertheless, very few studies consider this metric in both UAM passenger and good transportation network design. Only one study was found that considers some sort of safety metric in their location optimization tool [43] in the form of mid-air collision risk of Unmanned Aerial Vehicles (UAV). However, there are a lot more safety requirements, constraints and considerations that could be taken up in the model. This leaves room for models that are more advanced in terms of including safety metrics. Next to this, a lot of the current models for vertiport location optimization mainly consider one objective in their decision-making. For example, they only minimize general travel costs but they do not take into account other considerations such as noise annoyance, visual pollution, safety, vertiport capacity, available infrastructure space etc. In reality, decision-makers will, of course, have all these considerations to take into account. This leaves room for more advanced models. Finally, it was found that for vertiport location optimization only MILP models or the Variable Neighbourhood Search (VNS) algorithm or Genetic Algorithm are used. Whereas, in general, the Tabu Search algorithm has been used many times to solve other versions of the Hub Location Problem (HLP) and seems to perform well. Therefore it is interesting to see how it performs for vertiport location optimization and how the techniques transfer to this context. All of the mentioned considerations are best summarized by the following research gaps:

1. **The strategic placement of vertiports for Middle-Mile cargo operations with multiple warehouses is unexplored.**

2. **The incorporation of safety metrics in the strategic placements of vertiports is unexplored with the exception of mid-air collision risk in one paper.**
3. **Multi-objective vertiport location optimization is relatively unexplored, leaving room for more advanced models.**
4. **The Tabu Search algorithm has been used for HLPs but never in UAM context, making it interesting to see how the techniques transfer to this context.**

7.2. Research objective

The research objective to be identified stems from the research gaps that were stated in section 7.1. The main focus of this thesis is to develop an optimization model for the strategic positioning of vertiports. This is done in the context of Middle-Mile cargo operations in the area of Rotterdam. As there is currently no model out there that considers middle-mile cargo operations with multiple warehouses and multiple objectives the research objective is set to be the following:

Main research objective:

To develop and analyze an optimization model for the strategic placement of vertiports for middle-mile cargo operations, considering capacity, safety and societal impact, in the Rotterdam area.

In the development of the model there are three general areas that one could focus on to make it more advanced as compared to existing models out there. These are:

- **Case** - Most of the existing research on the process of vertiport location optimization focuses purely on network development and logistics planning. This leaves out the aerospace aspect, which is a very relevant aspect when developing a UAM network.
- **Method** - This relates to focusing on the method of optimization itself and could for example involve comparing the optimization method used to other existing methods.
- **Uncertainty** - Models in existing research do not incorporate uncertainties such as weather conditions and technical failure.

This thesis will focus mainly on the case rather than the method or adding uncertainty to the model. This is deemed the most interesting for this research as there are quite some insights to be added to models when looking at it with an aerospace engineering background such as battery discharge during flight and noise estimations for drones specifically.

7.3. Research questions

This section presents an overview of the identified research questions and their respective subquestions that are needed to answer the main research question.

1. **How can social impact factors be modelled?**
   - What is the impact of noise pollution nuisance on location suitability and how can it be modelled?
   - What is the impact of visual pollution nuisance on location suitability and how can it be modelled?
   - How does societal impact influence the suitability of locations?
   - How can safety metrics be incorporated into the design of a UAM cargo network?
   - What safety procedures and regulations should be taken into account?
   - What effect do safety requirements and constraints have on the imposed model?
2. **How do the demand for parcels and capacity of vertiports influence the optimization model?**
   - How can the demand for parcels in the area of Rotterdam be modelled?
   - What estimations can be made on the capacity of vertiports based on their size?

- How can the capacity of vertiports be incorporated in the model?

3. **What optimization methods can be used to determine strategic vertiport locations?**
    - How can the mathematical formulation of the HLP for on-demand UAM mobility be translated to a formulation for middle-mile cargo operations?
    - What is the effect of demand data clustering on the optimization method?
    - How can the Tabu Search algorithm be implemented in the context of UAM network design?
4. **How can the performance of the optimization model be analyzed?**
    - How sensitive is the model to the input of K in the K-means algorithm?
    - How sensitive is the model to changing the influence that different social impact factors have?
    - How do the assumptions influence the performance of the model?

8

Conclusion

The ever-increasing pace of urbanization and the high demand for efficient transportation alternatives have propelled cities into an era where the existing and traditional modes of transportation are being redefined. An exciting and promising mode of transportation is Urban Air Mobility (UAM). UAM can be employed for the transportation of people in the form of air taxis or the transportation of goods. The introduction of UAM into society and transport modes introduces the problem of finding and selecting good locations for vertiports to be built. The decision-making process of strategically positioning these vertiports is a complex problem that involves a lot of considerations. Safety, social acceptance, noise pollution, visual pollution, available land space for infrastructure, vertiport capacity, price of land and demand are all factors that can have an impact on deciding where to place vertiports. Furthermore, the application for which a UAM network is used will also have a large impact on the selection of vertiport locations. For this thesis middle-mile cargo operations were identified to be most interesting due to the lack of research considering this type of application and the market potential that it has.

This literature study has been aimed at scoping out literature on several factors of the decision-making process as well as some of the optimization methods that could be used in order to optimize the locations of vertiports. This was done with the goal of finding potential research gaps, to which this thesis could add. In doing so, the following gaps were found. Firstly, the strategic placement of vertiports for middle-mile cargo operations is unexplored in current scientific research. Secondly, the incorporation of safety metrics in vertiport location optimization models is unexplored. This research gap is particularly interesting as safety is the number one public concern in the implementation of UAM. Furthermore, another research gap that was identified is the fact that existing vertiport location optimization models generally do not consider many criteria. They mainly focus on optimizing a process in terms of time, costs or demand served while not considering important metrics such as safety and social acceptance for example. This leaves room for the development of more advanced models. Finally, in terms of solving the vertiport location optimization problem, it was found that there are several methods used in literature. As a result of a trade-off that was performed, it is proposed that the tabu algorithm be used as a solution method. This is partly because the tabu search algorithm is used often in existing research for general Hub Location Problems but it has never been applied to the context of UAM. This is another gap as it is interesting to see how the techniques of the tabu search algorithm translate to this context.

With the identified research gaps and the selected case study the following research objective was set for this thesis: **"To develop and analyze an optimization model for the strategic placement of vertiports for middle- mile cargo operations, considering capacity, safety and social acceptance, in the Rotterdam area."**

The Rotterdam area was chosen as a case study due to the data available on parcel demand by PostNL and others. Furthermore, Rotterdam is a major city with a large population, which results in a large demand for parcels throughout the entire city itself as well as the area surrounding it.

This extensive literature study provides the reader with background information on the problem to be solved in this master thesis.

III

Supporting work

1

Additional Results

As the paper presented that was presented in part I should be concise and to the point, not all results that were generated and found were included. Therefore, this chapter aims to provide additional results that were left out of the paper but could be of interest to the reader or for future research. To provide a complete overview of the results, all results shown in the paper are also included here. The chapter is divided into six sections with each of these dedicated to one of the experiments.

(The rest of this page have been left blank intentionally for formatting purposes)

1.1. Experiment A: Number of clusters K

Figure 1.1 shows the Pareto fronts that were obtained for experiment A for all three values of K (500,1000,2000). It was observed that the front is shifted downward left as the number of clusters increases, which means that better safety and noise scores are obtained for higher cluster amounts. This result is as expected as clustering more zones together will result in average safety and noise cluster scores that are higher and hence perform worse. Furthermore, little effect on the demand scores was observed.

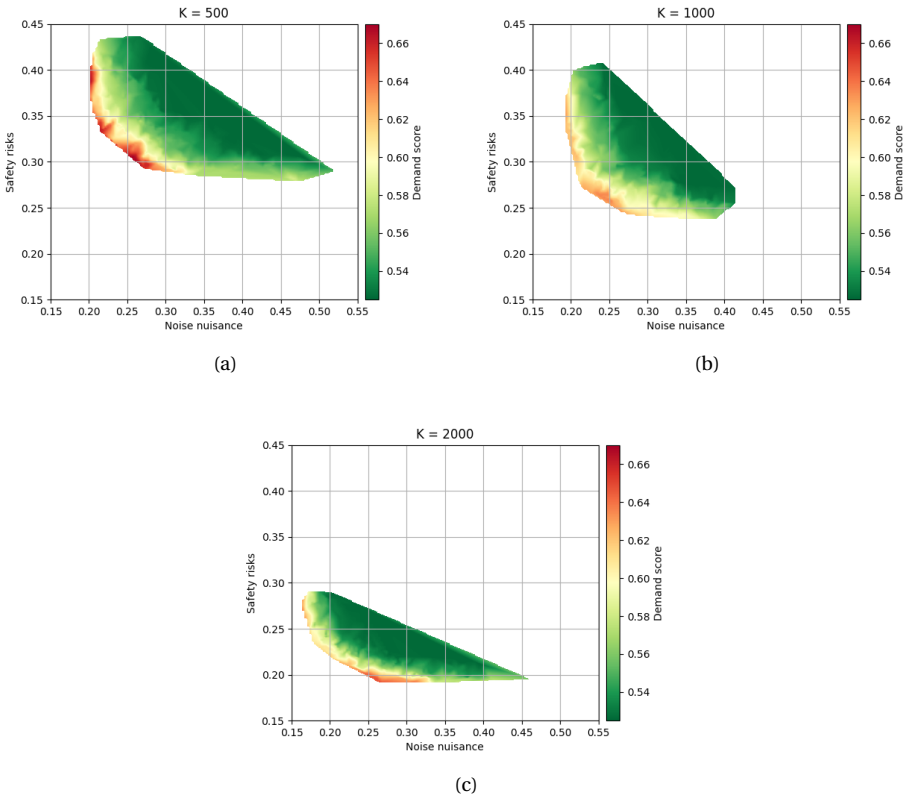

(a) (b)

(c)

Figure 1.1: Pareto front considering cluster amount of: (a) 500 (b) 1000 (c) 2000

Figure 1.2 shows the individual Pareto fronts when only two out of the three objectives are considered. From the figure it is evident that the cluster amount mainly affects the noise and safety scores as similar best demand scores are obtained and the Pareto fronts behave relatively similar in terms of demand.

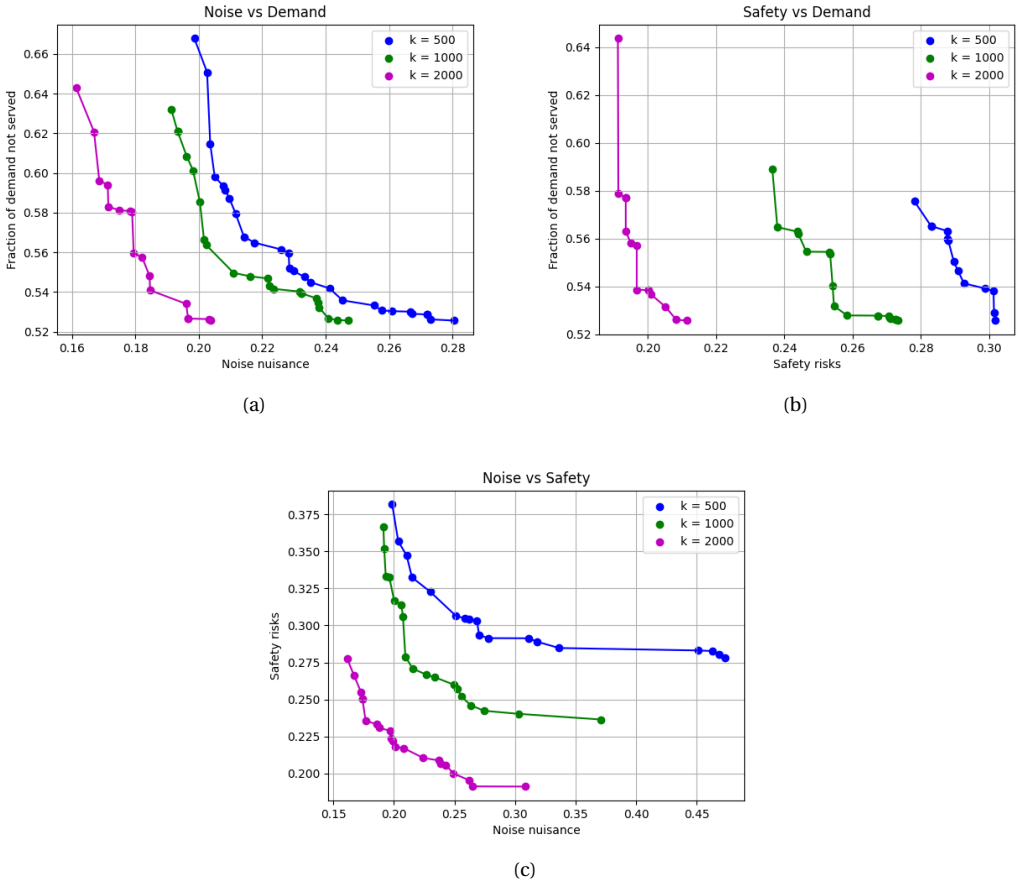

Figure 1.2: Pareto fronts when considering two out of three objectives: (a) Noise vs Demand (b) Safety vs Demand (c) Noise vs Safety

Figure 1.3 shows the boxplots associated with the demand, safety and noise scores for each of settings of K. Similar behaviour in demand for varying cluster sizes is observed as well as improvements in terms of safety and noise objective scores.

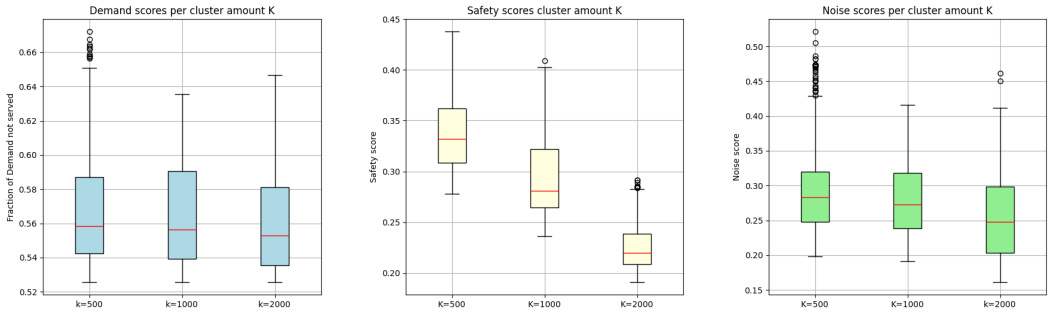

Figure 1.3: : Boxplot of collected objective scores from the Pareto front: (a) Fraction of demand not served (b) Safety (c) Noise

Figure 1.4 shows heatmaps containing information on how many times zones have been picked in the entire

Pareto front for each of the settings of K. To remove outliers, zones that have been picked less than 5% of the amount of times that the highest picked zone was selected, were removed from the map. The heatmaps could be used to identify potentially interesting areas for placing vertiports in combination with assessments of individual solutions. In general, it was found that similar areas are picked when using a number of 500 or 1000 clusters. It can be observed that the heatmap is somewhat different for the experiment with 2000 clusters. This indicates that there is some sensitivity to the amount of clusters that is used, which is rather logical as it radically changes the scoring system. This sensitivity should be noted when using the model for setting up a UAM network.

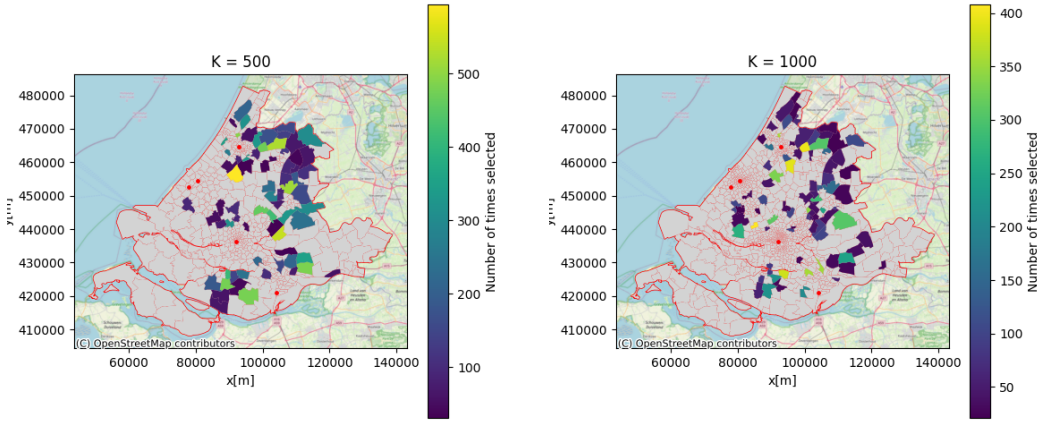

(a)

(b)

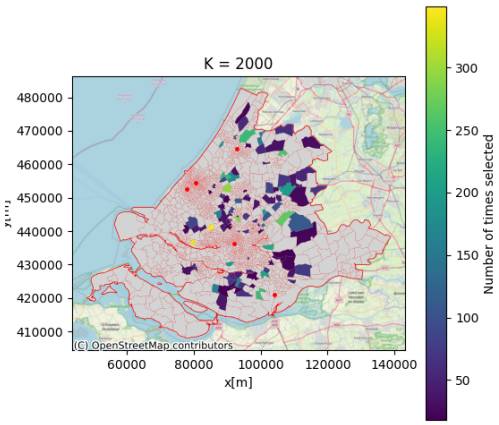

(c)

Figure 1.4: Heatmap of zones picked in Pareto front with (a) K = 500 (b) K = 1000 (c) K = 2000

Finally, Figure 1.5 shows the computation times that it took for the model to run for a total of 4000 iterations of the Tabu Search Algorithm.

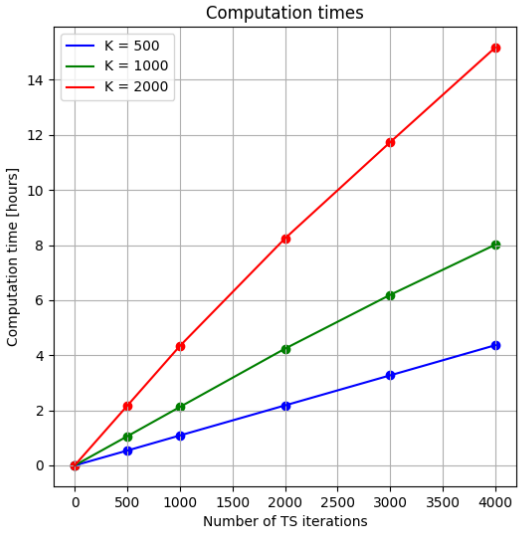

Figure 1.5: Computation times as a function of TS algorithm iterations

(The rest of this page have been left blank intentionally for formatting purposes)

1.2. Experiment B: Number of vertiports

Experiment B generates results for varying values of the amount of vertiports that are placed by the model. This was done for 10, 25, 50 and 100 vertiports. Figure 1.6 shows the resulting Pareto fronts. It can be observed that the Pareto front becomes smaller and moves in an upward right fashion for an increasing amount of vertiports. This is explained by the fact that the solution space is smaller for a larger amount of vertiports, which results in a more converged Pareto front. The upward right movement is explained by the fact that more zones will have to be selected that contain worse safety and noise scores when placing more vertiports. Furthermore, Figure 1.7 show the Pareto fronts only considering two out of the three objectives. No new results were drawn from this.

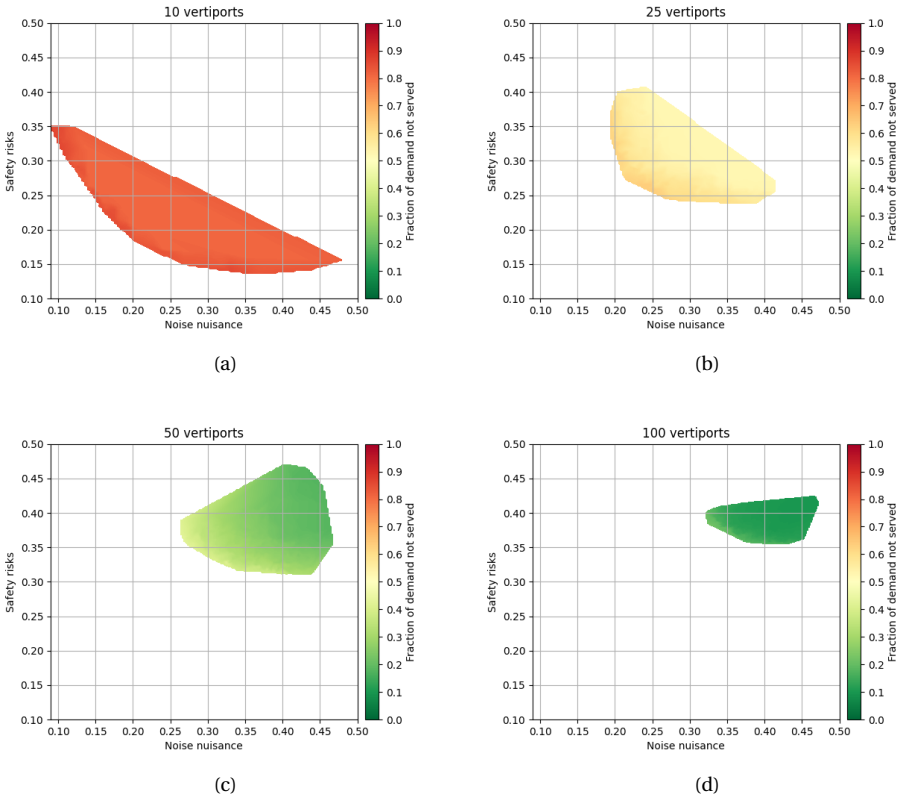

Figure 1.6: Pareto front considering a UAM network with a vertiport amount of: (a) 10 (b) 25 (c) 50 (d) 100

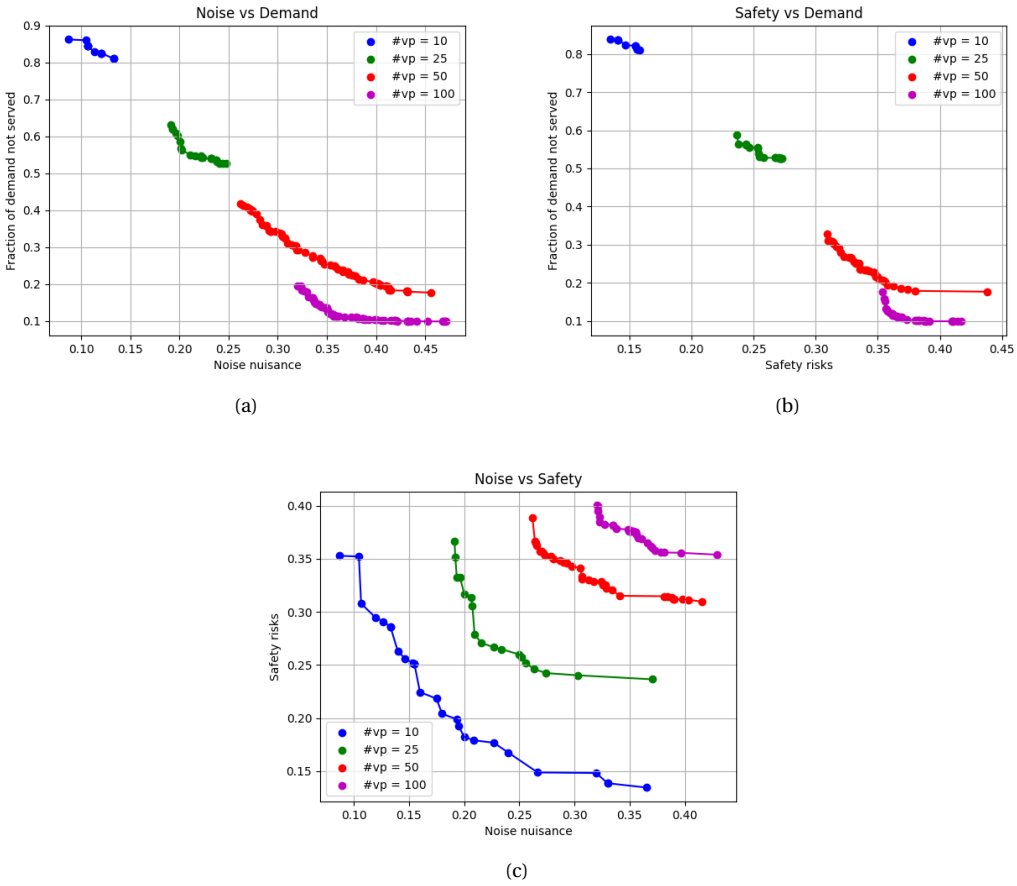

Figure 1.7: Pareto fronts when considering two out of three objectives: (a) Noise vs Demand (b) Safety vs Demand (c) Noise vs Safety

Figure 1.8 shows the boxplots containing the objective scores for each objective and vertiport amount. Again, a very clear relation is seen between an increase in vertiports and the amount of demand that can be served. Furthermore, the boxplots show that not only the best solutions in terms of safety and noise degrade when the amount of vertiports is increased, but the entire front is shifted, with the median and maximum scores also becoming higher.

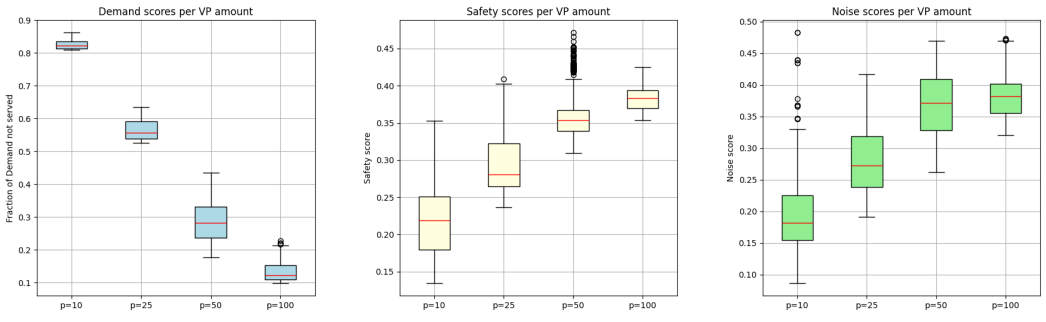

Figure 1.8: : Boxplot of collected objective scores from the Pareto front: (a) Fraction of demand not served (b) Safety (c) Noise

Figure 1.9 shows heatmaps of how many times zones are picked per vertiport amount setting, with outliers removed. In general, it is observed that the same general areas are picked over all settings of vertiport amount. The model mainly extends its selection to other and more zones when the amount of vertiports is increased.

Especially, an extension to the east and the south of the study area can be seen for an increased amount of vertiports.

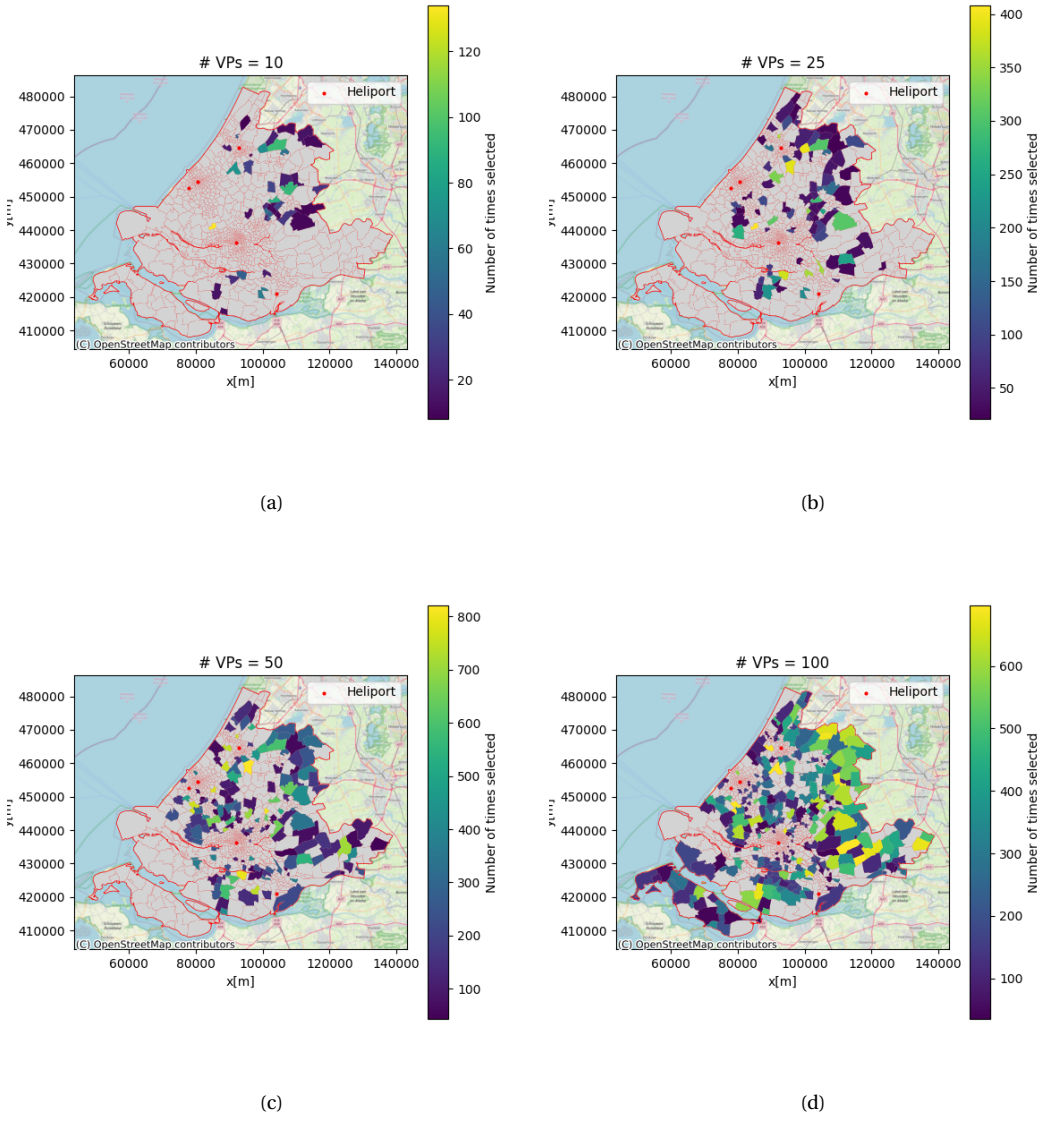

(a) (b)

(c) (d)

Figure 1.9: Heatmap of zones picked in Pareto front with (a) #VPs = 10 (b) #VPs = 25 (c) #VPs = 50 (d) #VPs = 1000

Finally, Figure 1.10 shows the computation times of the model for the different number of vertiport settings as a function of the number of TS algorithm iterations. It can be seen that the model runs a bit longer for higher amounts of vertiports.

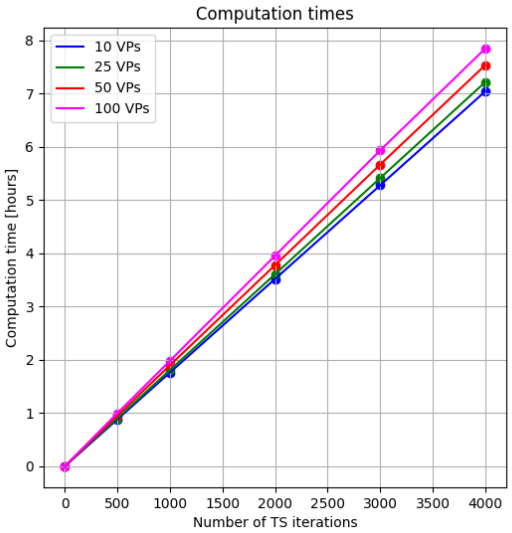

Figure 1.10: Computation times as a function of TS algorithm iterations

1.3. Experiment C: Drone range

The purpose of experiment C is to study the effect of a varying drone range on the objective scores and the model computation time. Figure 1.11 shows the Pareto fronts that were obtained for this experiment. As discussed in the paper, increasing the drone range will result in a better combination of all three objective scores. This can be deduced from the fact that the Pareto front retreats in a downward left fashion for an increasing drone range. This indicates that, while there are no improvements in the demand that can be served, the model is able to find better safety and noise scores for the same demand score.

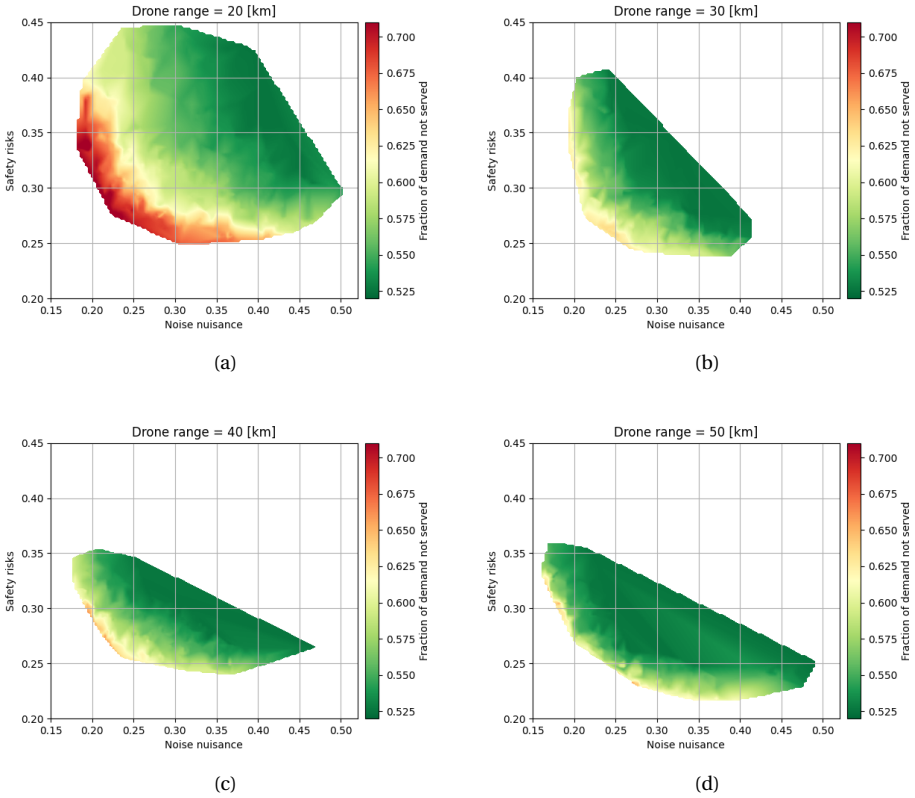

Figure 1.11: Pareto front considering a UAM network with a drone range of: (a) 20 [km] (b) 30 [km] (c) 40 [km] (d) 50 [km]

Figure 1.12 shows the Pareto fronts when considering two out of the objective scores. It can be seen that, with an increasing range, better noise and safety scores can be found for the same amount of demand served. In terms of the best scores found for noise and safety itself, there is a small shift of the fronts in a downward-left fashion, indicating better scores. However, these are very minor improvements.

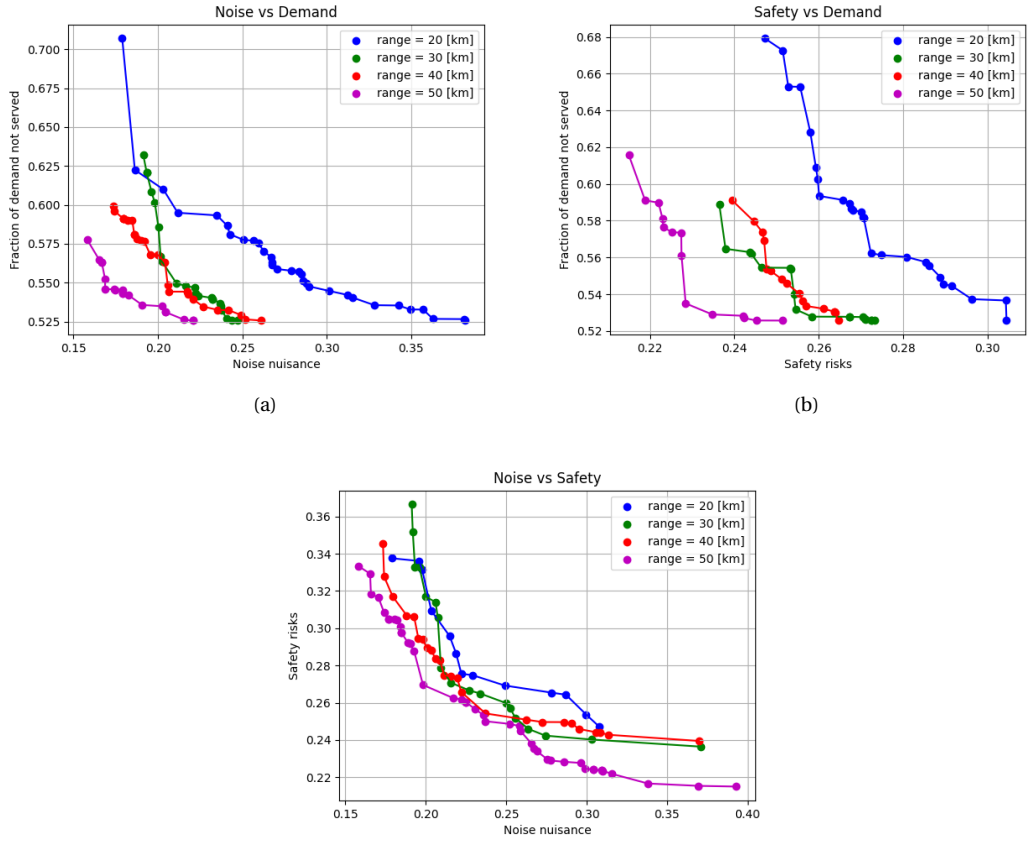

Figure 1.12: Pareto fronts when considering two out of three objectives: (a) Noise vs Demand (b) Safety vs Demand (c) Noise vs Safety

Figure 1.13 shows the boxplots of the collected objective scores from the Pareto fronts. No new insights were obtained from this.

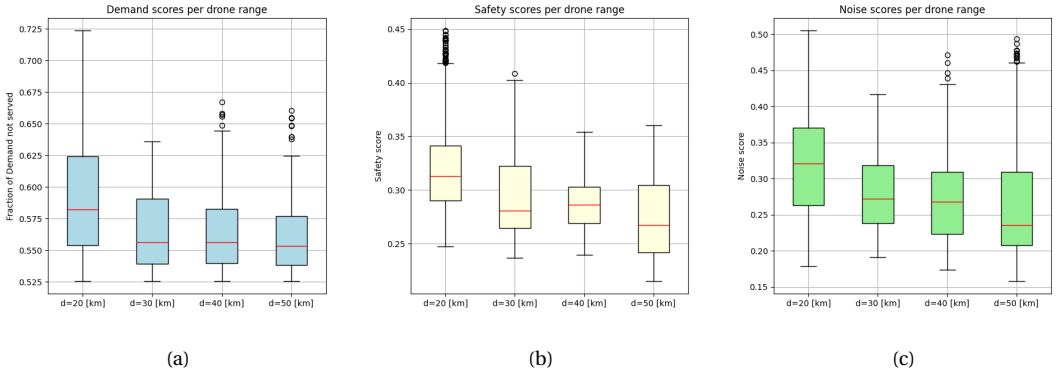

Figure 1.13: : Boxplot of collected objective scores from the Pareto front: (a) Fraction of demand not served (b) Safety (c) Noise

Figure 1.14 show heatmaps containing information on the amount of times each of the zones is picked in the solutions found in the Pareto front, with the outliers removed.

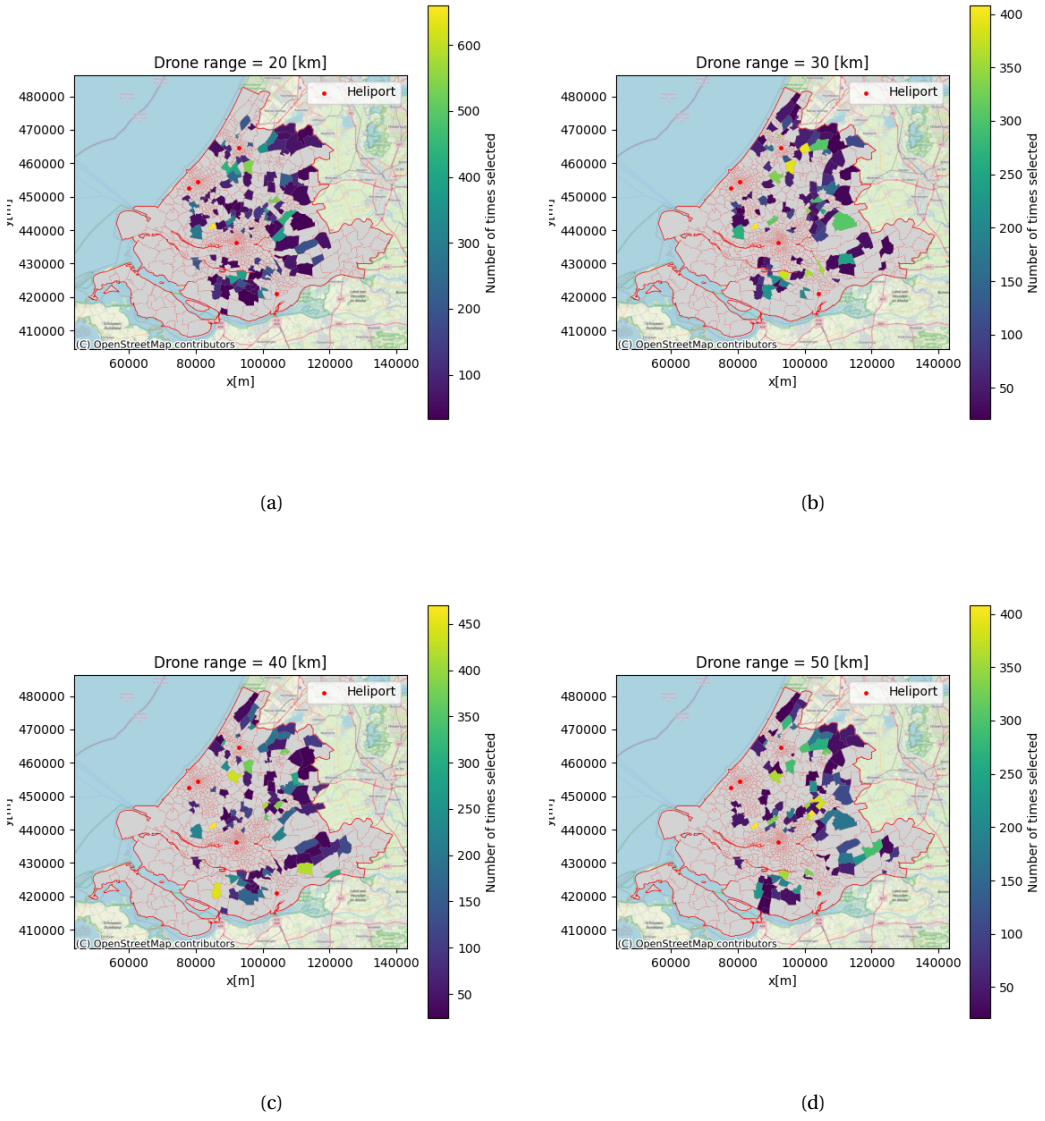

(a) (b)

(c) (d)

Figure 1.14: Heatmap of zones picked in Pareto front with drone range (a) 20 [km] (b) 30 [km] (c) 40 [km] (d) 50 [km]

Figure 1.15 shows the computation times for the various drone range settings as a function of TS algorithm iterations. It can be seen that there are no large differences in computation times and no relation is found between the drone range setting and the computation time.

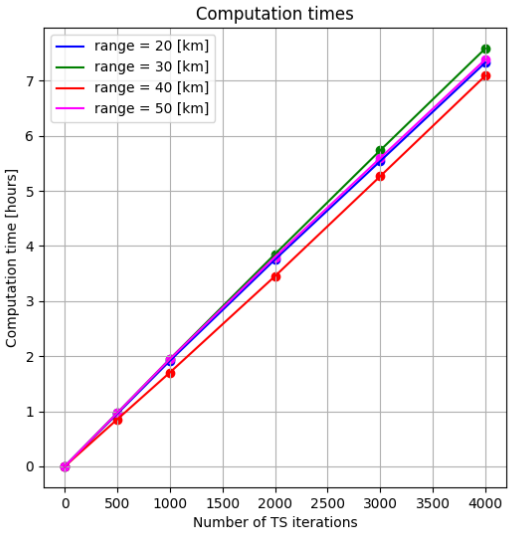

Figure 1.15: Computation times as a function of TS algorithm iterations

1.4. Experiment D: Maximum safety distance

Experiment D aims to find the relations between the set maximum safety distance and the performance of solutions in terms of the three objective scores as well as the computation time. Figure 1.16 shows the obtained Pareto fronts for this experiment. There is a small increase in best objective scores for the safety and noise objective scores and a small downward left shift of the Pareto front for an increasing maximum safety distance.

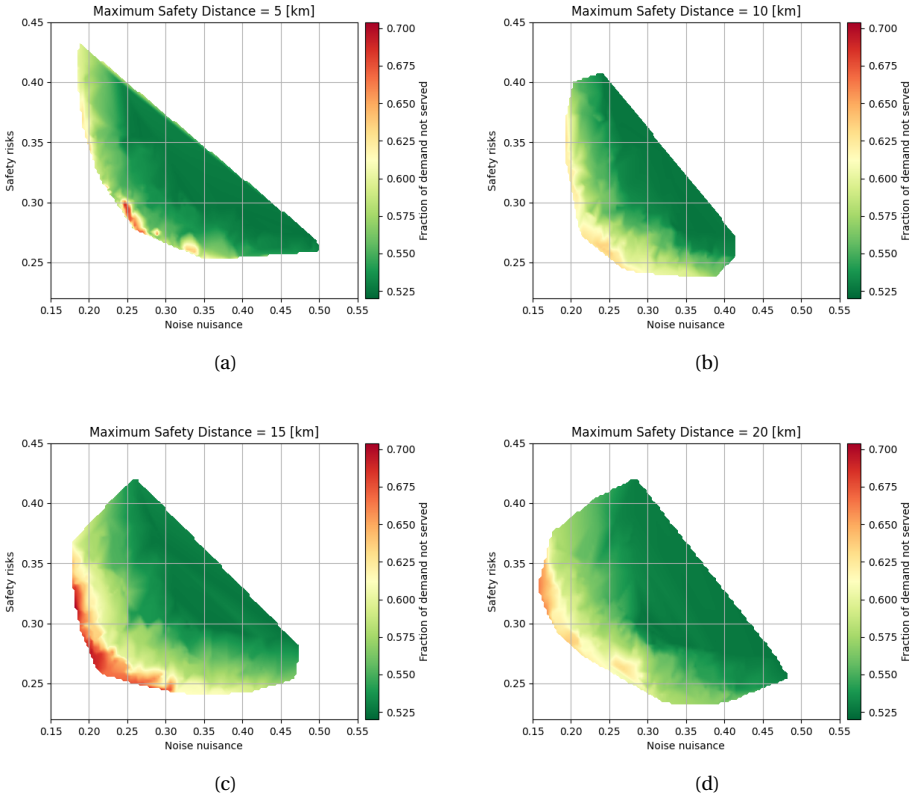

Figure 1.16: Pareto front considering a UAM network with a maximum safety distance of: (a) 5 [km] (b) 10 [km] (c) 15 [km] (d) 20 [km]

From the Pareto fronts considering only two out of three objectives, as shown in Figure 1.17, it can be seen that for higher safety distances, generally, a somewhat better safety score can be obtained. This is most noticeable when comparing a safety distance of 20 [km] to the others. For this safety distance, the best individual scores (indicated by the Nadir points), as well as combined scores (indicated by the entire front), were found.

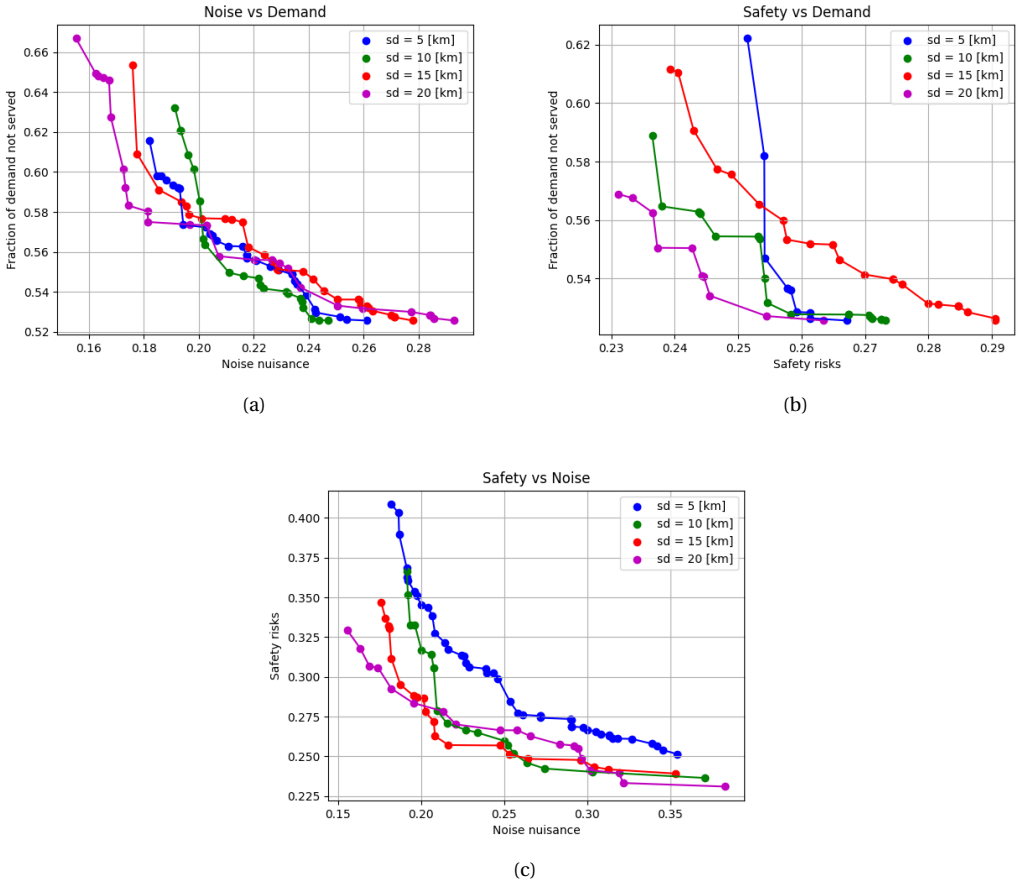

Figure 1.17: Pareto fronts when considering two out of three objectives: (a) Noise vs Demand (b) Safety vs Demand (c) Noise vs Safety

Figure 1.18 shows the boxplots of the collected objective scores from the Pareto fronts. Similar findings to the ones found from Figure 1.16 and Figure 1.17 are done.

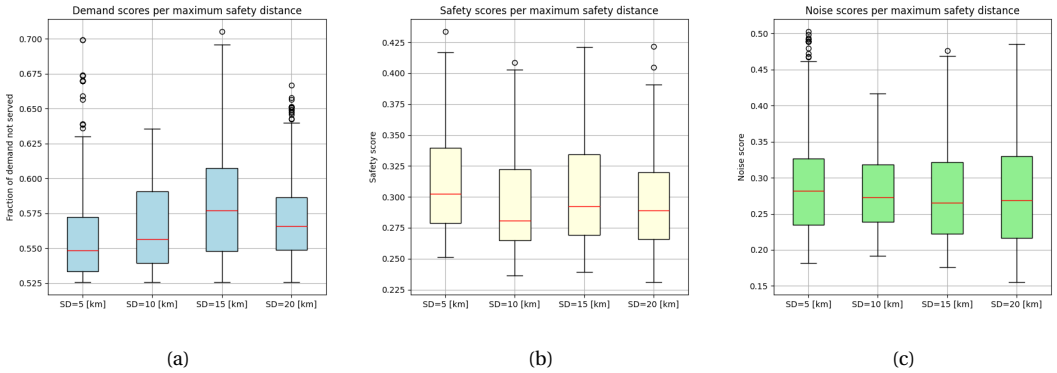

Figure 1.18: : Boxplot of collected objective scores from the Pareto front: (a) Fraction of demand not served (b) Safety (c) Noise

Figure 1.19 shows heatmaps containing information on the amount of times each of the zones is picked in

the solutions found in the Pareto front with the outliers removed. It can be seen that there are, generally, not completely new areas that are selected as a result of increasing the maximum safety distance. Therefore, it can be concluded that the increase in maximum safety distance mainly affects the individual solutions that are found and not the overall areas that are selected often.

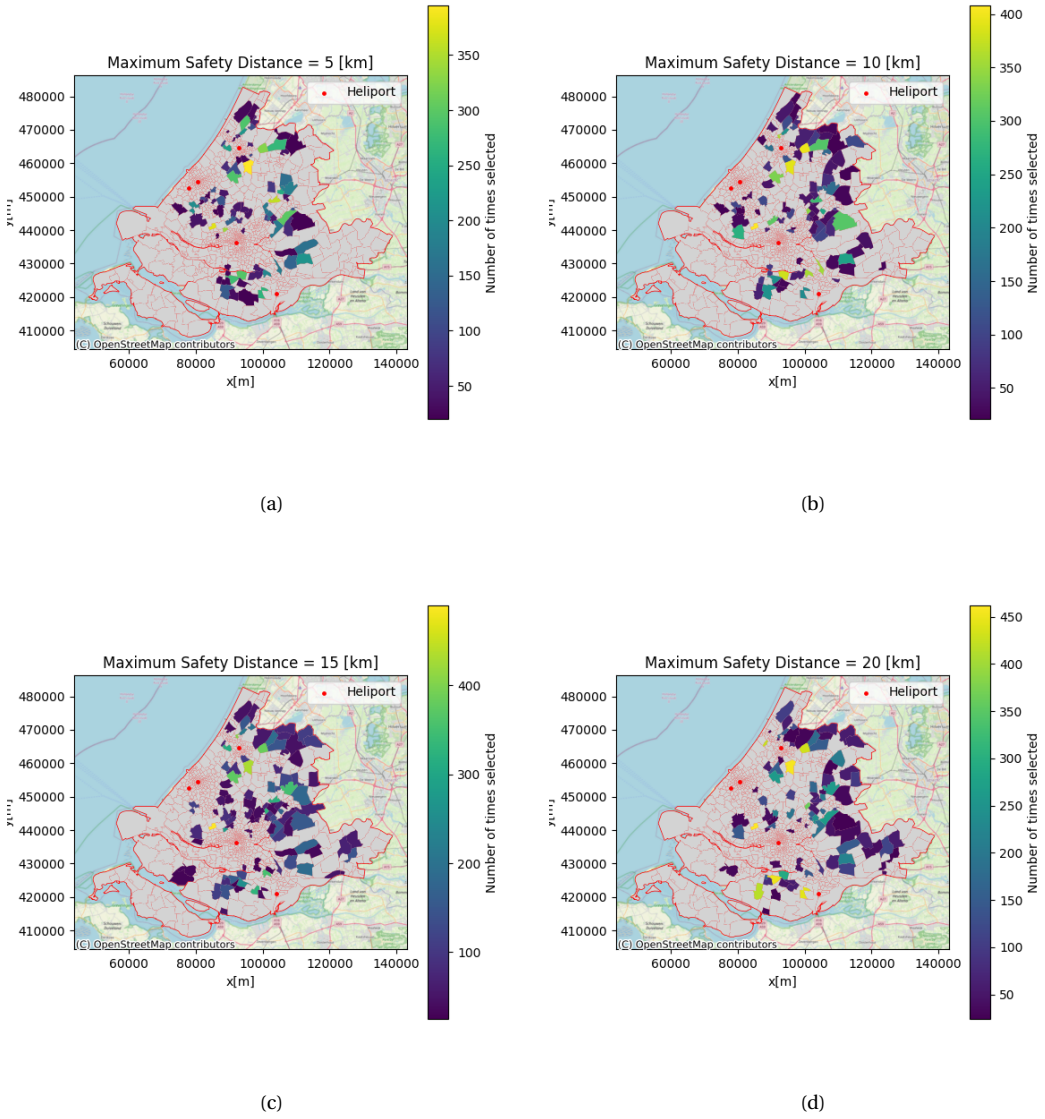

(a) (b)

(c) (d)

Figure 1.19: Heatmap of zones picked in Pareto front with maximum safety distance (a) 5 [km] (b) 10 [km] (c) 15 [km] (d) 20 [km]

Finally, Figure 1.20 shows the computation time for the model to run with the different values of maximum safety distance as a function of number of TS iterations. It can be seen that the only safety distance showing a significantly different computation time is 20 [km]. As this is a rather large maximum safety distance, it was concluded that, for general acceptable values of maximum safety distance, there is no relation with the computation time.

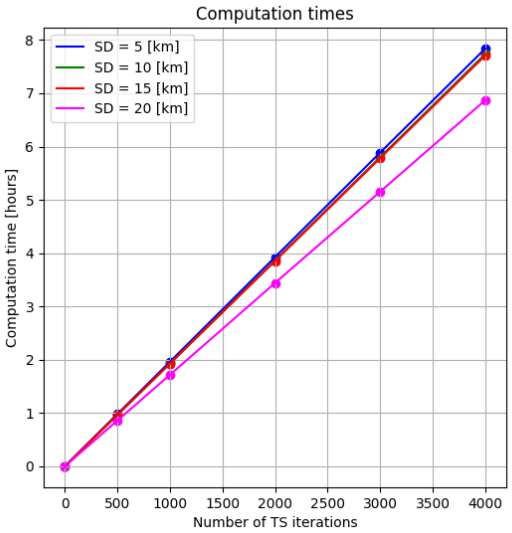

Figure 1.20: Computation times as a function of TS algorithm iterations

1.5. Experiment E: Turn Around Time

Experiment E aims to analyze the effects of varying the Turn Around Time (TAT) of drones at the destination vertiports, which mainly influences the vertiport capacity. The resulting obtained Pareto fronts are shown in Figure 1.21. Rather logically, a lower TAT results in a much better demand score. Moreover, a decrease in TAT does not result in a shift of the Pareto front in terms of safety and noise. It rather, extends the Pareto front in an upward right fashion as more solutions are found that contain good demand scores.

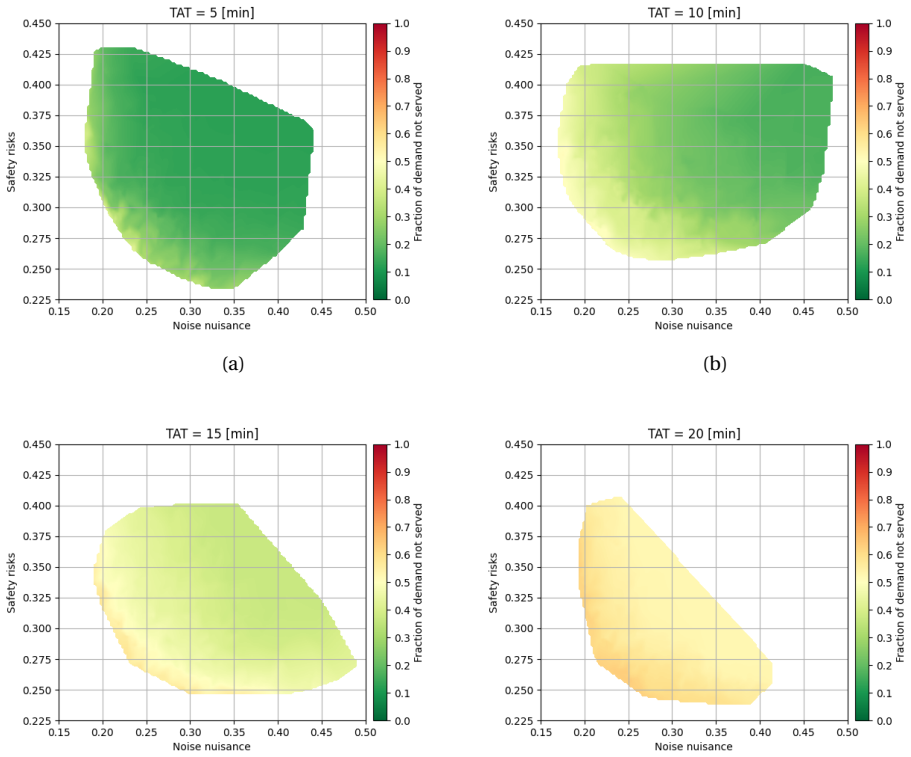

Figure 1.21: Pareto front considering a UAM network with a TAT of: (a) 5 [min] (b) 10 [min] (c) 15 [min] (d) 20 [min]

The individual Pareto fronts considering only two out of the three objectives are shown in Figure 1.22. From the figures, it becomes evident that there is a strong relation between the TAT and the demand that can be served, however, no conclusive findings were done in terms of the safety and noise objectives.

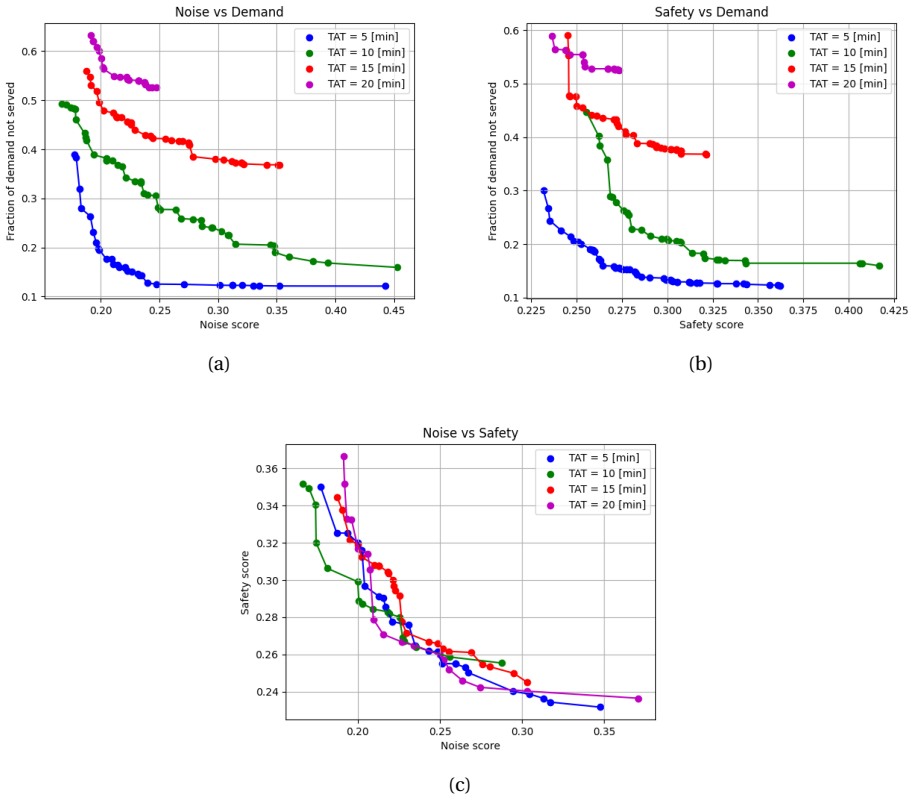

Figure 1.22: Pareto fronts when considering two out of three objectives: (a) Noise vs Demand (b) Safety vs Demand (c) Noise vs Safety

The boxplots of the collected objective scores from the Pareto fronts are shown in Figure 1.23. An interesting result is that there is somewhat of a shift downward of the medians of the safety and noise scores with an increasing TAT. This could be attributed to the fact that, due to demand being more constrained by the capacity for these values, the model is able to find more solutions that perform better in safety and noise. However, it should be noted that this shift is very small and therefore no conclusive statement on this relation can be made.

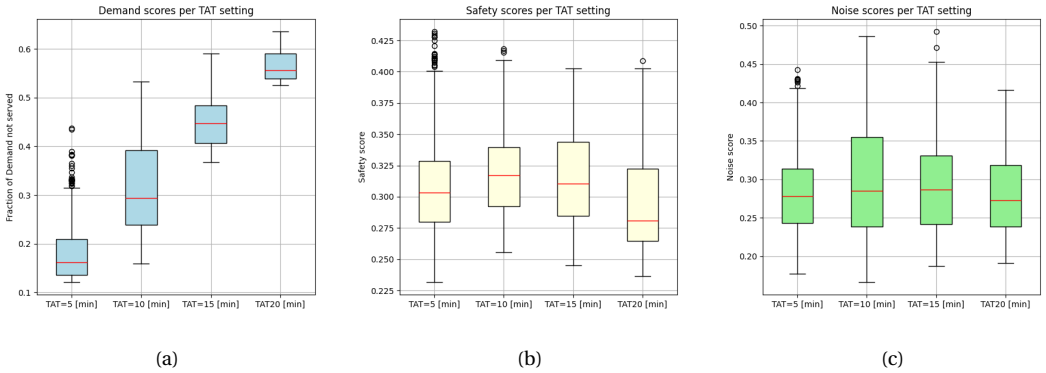

Figure 1.23: : Boxplot of collected objective scores from the Pareto front: (a) Fraction of demand not served (b) Safety (c) Noise

Figure 1.24 shows heatmaps containing information on the amount of times each of the zones is picked in

the solutions found in the Pareto front with the outliers removed. It can be seen that mostly, the same general areas are chosen, however, the zones that are picked more often, differ for the different values of TAT. This could be due to the fact that some areas have a very high demand. These areas would then be picked even more with a lower TAT as more of the demand in these areas can then be served, resulting in a better score for the demand objective.

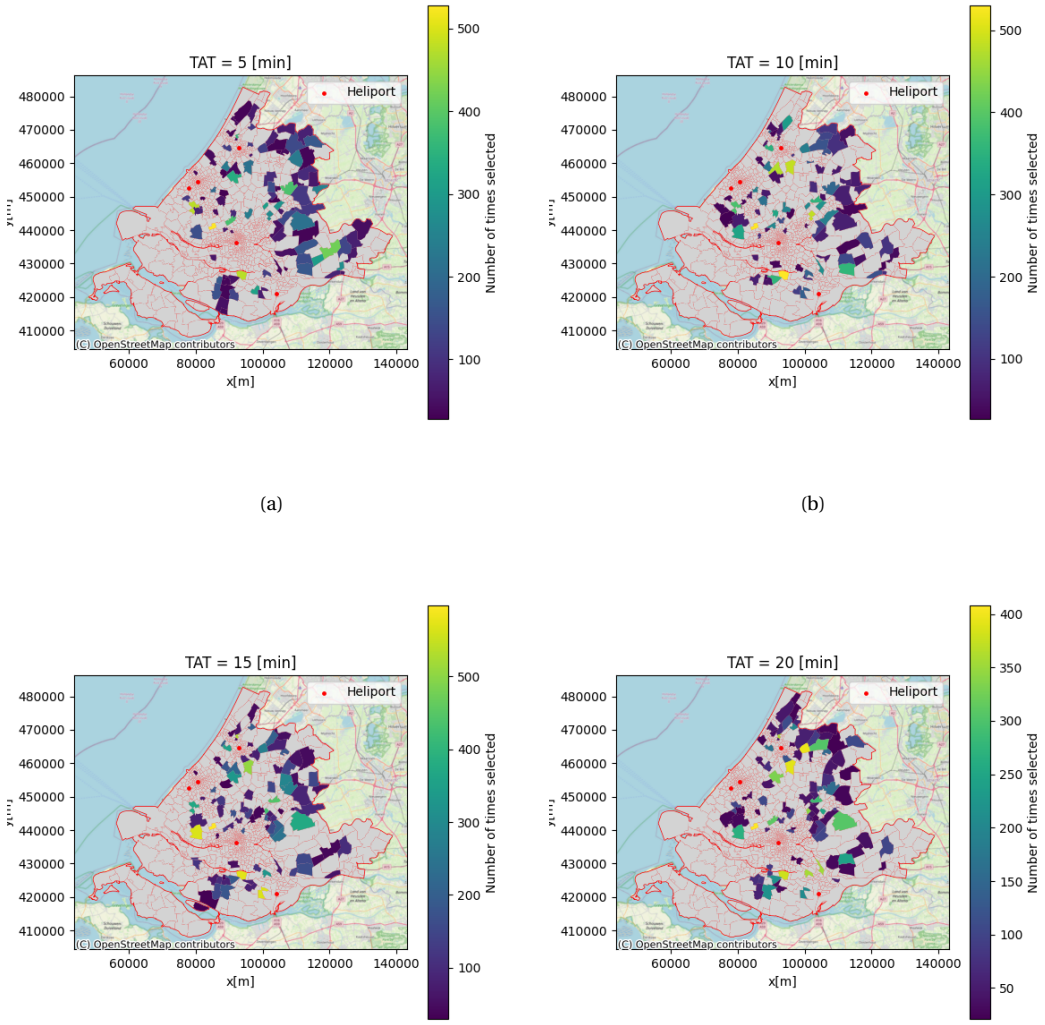

(a) (b)

(c) (d)

Figure 1.24: Heatmap of zones picked in Pareto front with maximum safety distance (a) 5 [km] (b) 10 [km] (c) 15 [km] (d) 20 [km]

Finally, Figure 1.25 shows the computation times of the model for the various settings of TAT. From the figure, it is evident that the setting of TAT has very little to no effect on the computation time.

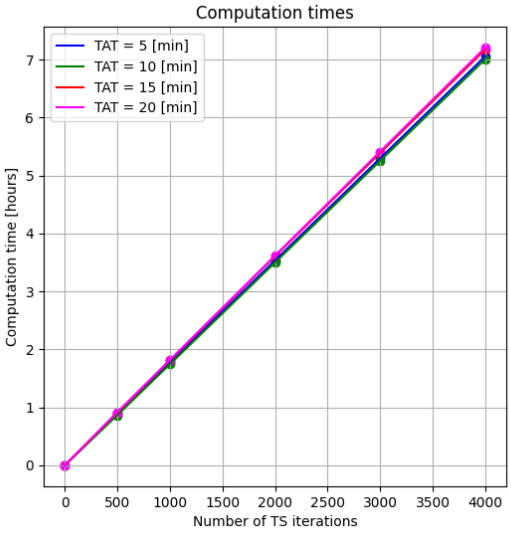

Figure 1.25: Computation times as a function of TS algorithm iterations

1.6. Experiment F: Existing heliport utilization

Experiment F aims to research the impact of using existing heliports as vertiports in the UAM MMD network. This entices constructing a network around the five existing heliports present in the region of South Holland. Figure 1.26 shows the resulting Pareto fronts considering 10 vertiports. It is evident that there is a major difference in performance when using existing heliports as opposed to not using them. It was observed that the Pareto front becomes very small for the scenario with heliports. This is due to the fact that the problem becomes highly constrained if five out of the ten vertiports are selected and locked beforehand. Figure 1.27 and Figure 1.28 show the resulting Pareto fronts for running the program with 25 and 50 vertiports respectively. Again, it was observed that the usage of heliports causes the acquired solutions to perform worse in all three model objectives.

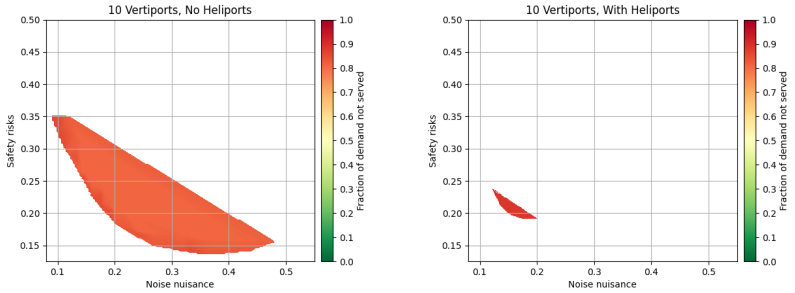

(a) (b)

Figure 1.26: Pareto front considering 10 vertiports (a) without heliport utilization (b) with heliport utilization

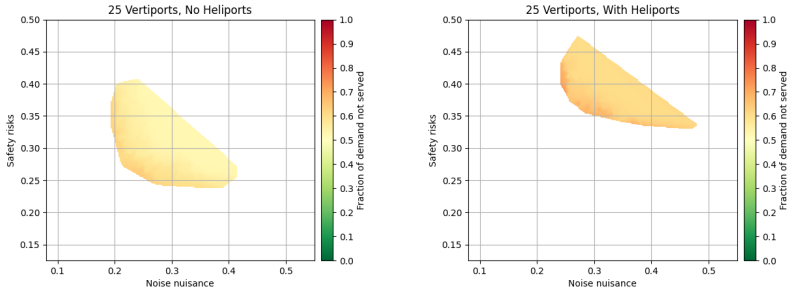

(a) (b)

Figure 1.27: Pareto front considering 25 vertiports (a) without heliport utilization (b) with heliport utilization

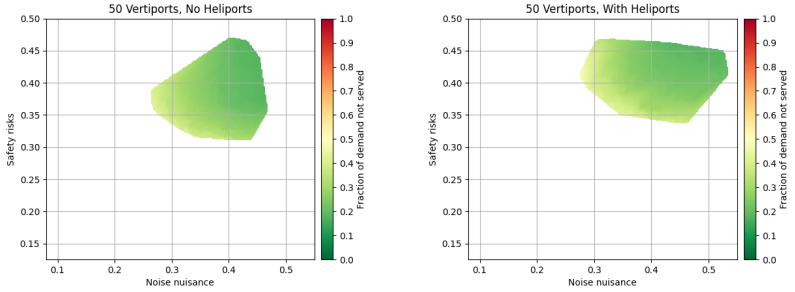

(a) (b)

Figure 1.28: Pareto front considering 50 vertiports (a) without heliport utilization (b) with heliport utilization

Figure 1.29 shows the obtained Pareto fronts when considering only two out of the three objectives. From this, similar conclusions can be drawn in the fact that the usage of heliports affects the Pareto fronts negatively. However, from subfigure c, it becomes evident that the effect of using heliports decreases as the number of vertiports to be placed increases, to the point where a network using 50 vertiports with no heliports almost performs as good as network of 25 vertiports for which the five heliports are used.

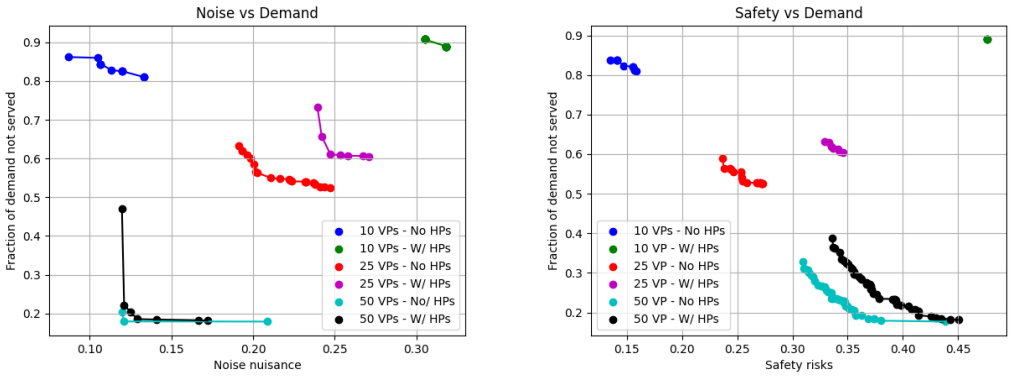

(a)

(b)

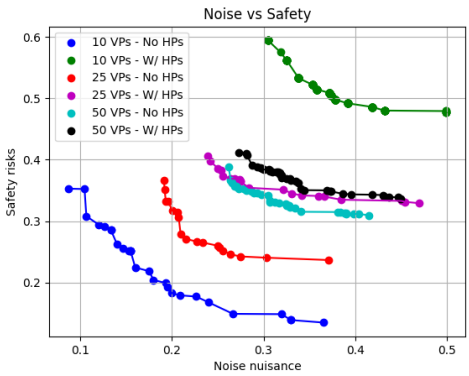

(c)

Figure 1.29: Pareto fronts when considering two out of three objectives: (a) Noise vs Demand (b) Safety vs Demand (c) Noise vs Safety

Figure 1.30 shows boxplots containing the collected objective scores from the Pareto fronts of each of the scenarios. Most noticeable is the demand boxplot for the scenario with 10 vertiports with the utilization of heliports. Due to the highly constrained optimization problem that this scenario poses, there is very little difference between the best and worst demand coverage that is accepted by the model (1.7%).

Finally, Figure 1.31, Figure 1.32 and Figure 1.33 show heatmaps of how many times zones are picked in the Pareto front for both scenarios for network size of 10, 25 and 50 vertiports respectively. It was observed that in all scenarios, the resulting Pareto fronts converge more to the same zones. This is indicated by the fact that fewer zones are picked if it is chosen to use existing heliports. Furthermore, it can be seen that irrespective of whether or not existing heliports are used, overall, the same areas are selected more often in the Pareto front. These are areas of high interest as they perform well in both scenarios.

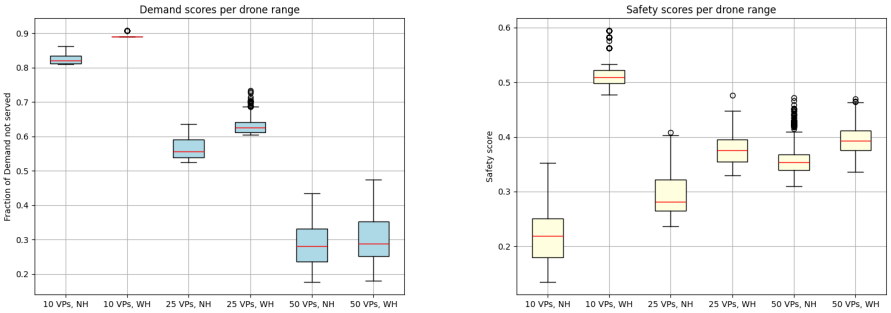

(a)

(b)

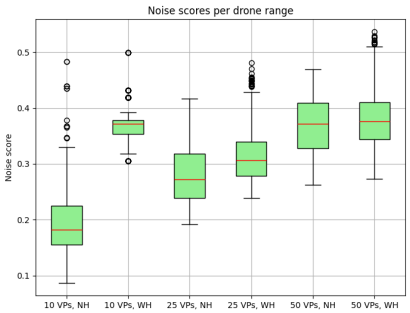

(c)

Figure 1.30: : Boxplot of collected objective scores from the Pareto front: (a) Fraction of demand not served (b) Safety (c) Noise

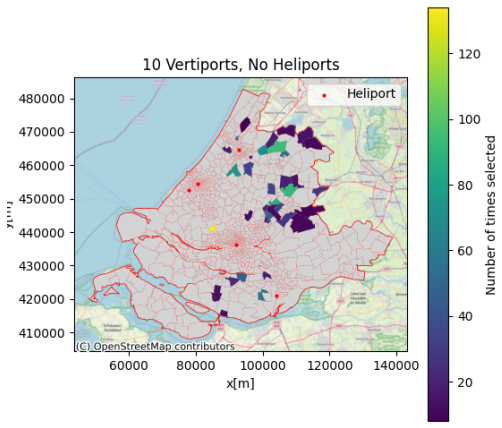

(a)

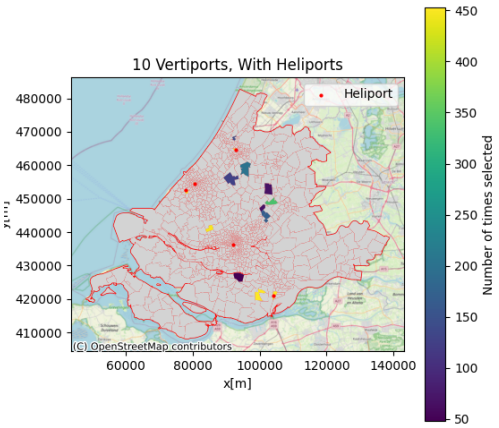

(b)

Figure 1.31: Heatmap of zones picked in Pareto front for 10 vertiports (a) without heliport utilization (b) with heliport utilization

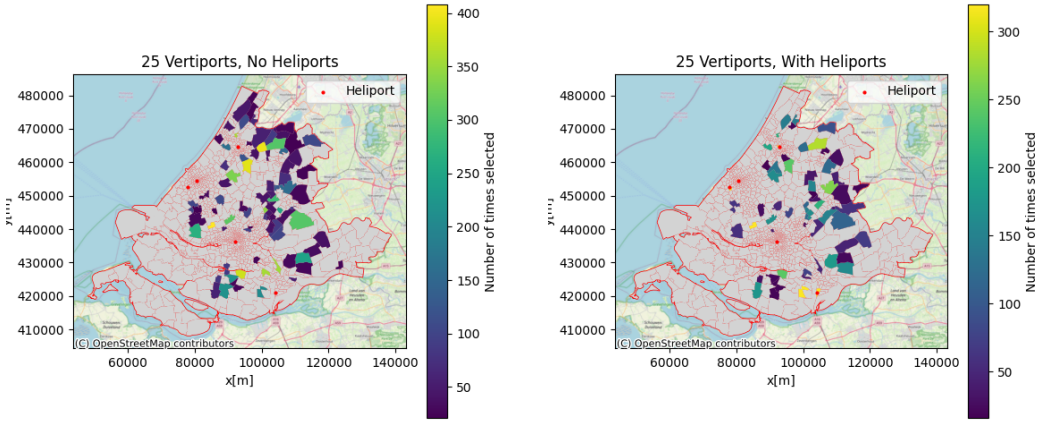

(a) (b)

Figure 1.32: Heatmap of zones picked in Pareto front for 25 vertiports (a) without heliport utilization (b) with heliport utilization

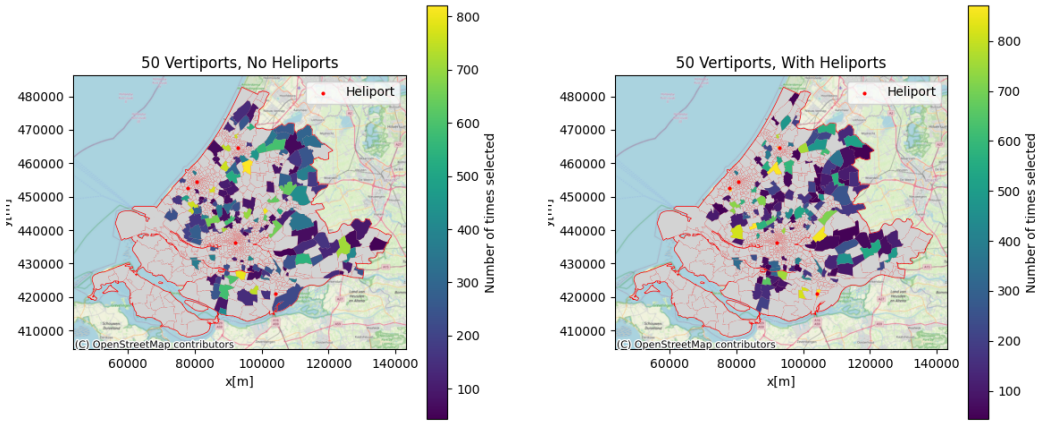

(a) (b)

Figure 1.33: Heatmap of zones picked in Pareto front for 50 vertiports (a) without heliport utilization (b) with heliport utilization

2

Spatial analysis

To assess the amount of infrastructural space available for the placement of vertiports in each of the 6625 zones, a spatial analysis was done using the Geographical Information System QGIS. For the spatial analysis, the most recent aerial pictures from 2024 were acquired from Publieke Dienstverlening Op de Kaart (PDOK) [74]. This chapter aims to give a small description of the approach for assessing infrastructural space and the scoring system that was used.

Since assessing 6625 zones visually was a very time-consuming task, the analysis was kept to a minimum, ensuring the zones could be rated as fast as possible. Therefore, the general approach to assessing the infrastructural space that is available in each of the zones was based on the estimation of how many vertiport pads would be able to fit next to each other either in a square or rectangle, depending on the available space. The size of each of the pads is assumed to be similar to the size of a helicopter pad. Each of the zones was given a rating, being 1,2,3 or 4 which was used as an indication of how much space was available. The ratings were defined as follows.

- **Score 1** - A score of one means that the rated zone has no available space to accommodate a vertiport.
- **Score 2** - A score of two means that the rated zone has a small amount of space available to accommodate a vertiport. A single vertiport pad can be placed in the zone.
- **Score 3** - A score of three means that the rated zone has a good amount of space available to accommodate a vertiport. Four vertiport pads can be placed in the zone.
- **Score 4** - A score of two means that the rated zone has a large amount of space available to accommodate a vertiport. Sixteen vertiport pads can be placed in the zone.

To provide the reader with an idea of the rating process, Figure 2.1 gives an example of a zone for each of the rating categories. Subfigure A shows a zone with no space at all as the entire zone is used for houses. Subfigure B shows a zone with a rating of 2 as there is a small patch of land available at the bottom. Subfigure C shows a zone with a rating of 3 as there is quite some space available (where currently trees are present), but it is not a very large zone or a very large amount of space. Finally, subfigure D shows a zone with a rating of 4 as there is a very large amount of space available.

(a) (b)

(c) (d)

Figure 2.1: Example zone with infrastructural space score rating (a) 1 (b) 2 (c) 3 (d) 4

3

Model analysis

3.1. Number of iterations

For the execution of the experiments, 4000 iterations of the Tabu Search algorithm were performed to search the solution space. Generally, it would be beneficial to perform more iterations of the algorithm as a larger amount of the solution space is then explored. This section aims to provide the rationale for the set amount of iterations of 4000.

The main driving factors for the decision on the number of iterations are the found solutions (model performance) and the computational effort it takes to run the set amount of iterations. The goal was to set the iteration limit to an amount that is able to find good solutions within a reasonable amount of time due to time restrictions on this work. To determine this, the model was run for 6000 iterations and the difference in obtained solution scores was monitored using the Mann-Whitney U statistical significance test. As shown in Table 3.1, with a significance level of $\alpha = 0.05$, 4000 is the lowest amount of iterations for which no significant difference was found in the obtained objective scores as compared to running the model with 6000 iterations. The boxplots, shown in Table 3.1, show that better solution scores can be obtained for more iterations, however, especially in the median, somewhat of a stabilization is observed around 4000 iterations.

Table 3.1: Mann Whitney U statistical test p-values per objective type with each dataset compared to the set obtained from running with 6000 iterations.

	Number of iterations				
	1000	**2000**	**3000**	**4000**	**5000**
Demand	6.448 E-6	3.186 E-6	0.015	0.174	0.122
Safety	1.385 E-6	1,728 E-4	3.095 E-5	0.949	0.302
Noise	1.918 E-17	2.55 E-10	0.14	0.137	0.886

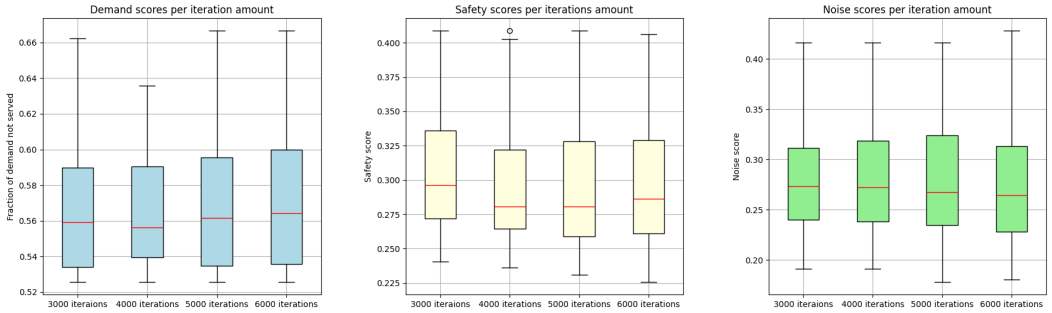

(a) (b) (c)

Figure 3.1: : Boxplot of collected objective scores from the Pareto front: (a) Demand (b) Safety (c) Noise

While a higher number of iterations is preferred as it explores more of the solution space, the computation time increases heavily for an increase in iterations. As can be seen in Figure 3.2, the computation time almost increases linearly with an increasing number of iterations. It was chosen to set the number of iterations to 4000 as this is the most amount of iterations for which time restrictions allowed.

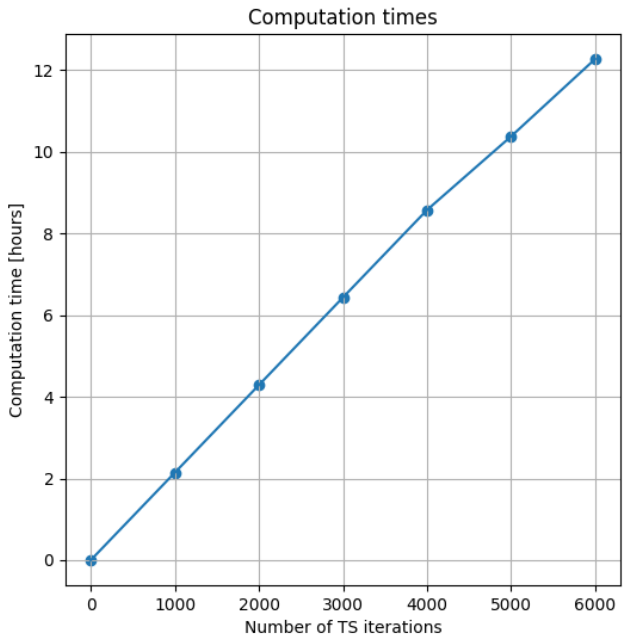

Figure 3.2: Computation times of running the algorithm as a function of iteration count

3.2. Initial solution sensitivity

While the experiments were all run with the same randomly chosen initial solution, the effect that this solution has on the model should also be discussed as different initial solutions might lead to searching different sections of the solution space. Therefore, this section aims to discuss the effects of changing the initial solution that is inputted into the model. First of all, looking at the boxplots shown in Figure 3.3, it is apparent that the initial solution does have some effect on the solution scores that were obtained. Some differences can be seen in both the best-obtained scores per objective type, but also in the median. The observed differences are not very large, however, they should be noted in case of using the model in real-life situations where potential suitable UAM networks are assessed.

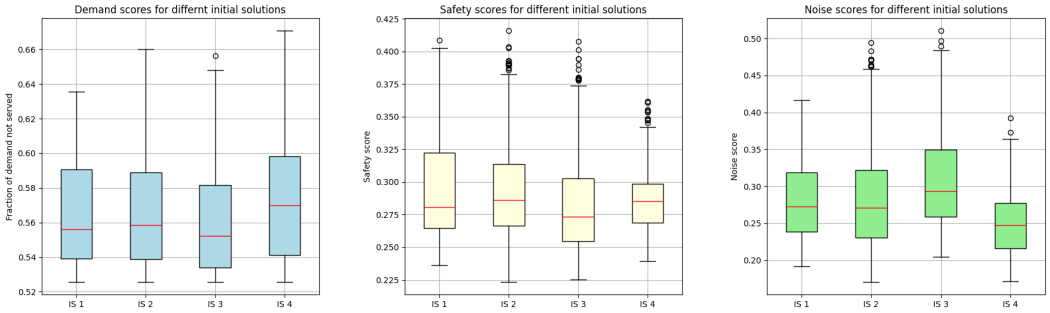

(a) (b) (c)

Figure 3.3: : Boxplot of collected objective scores from the Pareto front: (a) Demand (b) Safety (c) Noise

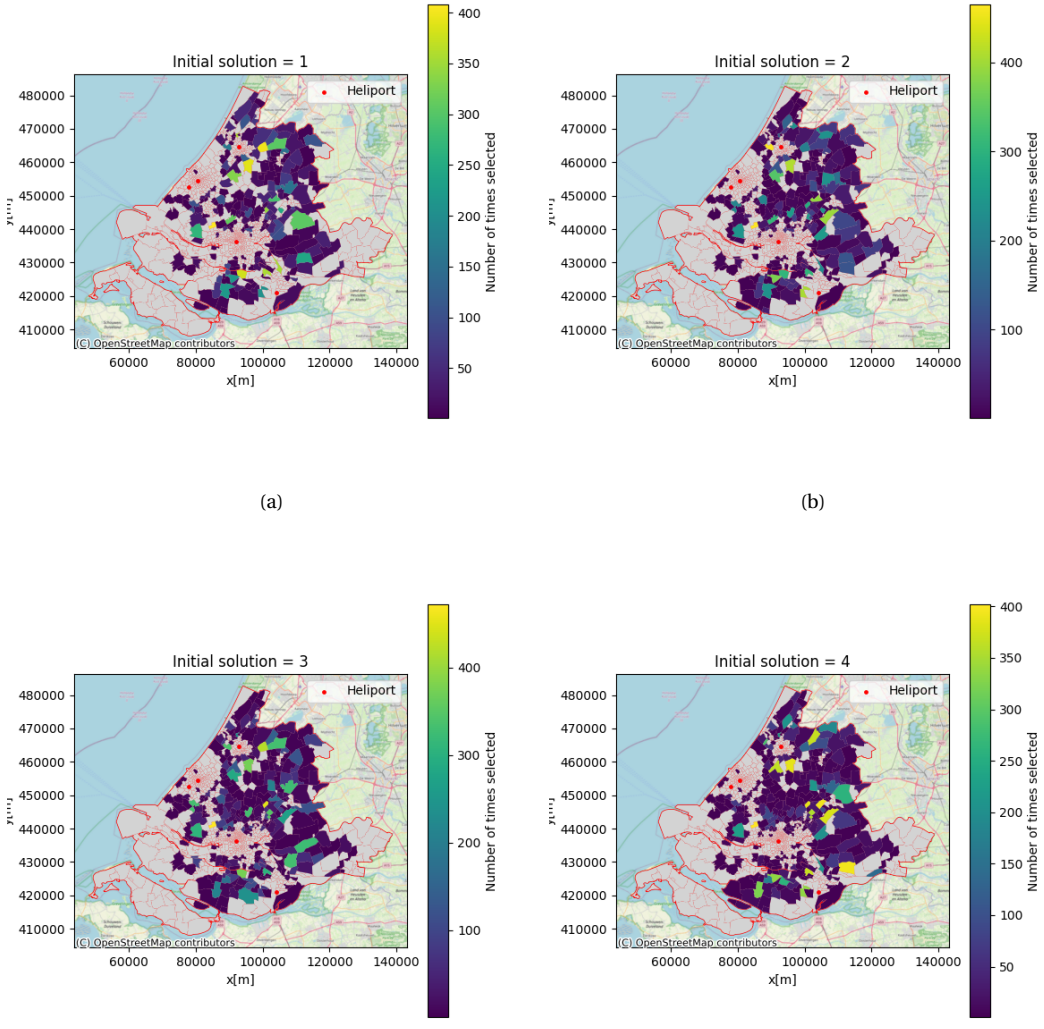

(a) (b)

(c) (d)

Figure 3.4: Heatmap of zones picked in Pareto front with different initial solutions

As the solution space of the proposed model is very large, it comes as no surprise that there are some differences in the obtained solution scores. From the heatmaps, shown in Figure 3.4, it was found that, while there are some differences in the found solution scores, generally, the same areas are selected more often. This makes it easier to identify potentially interesting locations. Nevertheless, it is advisable, when using the model for identifying entire networks, to run the model with multiple initial solutions with as many iterations as possible within time limitations.

3.3. Verification & Validation

To ensure the robustness and integrity of the model, various verification steps were taken. Several unit and system tests were done to ensure that the model works as proposed. This was done either by hand calculation of some model steps, performing the same computation with different methods or by inspection of altered data. For instance, for the assignment of parcels to vertiports, it was checked that no capacity limits were exceeded and all origin-destination pairs were assigned to no more than one vertiport. In the case that only part of the demand could be served by a vertiport, it was made sure that for the remaining parcels, a new request and origin-destination pair was created. Next to the verification of this constraint, it was also made sure that no zones could be chosen that have no infrastructural space, by removing them from the set and visually inspecting if these zones were all removed. For the separation between vertiports and heliports, a function was written that tests whether a proposed solution network violates any of the constraints with minimum and maximum safety distances. In case the function returned true, the solution was feasible and could used for the optimization. If this was not the case, the solution was emitted.

For validation of the framework various system tests in the form of visual inspections and sanity tests were performed. An example is given by Figure 3.5 which shows a visual inspection of the minimum distance between vertiports and the minimum distance to existing heliports. In subfigure A, a single solution for the experiment with 100 vertiports is shown. As this is the most challenging situation to have all vertiports spaced 2440 metres apart, it is the most interesting result to use for evaluating this constraint. In the figure, all centroids of the selected zones are shown with a circle of radius 2440 metres around them. It can be seen that no other centroids are in any of these circles that indicate prohibited areas. This was randomly checked for a number of solutions. Furthermore, in subfigure B, all selected zones in the found Pareto front are shown in a heatmap, as well as the existing heliports and a circle of radius 2440 metres surrounding the heliports. Again, none of the centroids of the selected zones are within these circles indicating prohibited areas. The same type of approach was used for other constraints, for example, for the maximum safety distance, flight restricted areas and restricted zones due to the presence of the city centres of Rotterdam and The Hague. In addition to this, we talked with policy makers on unmanned aviation from the ministry of Infrastructure and Water Management of the Netherlands. This was done to validate if the framework adheres to the high level requirements of policy makers for the usage of such a framework. While actual policy making requires deeper investigation of the area of interest (e.g. identifying more specific areas containing safety risks), the framework is still of interest as it is able to provide meaningful insight. Furthermore, the desired outcome of the more specific area analysis can rather easily be added to the framework by including additional constraints.

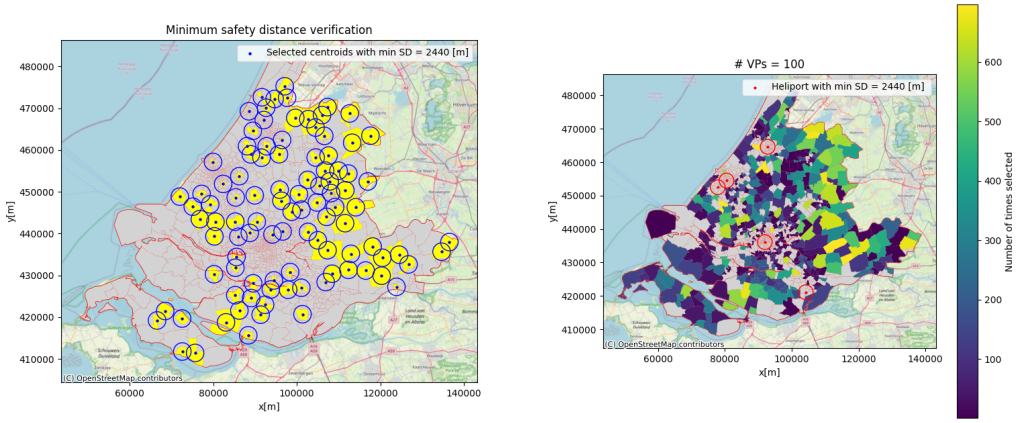

(a) (b)

Figure 3.5: Visual inspection of minimum safety distances (a) between vertiports (b) to existing heliports

4

Business case example: South Holland

This chapter aims to illustrate how the model can be used for the analysis of a business case in the region of South Holland. It therefore demonstrates the value of the model for potential UAM network operators and the Ministry of Infrastructure and Water Management of the Netherlands. For this business case example, the base scenario as described in Part I, Scientific Paper, Section 5 is used. It is assumed that there is a desire to evaluate the viability and effectiveness of a UAM network considering 25 vertiports. Further settings for the independent variables are shown in Table 4.1.

Input	Value
Number of clusters K	1000
Number of vertiports P	25
Drone range	30 [km]
Maximum safety distance	10 [km]
TAT	20 [min]

Table 4.1: Independent variable settings used for business case example

For the described scenario and settings, the model outputs the Pareto front as shown in Figure 4.1. This contour can be used to provide insights into the trade-off between the three objectives, being demand coverage, safety risks and noise nuisance. All possible solutions that are found during the optimization are mapped in the Pareto front. In case there is a heavy preference for one of the three objectives, decision-makers could choose for one of the solutions that perform best in a single objective. These are indicated in the figure by the star markers. The scores that are obtained for the other objectives for these solutions are given in Table 4.1.

Table 4.2: Objective scores for solutions prioritizing one objective

	Additional objective scores		
	Demand	**Safety**	**Noise**
Primary objective			
Demand	0.525	0.341	0.320
Safety	0.588	0.236	0.370
Noise	0.632	0.366	0.191

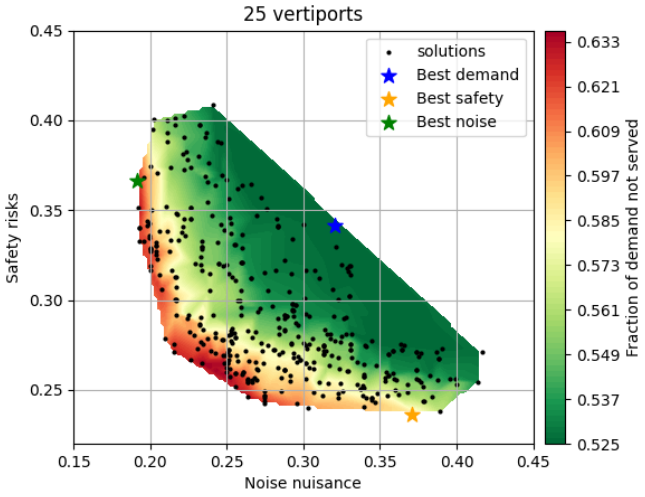

Figure 4.1: Pareto front for business case example scenario

(The rest of the page is left blank intentionally for formatting purposes)

The model then provides the areas that correspond to the selected solutions and maps them. The solutions corresponding to selecting any one of the three solutions that fully prioritize one objective are shown in Figure 4.2.

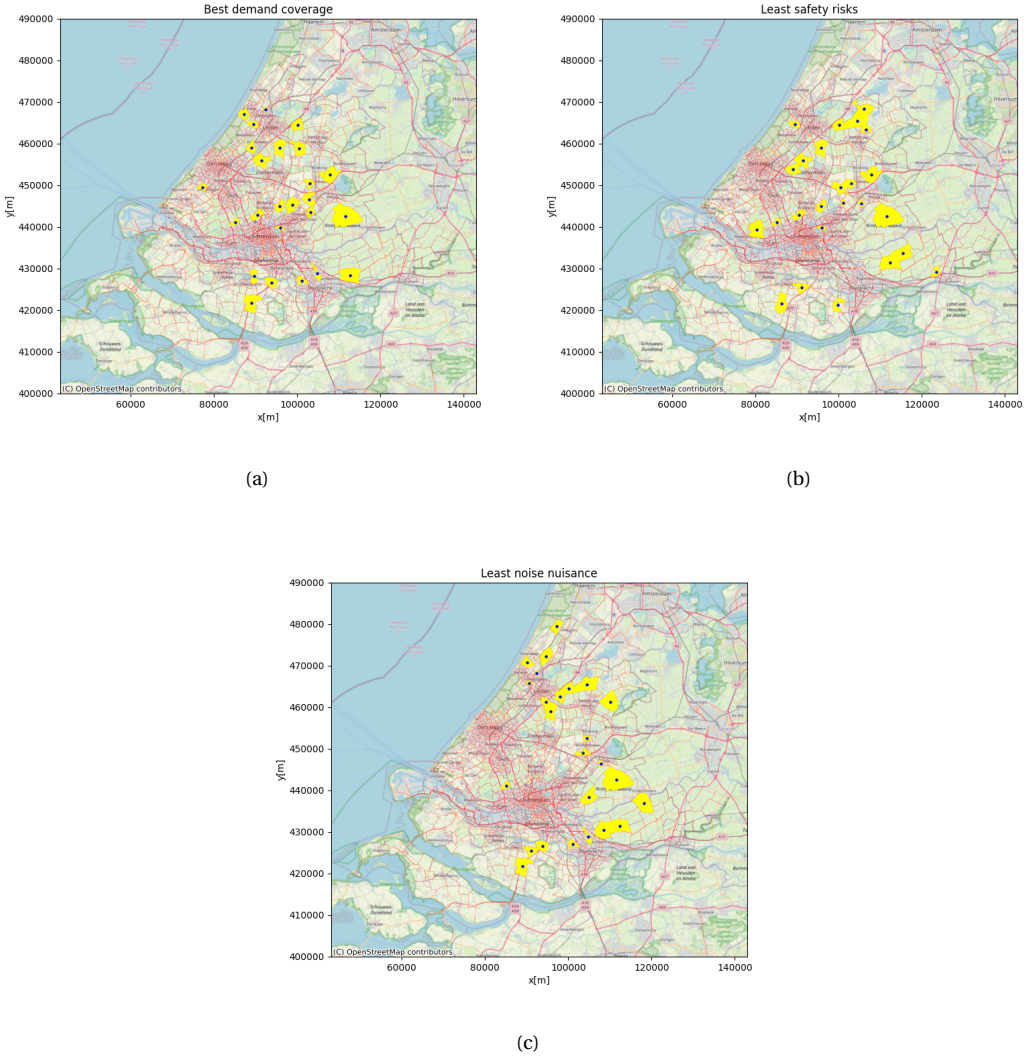

Figure 4.2: Vertiport locations for (a) best demand coverage (b) least safety risks (c) least noise nuisance

In reality, the selection of a suitable solution will most probably not be based on a complete priority of a single objective. Rather, it will be based on a trade-off between the three objectives subject to minimum requirements. For example, whether or not a UAM MMD network is implemented, is likely dependent on the demand coverage that can be realized. The highest attainable demand coverage for a network with 25 vertiports is 47.5%. If this is deemed insufficient, considerations should be made whether it is worth investing in more vertiports or if the implementation area is unsuitable for the UAM MMD network.

For the purpose of demonstration, we assume that a minimum coverage of 45%is deemed to be acceptable to implement a network. In this case, a lot of solutions located in the bottom left of the Pareto front become non-viable solutions. With the leftover viable solutions, a new sub Pareto front can be constructed considering the safety and noise objectives. This is illustrated by Figure 4.3. This Pareto front contains the most interesting solutions as they adhere to demand coverage constraint while performing the best in terms of safety risks and noise nuisance. Decision-makers can then decide upon preference between safety and noise and select a solution on this Pareto front. Figure 4.3 shows such a selection. The selected solution performs quite well in

both the noise and safety objective and the act of moving towards another solution on the sub Pareto front in any direction will result in little improvement of one of the objective scores while significantly deteriorating the other objective score. E.g. moving towards the closest solution that performs better in terms of safety risks, causes very little improvement in safety and worsens the noise score largely. The same holds the other way around.

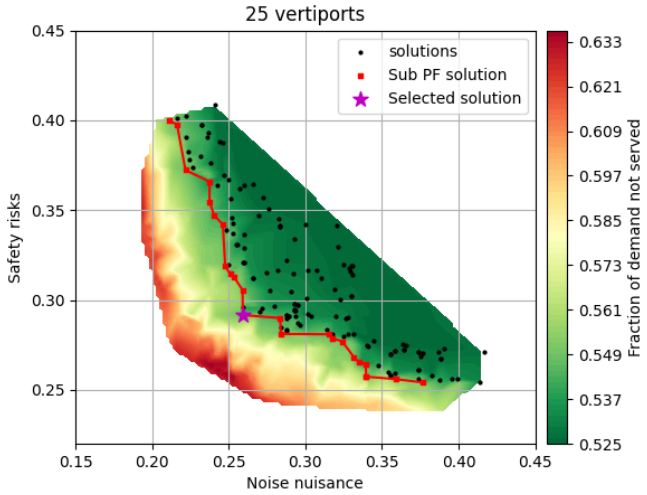

Figure 4.3: Pareto from only considering solution with a minimum of 45% demand coverage

The vertiport locations as a result of the selected solution are then outputted by the model and shown in Figure 4.4. In this way vertiport locations can be determined by decision-makers, demonstrating the business value of the developed model.

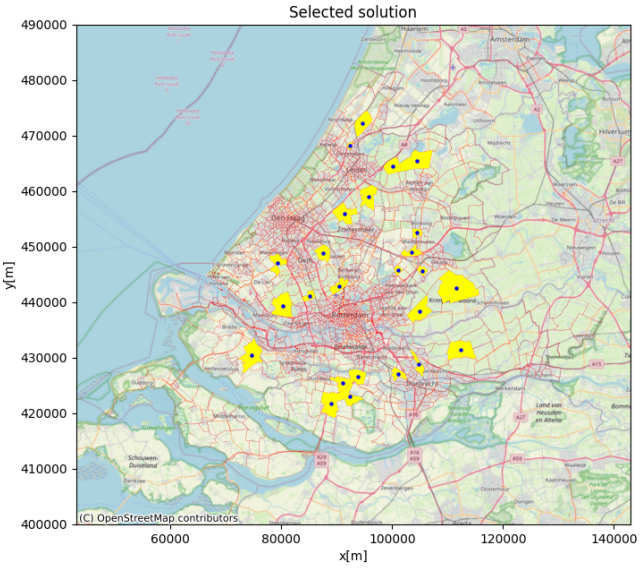

Figure 4.4: Vertiport locations for selected solution

Bibliography

[1] Wave Aerospace. Falcon ii le sales brochure. https://waveaerospace.com/wp-content/uploads/Falcon-II-LE-Sales-Brochure.pdf, . Accessed: 2023-10-26.

[2] Wave Aerospace. Huntress sales brochure. https://waveaerospace.com/wp-content/uploads/Huntress-Sales-Brochure.pdf, . Accessed: 2023-10-26.

[3] B. Ahn and H. Hwang. Design criteria and accommodating capacity analysis of vertiports for urban air mobility and its application at gimpo airport in korea. *Applied Sciences (2022),12,6077*, 2022.

[4] Joby Aviation. Our story. https://www.jobyaviation.com/about/. Accessed: 2023-09-27.

[5] J.F. Benders. Partitioning procedures for solving mixed-variables programming problems. *Numerisch Mathematik 1962;4:23852*, 1962.

[6] N. Boysen, S. Fedtke, and S. Schwerdfeger. Last-mile delivery concepts: a survey from an operational research perspective. *OR Spectrum*, 2021.

[7] J.F. Campbell. Integer programming formulations of discrete hub location problems. *European Journal of Operational Research, 72, 387-405*, 1994b.

[8] Luigi Cardarella. Understanding simulated annealing. https://www.luigicardarella.it/understanding-simulated-annealing/. Accessed: 2023-11-07.

[9] D.L. Davies and D.W. Bouldin. A cluster separation measure. *EEE Trans. Pattern Anal. Mach. Intell. 2, 224227*, 1979.

[10] M. de Bok and L. Tavasszy. n empirical agent-based simulation system for urban goods transport (mass-gt). *Procedia Computer Science, 130:126133, 2018. ISSN 1877-0509. The 9th International Conference on Ambient Systems, Networks and Technologies (ANT 2018) / The 8th International Conference on Sustainable Energy Information Technology (SEIT-2018) / Affiliated Workshops*, 2018.

[11] R.S. de Camargo, G. Miranda Jr., and H.P. Luna. Benders decomposition for the uncapacitated multiple allocation hub location problem. *Computers & Operations Research 35 (2008) 1047 1064*, 2008.

[12] TU Delft. Ambulance drone. https://www.tudelft.nl/io/onderzoek/research-labs/applied-labs/ambulance-drone, 2022.

[13] Draganfly. Draganfly products, heavy lift drone. https://draganfly.com/products/heavy-lift/. Accessed: 2023-10-26.

[14] EASA. Prototype technical specifications for the design of vfr vertiports for operation with manned vtol-capable aircraft certified in the enhanced category. Technical report, EASA, 2022.

[15] European Union Aviation Safety Agency (EASA). Study on the societal acceptance of urbain air mobility in europe. Technical report, EASA, 2021.

[16] European Union Aviation Safety Agency (EASA). Easy access rules for unmanned aircraft systems. Technical report, EASA, 2022.

[17] T. Edwards and G. Price. evtol passenger acceptance. Technical report, NASA, 2020.

[18] Elistair. Orion 2.2 te tactical tethered drone. https://elistair.com/solutions/tethered-drone-orion/. Accessed: 2023-10-26.

[19] H. Eskandaripour and E. Boldsaikhan. Last-mile drone delivery: Past, present, and future. *Drones. 2023; 7(2):77*, 2023.

[20] C. Lin et al. The capacitated p-hub median problem with integral constraints: An application to a chinese air cargo network. *Applied Mathematical Modelling Volume 36, Issue 6, June 2012, Pages 2777-2787*, 2012.

[21] F. Yunus et al. Efficient prediction of urban air mobility noise in a vertiport environment. *Aerospace Science and Technology Volume 139, August 2023, 108410*, 2023.

[22] H. Calik et al. A tabu-search based heuristic for the hub covering problem over incomplete hub networks. *Computers & Operations Research 36 (2009) 3088-3096*, 2009.

[23] H. Schütze et al. *Introduction to Information Retrieval.* Cambridge University Press, 2008.

[24] J. Jeong et al. Selection of vertiports using k-means algorithm and noise analyses for urban air mobility (uam) in the seoul metropolitan area. *Applied Sciences 11 (12), 119*, 2021.

[25] J. Macias et al. An integrated vertiport placement model considering vehicle sizing and queuing: A case study in london. *Journal of Air Transport Management, Volume 113*, 2023.

[26] K.R. Antcliff et al. Silicon valley as an early adopter for on-demand civil vtol operations. *16th AIAA Aviation Technology, Integration, and Operations Conference*, 2016.

[27] L. Chen et al. Scalable vertiport hub selection for air taxi operations in a metropolitan region. *Informs Journal On Computing, Vol. 34, No. 2, March-April 2022, pp. 834-865*, 2022.

[28] L. Preis et al. Ground operation on vertiports introduction of an agent-based simulation framework. *AIAA Scitech 2021 Forum*, 2021.

[29] L. Wei et al. Optimal placement of airparks for stol-based urban and suburban air mobility. *AIAA Scitech 2020 Forum*, 2020.

[30] M. Brink et al. Conversion between noise exposure indicators leq24h, lday, levening, lnight, ldn: Principles and practical guidance. *Int. J. Hyg. Environ. Health 2018, 211, 5463*, 2018.

[31] M. Brunelli et al. A framework to develop urban aerial networks by using a digital twin approach. *Drones 2022, 6, 387*, 2022.

[32] M. Brunelli et al. New infrastructures for urban air mobility systems: A systematic review on vertiport location and capacity. *Journal of Air Transport Management 112 (2023) 102460 Available*, 2023.

[33] M. Guerreiro et al. Capacity and throughput of urban air mobility vertiports with a first-come, first-served vertiport scheduling algorithm. *AIAA AVIATION 2020 FORUM*, 2020.

[34] M.A. Albadr et al. Genetic algorithm based on natural selection theory for optimization problems. *Symmetry 2020, 12, 1758*, 2020.

[35] M.A. Arostegui Jr. et al. An empirical comparison of tabu search, simulated annealing, and genetic algorithms for facilities location problems. *Int. J. Production Economics 103 (2006) 742754*, 2006.

[36] M.A.S. Mohamed et al. isual pollution manifestations negative impacts on the people of saudi arabia. *Int. J. Adv. Appl. Sci. 2021, 8, 94101*, 2021.

[37] M.J. Duffy et al. A study in reducing the cost of vertical flight with electric propulsion. *17th AIAA Aviation Technology, Integration, and Operations Conference*, 2017.

[38] N. Gunandy et al. Evaluating future electrified urban air mobility cargo delivery operations. *AIAA Aviation Forum*, 2022.

[39] R. Howard et al. Assessing the suitability of urban air mobility vehicles for a specific aerodrome network. *AIAA AVIATION 2021 FORUM, 2021, p. 3208*, 2021.

[40] R.Z. Faharani et al. Hub location problems: a review of models, classification, solution techniques, and applications. *Comput. Ind. Eng. 64 (4), 10961109*, 2013.

[41] R.Z. Farahani et al. Hub location problems: A review of models, classification, solution techniques, and applications. *Computers & Industrial Engineering Volume 64, Issue 4, April 2013, Pages 1096-1109*, 2013.

[42] S.A. Alumur et al. Perspectives on modelling hub location problems. *European Journal of Operational Research Volume 291, Issue 1, 16 May 2021, Pages 1-17*, 2021.

[43] Shin et al. Skyport location problem for urban air mobility system. *Computers and Operations Research, 138 (105611), 113*, 2022.

[44] Y. Zeng et al. Future demand and optimum distribution of droneports. *2020 IEEE 23rd International Conference on Intelligent Transportation Systems (ITSC)*, 2020.

[45] Federal Aviation Administration (FAA). Heliport design, ac no: 150/5390-2c. Technical report, FAA, 2012.

[46] D.N. Fadhill. A gis-based analysis for selecting ground infrastructure locations for urban air mobility (master thesis, 2018.

[47] E. Feldhoff and G.S. Roque. Determining infrastructure requirements for an air taxi service at cologne bonn airport. *CEAS Aeronautical Journal (2021) 12:821833*, 2021.

[48] Flargo. Our vtol solutions for cargo delivery and passenger transportation. https://flargo.tech/vtol-solutions/. Accessed: 2023-10-26.

[49] Gadfin. Gadfin products. https://www.gadfin.com/products/. Accessed: 2023-10-26.

[50] B.J. German and M.J. Daskilewicz et al. Cargo delivery by passenger evtol aircraft: A case study in the san francisco bay area. *2018 AIAA Aerospace Sciences Meeting*, 2018.

[51] F. Glover. Improved linear integer programming formulations of nonlinear integer problems. *Management Science, 22(4), 455-460*, 1975.

[52] F. Glover. Tabu search - part 1. *ORSA Journal on computing Vol 1, No. 3, Summer 1989*, 1989.

[53] C.J. Delgado Gonzales. *Rooftop-place suitability analysis for urban air mobility hubs: A GIS and Neural network Approach (Doctoral Dissertation)*. PhD thesis, Universitat Jaume I, 2020.

[54] K.H. Goodrich and B.E. Barmore. Exploratory analysis of the airspace throughput and sensitivities of an urban air mobility system. *2018 Aviation Technology, Integration, and Operations Conference*, 2018.

[55] J. Holden and N. Goel. Uber elevate: Fast-forwarding to a future of on-demand urban air transportation. Technical report, Uber, 2016.

[56] International Civil Aviation Organization (ICAO. Annex 14 - aerodromes - volume ii - heliports. Technical report, ICAO, 2013.

[57] Mordor intelligence. Air taxi market size & share analysis - growth trends & forecasts (2023-2035). https://www.mordorintelligence.com/industry-reports/air-taxi-market, 2023. Accessed: 2023-09-27.

[58] R. Ishfaq and C.R. Sox. Design of intermodal logistics networks with hub delays. *European Journal of Operational Research Volume 220, Issue 3, 1 August 2012, Pages 629-641*, 2012.

[59] Jaunt. Technology. https://jauntairmobility.com/technology/. Accessed: 2023-09-27.

[60] B.Y. Kara and B.C. Tansel. The single-assignment hub covering problem: Models and linearizations. *Journal of the Operational Research Society, 54(1) 59-64*, 2003.

[61] N. Kim and Y. Yoon. Regionalization for urban air mobility application with analyses of 3d urban space and geodemography in san francisco and new york. *Procedia Computer Science 184 (2021) 388395*, 2021.

[62] G. Laporte, S. Nickel, and F.S. da Gama. *Location Science*. Springer, 2019.

[63] G.J. Lieberman and F.S Hillier. *Introduction to operations research, volume 11.* McGrawHill New York, USA, 2021.

[64] Lilium. Jet. https://lilium.com/jet?_gl=1*l2254a*_up*MQ..*_ga*NDgwNjcyNzA4LjE2OTU5MDk2ODE.*_ga_9YC7ETNZ98*MTY5NTkwOTY4MC4xLjAuMTY5NTkwOTY4MC4wLjAuMA.. Accessed: 2023-09-27.

[65] E. Lim and H. Hwang. The selection of vertiport location for on-demand mobility and its application to seoul metro area. *International Journal of Aeronautical and Space Sciences, 20:260272*, 2019.

[66] Walter Living. Housing market in rotterdam (october 2023). https://walterliving.com/city/rotterdam. Accessed: 2023-10-30.

[67] V. Marianov and D. Serra. Location models for airline hubs behaving as m/d/c queues. computers and operations research, 30, 9831003. *Computers and Operations Research, 30, 9831003*, 2003.

[68] H.M. Miedema and C. G. Oudshoorn. Annoyance from transportation noise: relationships with exposure metrics dnl and denl and their confidence intervals. *Environmetal health perspectives 109(4):409-416*, 2001.

[69] N. Mladenovic and P. Hansen. Variable neighborhood search. *Computers & Operations Research, 24(11), 1097-1100*, 1997.

[70] J. Mwemezi and Y. Huang. Optimal facility location on spherical surfaces: Algorithm and application. *New York Science Journal, 4, 21-28*, 2011.

[71] Ministry of Infrastructure and Water Management. Dataset: Actueel hoogtebestand nederland (ahn). https://www.pdok.nl/introductie/-/article/actueel-hoogtebestand-nederland-ahn. Accessed: 2023-10-26.

[72] Port of Rotterdam. Drone port of rotterdam: U-space airspace prototype whitepaper. Technical report, Port of Rotterdam, 2023.

[73] M.E. O'Kelly. A quadratic integer program for the location of interacting hub facilities. *European Journal of Operational Research, 32(3), 393-404*, 1987.

[74] Publieke Dienst op de Kaart (PDOK). Dataset: Pdok luchtfoto rgb (open), 2024. URL https://www.pdok.nl/introductie/-/article/pdok-luchtfoto-rgb-open-.

[75] F.S. Pamuk and C. Sepil. A solution to the hub center problem via a single-relocation algorithm with tabu search. *IIE Transactions (2001) 33, 399-411*, 2001.

[76] P. Panchal, L. Meyer, and T.A. Granberg. Introduction to uam risk, noise and visual pollution. Webinar Date: 26-10-2023.

[77] B.T. Park and S. H. Kim. Vertiport design optimization using integer programming. *2022 IEEE/AIAA 41st Digital Avionics Systems Conference (DASC)*, 2022.

[78] M. Peker and B.Y. Kara. The p-hub maximal covering problem and extensions for gradual decay functions. *Omega 53, 158-172*, 2015.

[79] Pipistrel. Pipistrel air cargo. https://www.pipistrel-aircraft.com/air-cargo/. Accessed: 2023-10-26.

[80] L. Preis. Quick sizing, throughput estimating and layout planning for vtol aerodromesa methodology for vertiport design. *AIAA Aviation 2021 Forum, 2372, pp. 119*, 2021.

[81] L. Preis and M. Hornung. Identification of driving processes for vertiport operations using agent-based simulation. *AIAA SCITECH 2022 Forum*, 2022.

[82] S. Rajendran and J. Zack. "insights on strategic air taxi network infrastructure locations using an iterative constrained clustering approach". *Transportation Research Part E 128, 470505*, 2019.

[83] S. Rath and Y.J. Chow. Air taxi skyport location problem with single-allocation choice-constrained elastic demand for airport access. *Journal of Air Transport Management, Volume 105*, 2022.

[84] S. Ray and H. Turi. Determination of number of clusters in k-means clustering and application in colour image segmentation. *In: Proceedings of the 4th International Conference on Advances in Pattern Recognition and Digital Techniques, December, pp. 137143*, 1999.

[85] Allied Market Research. Air taxi market by propulsion type (parallel hybrid, electric, turboshaft, and turboelectric), aircraft type (multicopter, quadcopter, and others), and passenger capacity (one, two, four, and more than six): Global opportunity analysis and industry forecast, 2021-2030. https://www.alliedmarketresearch.com/air-taxi-market, 2019. Accessed: 2023-09-27.

[86] Rijksoverheid and LVNL. Official no-fly zones provided by the dutch central government. https://map.godrone.nl/, 2023. Accessed: 2023-10-17.

[87] M. Rimjha and A. Trani. Urban air mobility: Factors affecting vertiport capacity. *2021 Integrated Communications Navigation and Surveillance Conference (ICNS)*, 2021.

[88] Velos Rotors. Velos v3 brochure. https://velos-rotors.com/wp-content/uploads/2020/11/Velos-V3-Brochure-8.5-%C3%97-11-in-WEB.pdf. Accessed: 2023-10-26.

[89] P.J. Rousseeuw. Silhouettes: a graphical aid to the interpretation and validation of cluster analysis. *Comput Appl Math 20:5365*, 1986.

[90] RSP. Drone inspecties. https://www.rps.nl/expertise/field-services/infrastructuur-inspecties/drone-inspecties/. Accessed: 2023-10-26.

[91] T.J. Schultz. Synthesis of social surveys on noise annoyance. *J.Acoust. Soc.Am. 64, 377405*, 1978.

[92] K. Schweiger and L. Preis. Urban air mobility: Systematic review of scientific publications and regulations for vertiport design and operations. *Drones 2022, 6, 179*, 2022.

[93] K. Schweiger, F. Knabe, and B. Korn. An exemplary definition of a vertidromes airside concept of operations. *Aerospace Science and Technology 125 (2022) 107144*, 2022.

[94] A.A. Sinha and S. Rajendran. A novel two-phase location analytics model for determining operating station locations of emerging air taxi services. *Decision Analytics Journal 2 (100013), 115*, 2022.

[95] Skydio. Public safety: Fire fighting drones. https://www.skydio.com/fire-fighting-drones. Accessed: 2023-10-26.

[96] QGIS Development Team. Qgis geographic information system. http://qgis.osgeo.org.

[97] K. Thomas and T.A. Granberg. Quantifying visual pollution from urban air mobility. *Urban Air Mobility. Drones 2023, 7, 396*, 2023.

[98] V. Tokarev and V. Makarenko. Prediction of noise generated by small unmanned aerial vehicles' operation in vertiport vicinity. *International Journal of Sustainable Aviation (IJSA), Vol. 7, No. 2, 2021]*, 2021.

[99] Ziyan UAS. Ziyan uas products, blowfish a2g. https://www.ziyanuav.com/en/list/306.html, . Accessed: 2023-10-26.

[100] Ziyan UAS. Ziyan uas products, blowfish a3. https://www.ziyanuav.com/en/list/374.html, . Accessed: 2023-10-26.

[101] UPS. About ups, ups flight forward adds innovative new aircraft, enhancing capabilities and network sustainability. https://about.ups.com/ae/en/newsroom/press-releases/innovation-driven/ups-flight-forward-adds-new-aircraft.html. Accessed: 2023-10-24.

[102] G. Usman, U. Ahmad, and M. Ahmad. Improved k-means clustering algorithm by getting initial cenroids. *World Applied Science Journal 27 (4), 543551*, 2013.

[103] P.D. Vascik and R.J. Hansman. Development of vertiport capacity envelopes and analysis of their sensitivity to topological and operational factors. *AIAA Scitech 2019 Forum, pp. 126*, 2019.

[104] Volocopter. Solutions. https://www.volocopter.com/solutions/volocity/. Accessed: 2023-09-27.

[105] Voltaero. Cassio. https://www.voltaero.aero/en/. Accessed: 2023-09-27.

[106] P.J. Vossen. Sustainability and cost assessment of lithium battery health management strategies for electric unmanned aerial vehicles. *Master Thesis*, 2022.

[107] VZinfo. Informatie over volksgezondheid en zorg, bevoling|regionaal. https://www.vzinfo.nl/bevolking/regionaal. Accessed: 2023-10-26.

[108] B. Wagner. Model formulations for hub covering problems. *Journal of the Operational Research Society, 59, 932-938*, 2008b.

[109] Z. Whu and Y. Zhang. Integrated network design and demand forecast for on-demand urban air mobility. *Engineering Volume 7, Issue 4, April 2021, Pages 473-487*, 2021.

[110] L.C. Willey and J.L. Salmon. A method for urban air mobility network design using hub location and subgraph isomorphism. *Transportation Research, Part C 125*, 2021.

[111] B. Yutko and G. Gysin. Concept of operations for uncrewed urban air mobility. Technical report, Wisk and Boeing, 2022.

[112] S. Zelinski. Operational analysis of vertiport surface topology. *IEEE 39th Digital Avionics Systems Conference (DASC)*, 2020.

[113] Zipline. About zipline. https://www.flyzipline.com/about/. Accessed: 2023-09-27.